Overview of Physics results at ATLAS

VIII International Conference on High Energy Physics in the LHC Era - HEP2023
(9-13 January 2023) Universidad Técnica Federico Santa María (UTFSM), Valparaíso, Chile.

Rebeca Gonzalez Suarez - Uppsala University

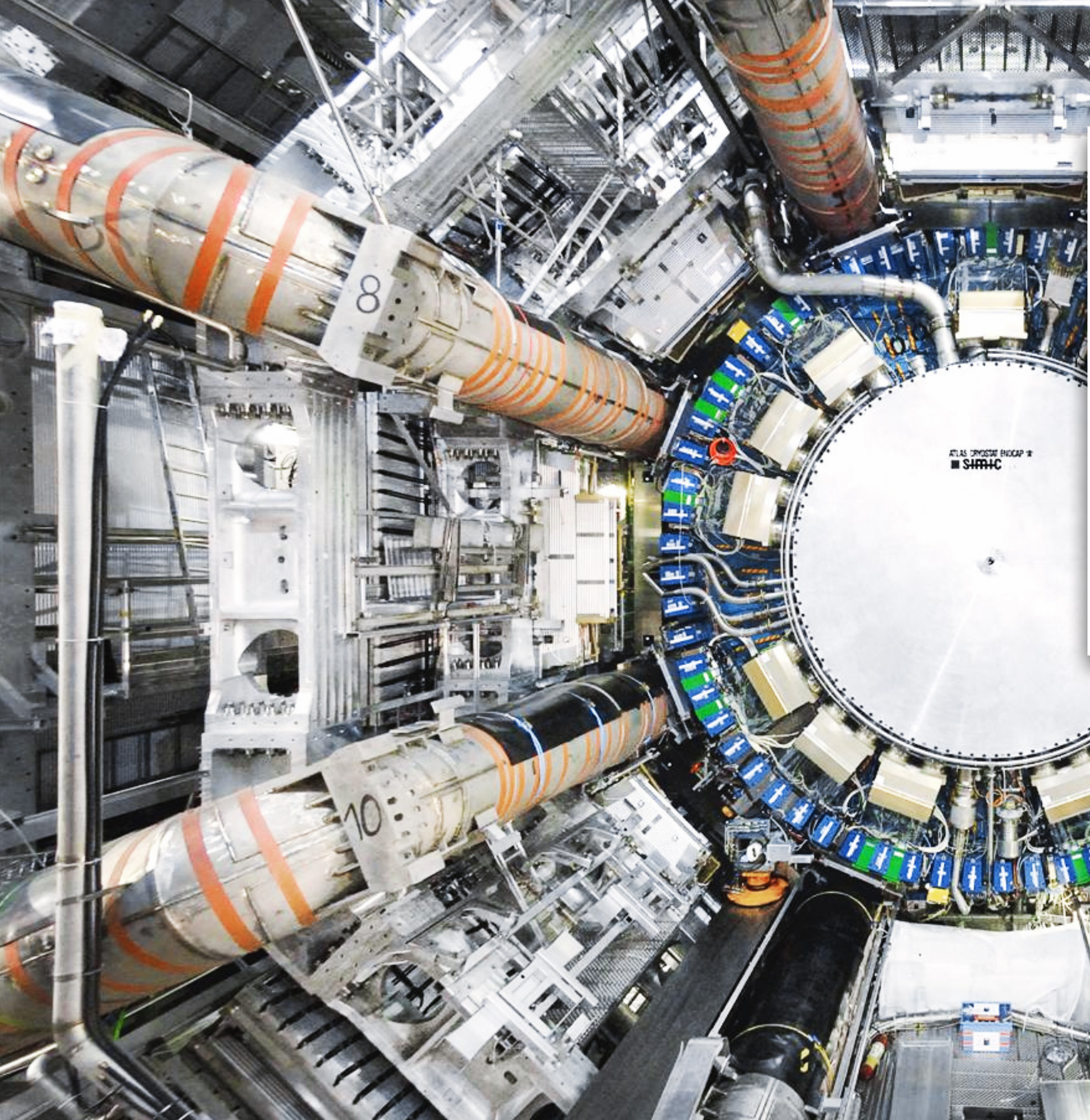

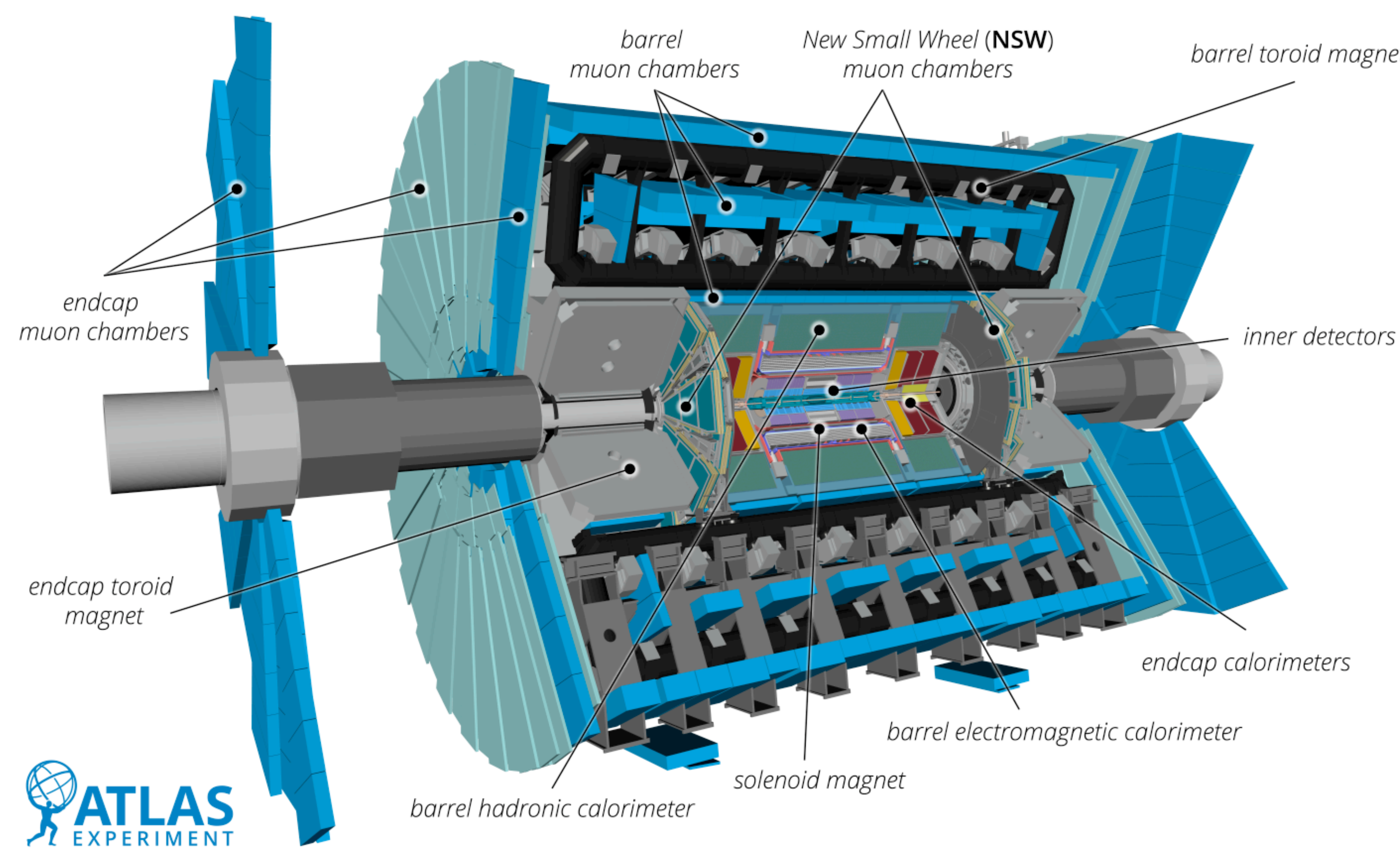

- Public results - Main website
- **Follow ATLAS in social media:**
  - Twitter | Facebook | Instagram | TikTok | LinkedIn | YouTube | Flickr | Mastodon

2022 was a very exciting year for ATLAS

The start of the LHC Run-3

- On July 5
  - https://atlas.cern/Updates/Press-Statement/Run3-first-collisions
  - https://atlas.cern/Updates/Press-Statement/LHC-Run3-Starts
- **13.6 TeV pp collision data - more than 30fb^{-1} already recorded**

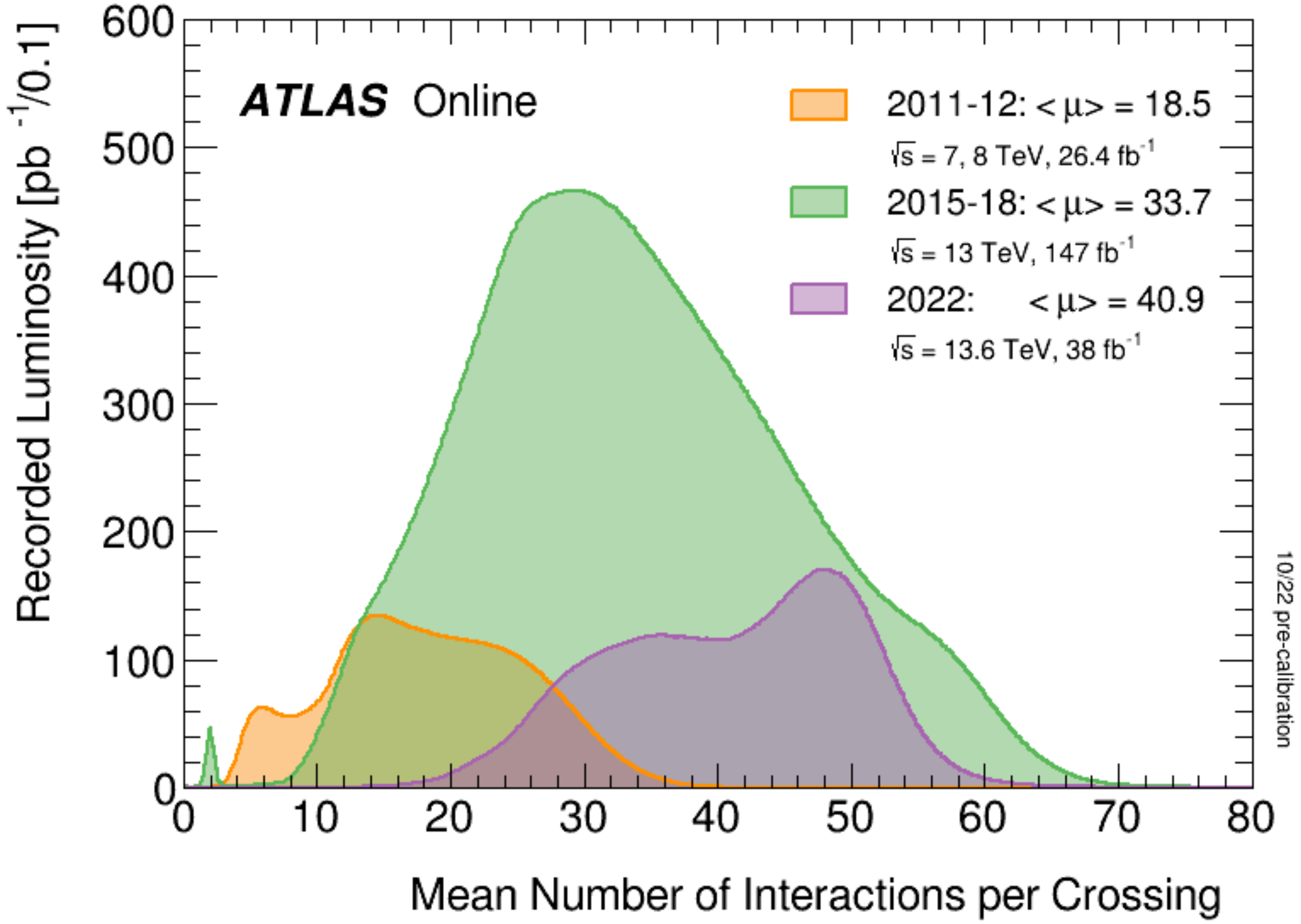

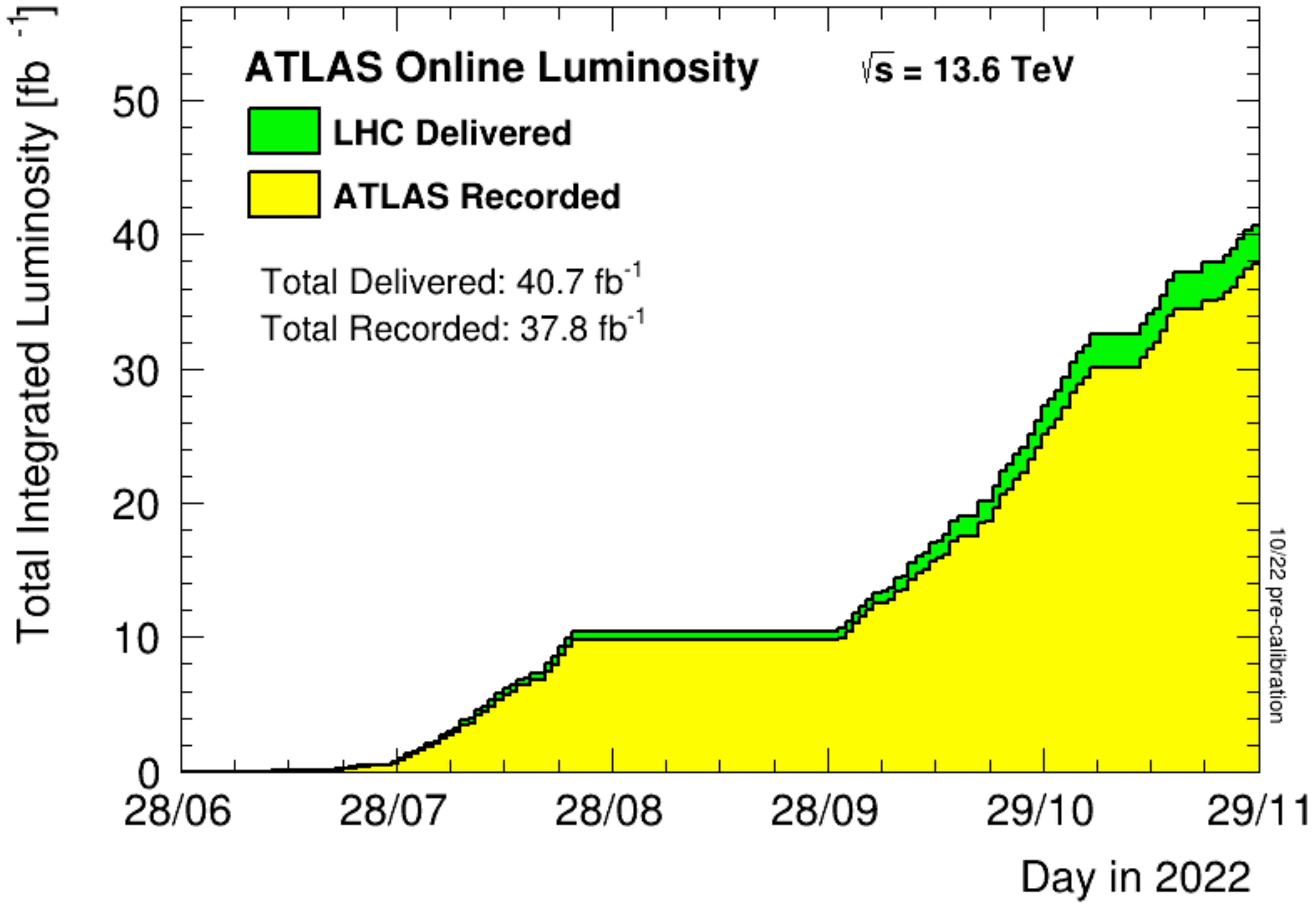

First Run-3 results already underway!

Still a lot to learn from Run-2 and Run-1

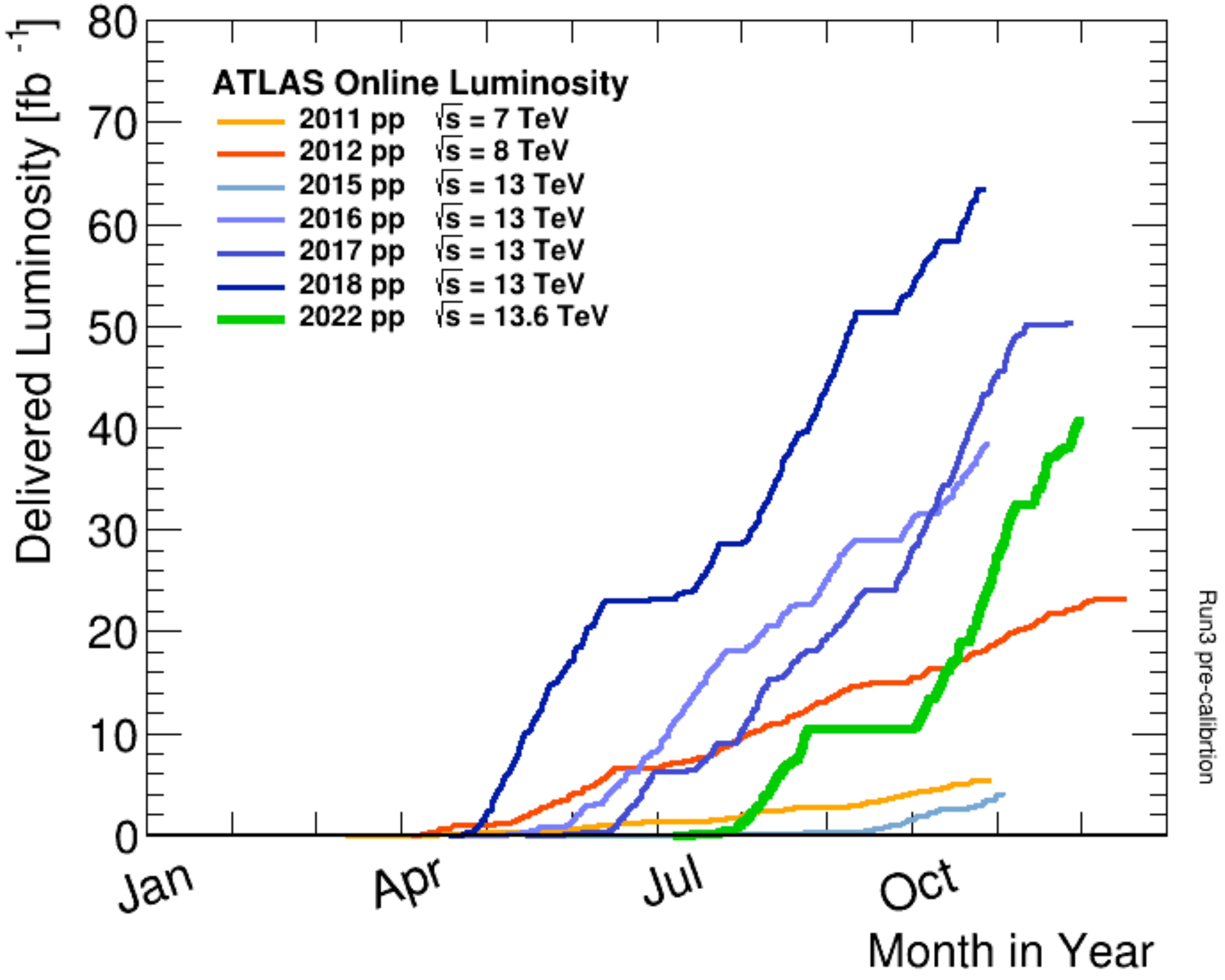

- **Run-2 dataset**
  - **pp 13 TeV - 139fb^{-1}**
    - 94% data quality efficiency
  - **Heavy ion datasets**
    - PbPb 5.02 TeV - 1.82 nb^{-1}
    - XeXe 5.44 TeV - 3μb^{-1}
    - pPb 8.16 TeV - 165 nb^{-1}
  - **Low PU pp reference runs**
    - 5.02 TeV - 0.26 fb^{-1}
    - 13 TeV - 0.15fb^{-1}
- **Run-1 pp dataset:** 5fb^{-1} @ 7 TeV & 20fb^{-1} @ 8 TeV

The most precise luminosity measurement to date

- Integrated luminosity, full Run 2 dataset recorded by ATLAS and certified as good for physics: 140.1 ± 1.2fb^{-1}
  - **Uncertainty: 0.83% → most precise luminosity measurement at a hadron collider to date.**
  - Absolute luminosity scale via Van der Meer scans, extrapolated using complementary measurements from luminosity-sensitive detectors
  - Extremely important for e.g.: cross-section measurements - leading source of uncertainty

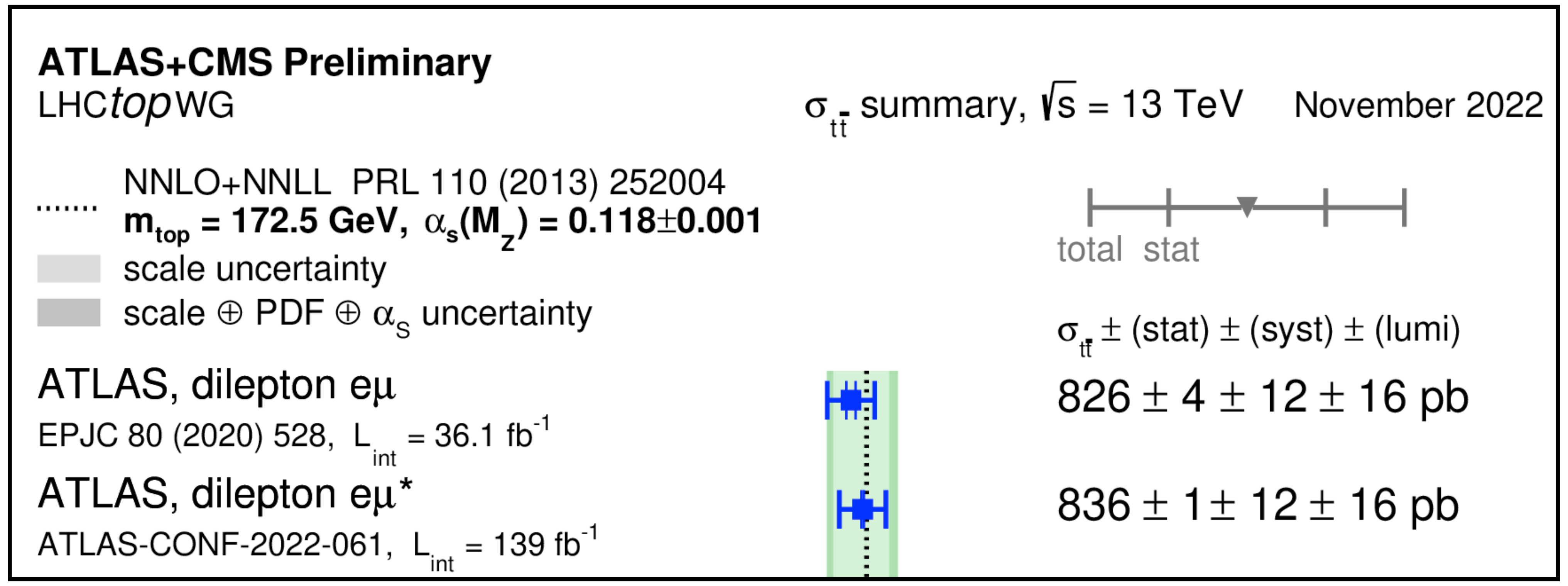

arXiv:2212.09379

DAPR-2021-01/

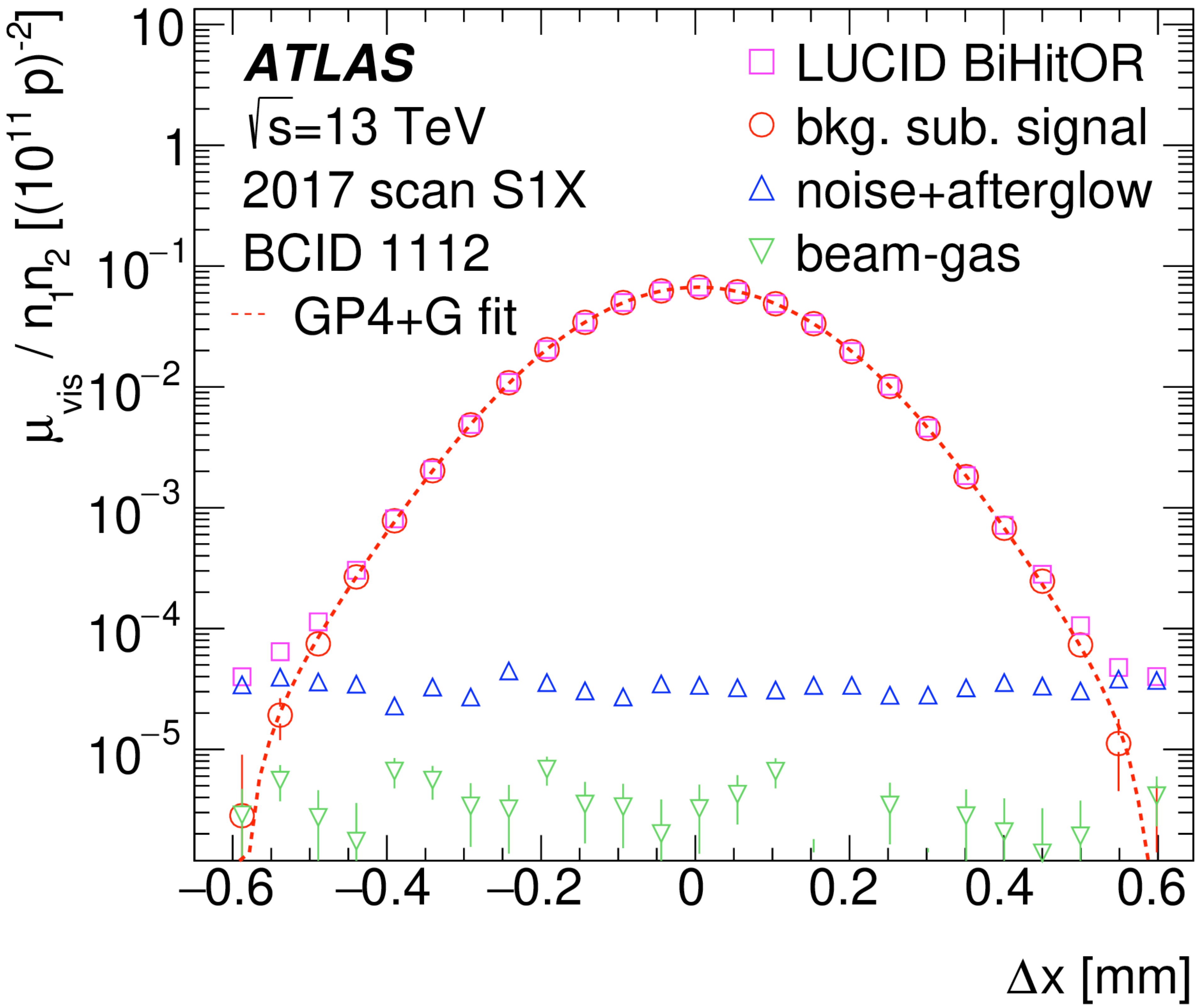

Van der Meer (vdM) scan curve, obtained when the LHC proton beams are displaced from their normal position in the horizontal and vertical planes for the experiments to record the counts in the luminosity detectors. The curve is fitted and backgrounds are subtracted

10 years since the Higgs discovery

https://atlas.cern/Updates/Press-Statement/10-year-higgs
https://atlas.cern/Updates/News/ATLAS-CMS-Higgs-2022

There is a lot to celebrate

- More than 30 times as many Higgs bosons have been recorded by ATLAS since the observation, allowing for **very precise measurements and new tests of the SM**
- Nature paper: a wealth of tests, the Higgs boson is very consistent with the predictions of the theory, stringent constraints on many BSM models can be set
- Inclusive Higgs boson production rate relative to the SM prediction:

$$\mu = 1.05 \pm 0.06 = 1.05 \pm 0.03\,(\text{stat.}) \ \pm 0.03\,(\text{exp.}) \ \pm 0.04\,(\text{sig. th.}) \ \pm 0.02\,(\text{bkg. th.}).$$

arXiv:2207.00092

HIGG-2021-23

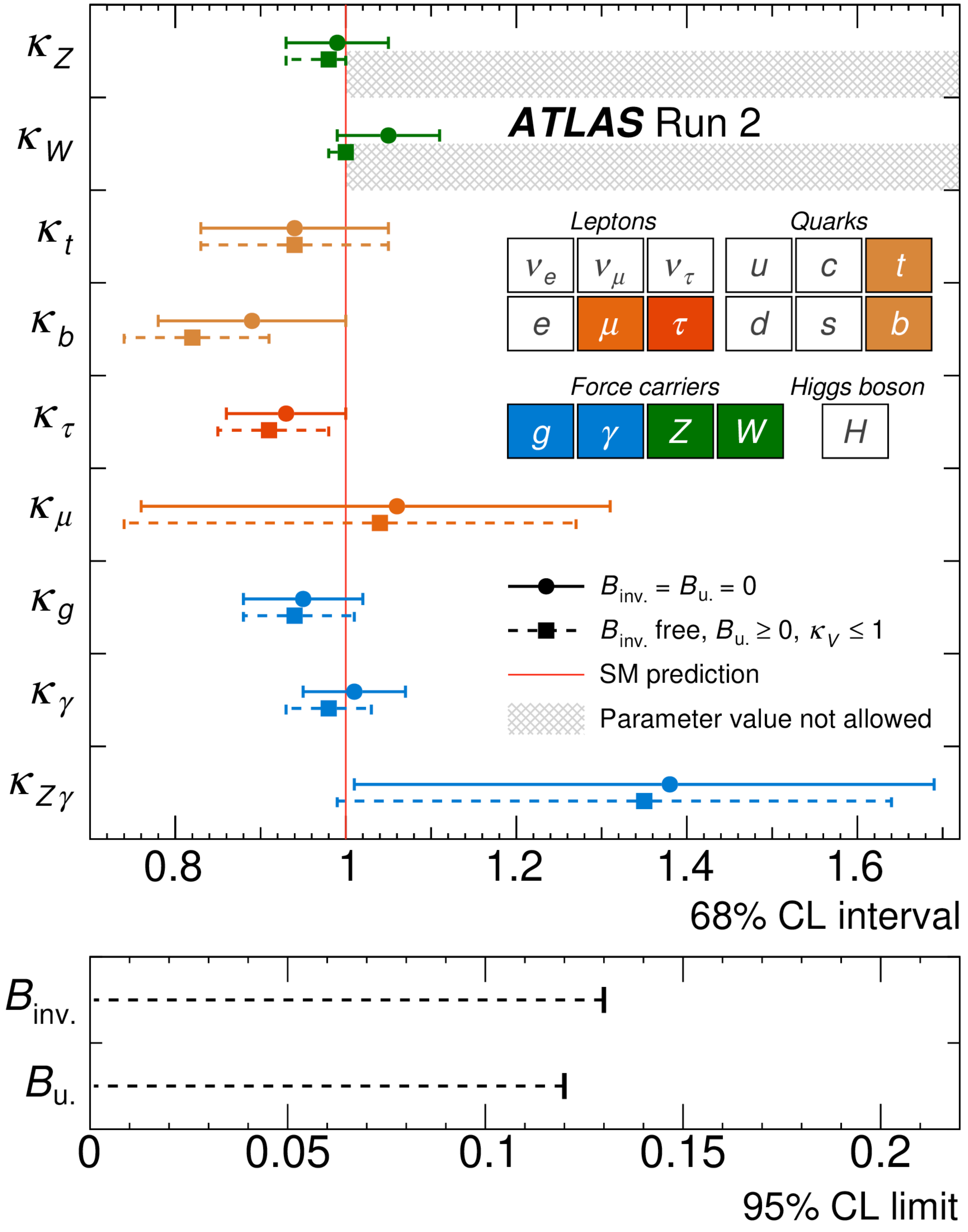

Mass, off-shell production and total width

HIGG-2020-07 arXiv:2207.00320

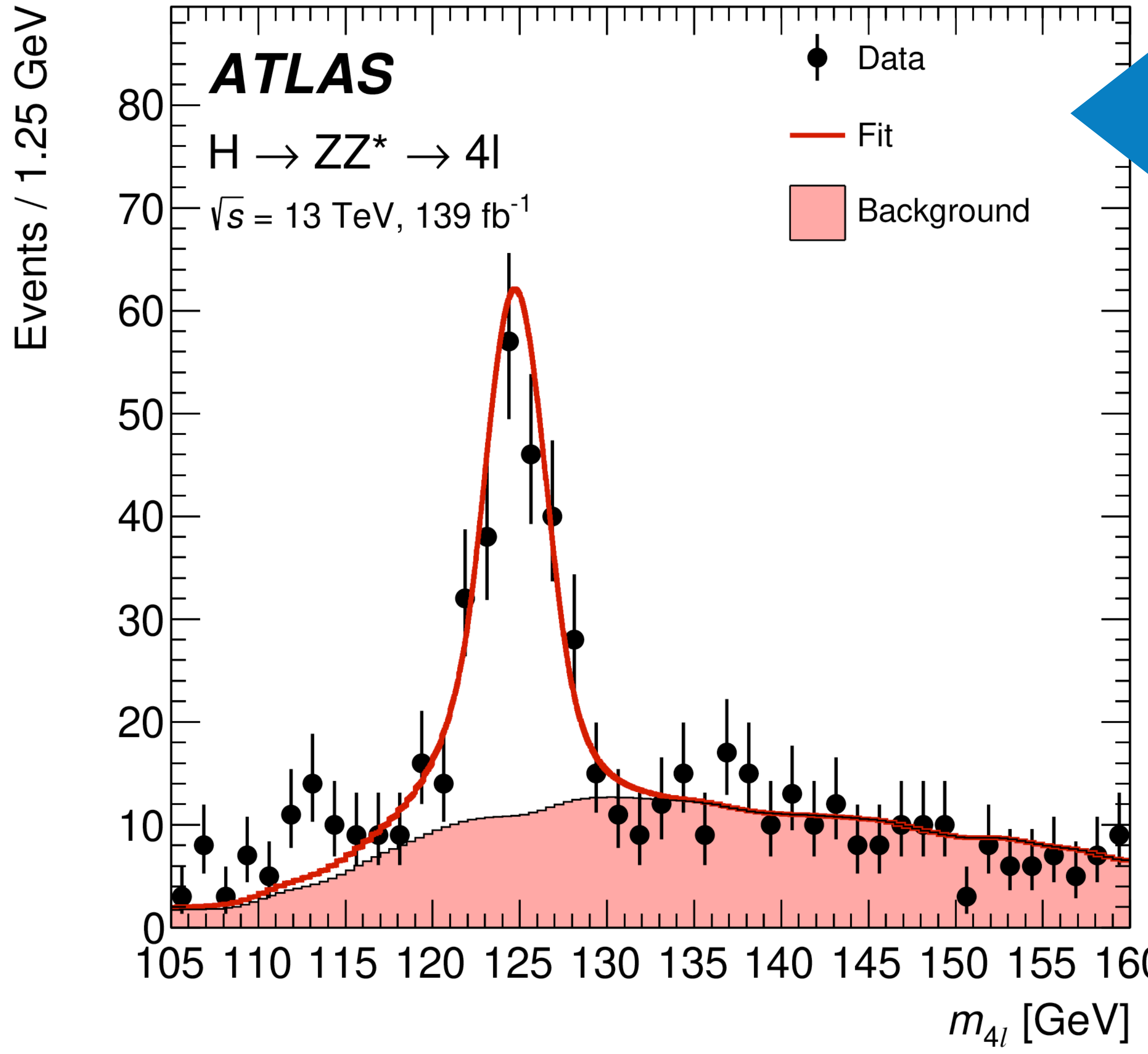

H → ZZ
Full Run-2 dataset

- **Mass** (combined with Run-1 measurements):
  - 124.94±0.17(stat.)±0.03(syst.) GeV
- **Total width**
- Direct measurement: not possible
- Comparing on-shell (depends on width) and off-shell (independent, sensitive to BSM) regions.
- 3.2 (2.4) σ evidence of off-shell Higgs production
- Measured total width:
  - 4.6 +2.6–2.5 MeV (4.1 MeV predicted)

ATLAS-CONF-2022-068

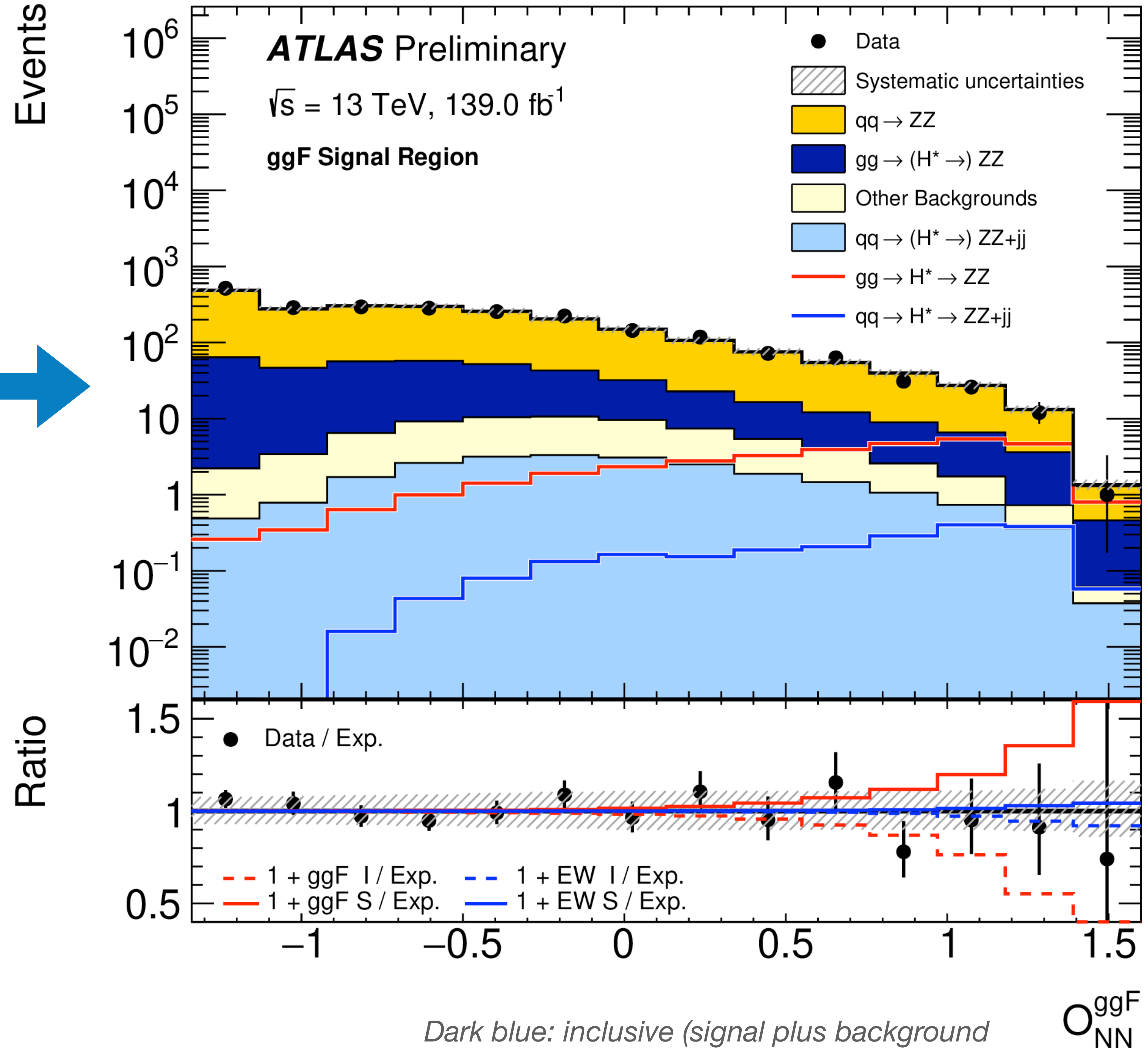

Dark blue: inclusive (signal plus background plus interference) ggZZ

https://atlas.cern/Updates/Briefing/Higgs-Total-Width https://atlas.cern/updates/briefing/combined-Higgs-discovery-channels

Cross-sections

- **Total and differential:**

arXiv:2207.08615

HIGG-2022-04

  - $H \to ZZ_* \to 4\ell$ and $H \to \gamma\gamma$
  - σ_{tot} = 55.5+4.0–3.8pb (SM prediction: 55.6±2.8pb)

Full Run-2 dataset

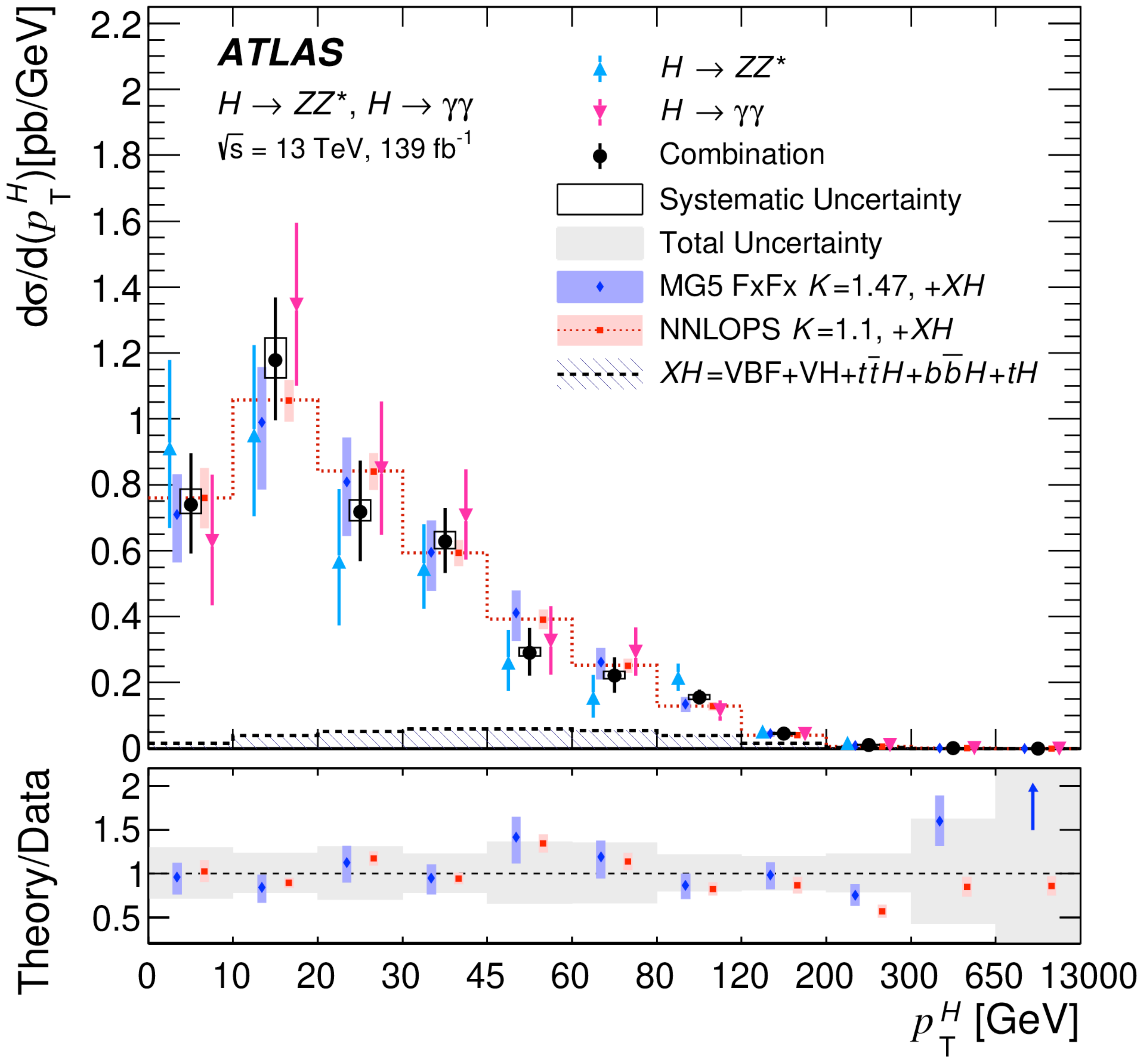

ATLAS-CONF-2022-067

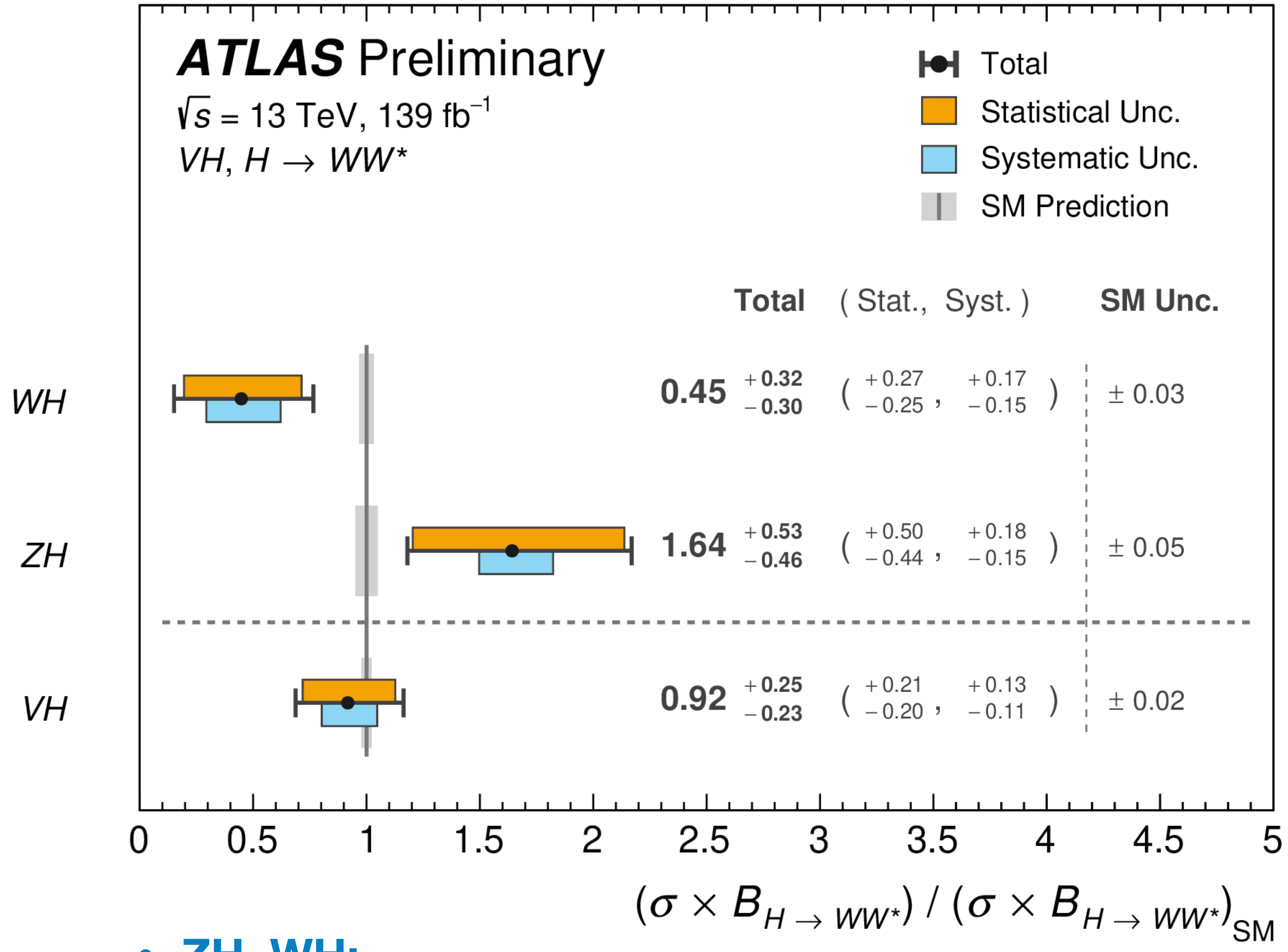

- **ZH, WH:**
  - $H \to WW$
    - *WH: 0.13+0.08–0.07(stat.) +0.05–0.04(syst.) pb*
    - *ZH:* 0.31+0.09–0.08(stat.)±0.03(syst.) pb

https://atlas.cern/updates/briefing/higgs-charm-beauty

Couplings

Full Run-2 dataset

HIGG-2021-12 arXiv:2201.11428

- **Search for H→cc**
- Combined with H→bb
- Ratio: $|\kappa_c/\kappa_b| < 4.5$ at 95% CL, smaller than the ratio of b- and c-quark masses
- For the first time:
  - Higgs-charm coupling determined to be weaker than the Higgs-bottom coupling at 95% CL
  - Higgs interacts differently with quarks of the 2nd and 3rd generation

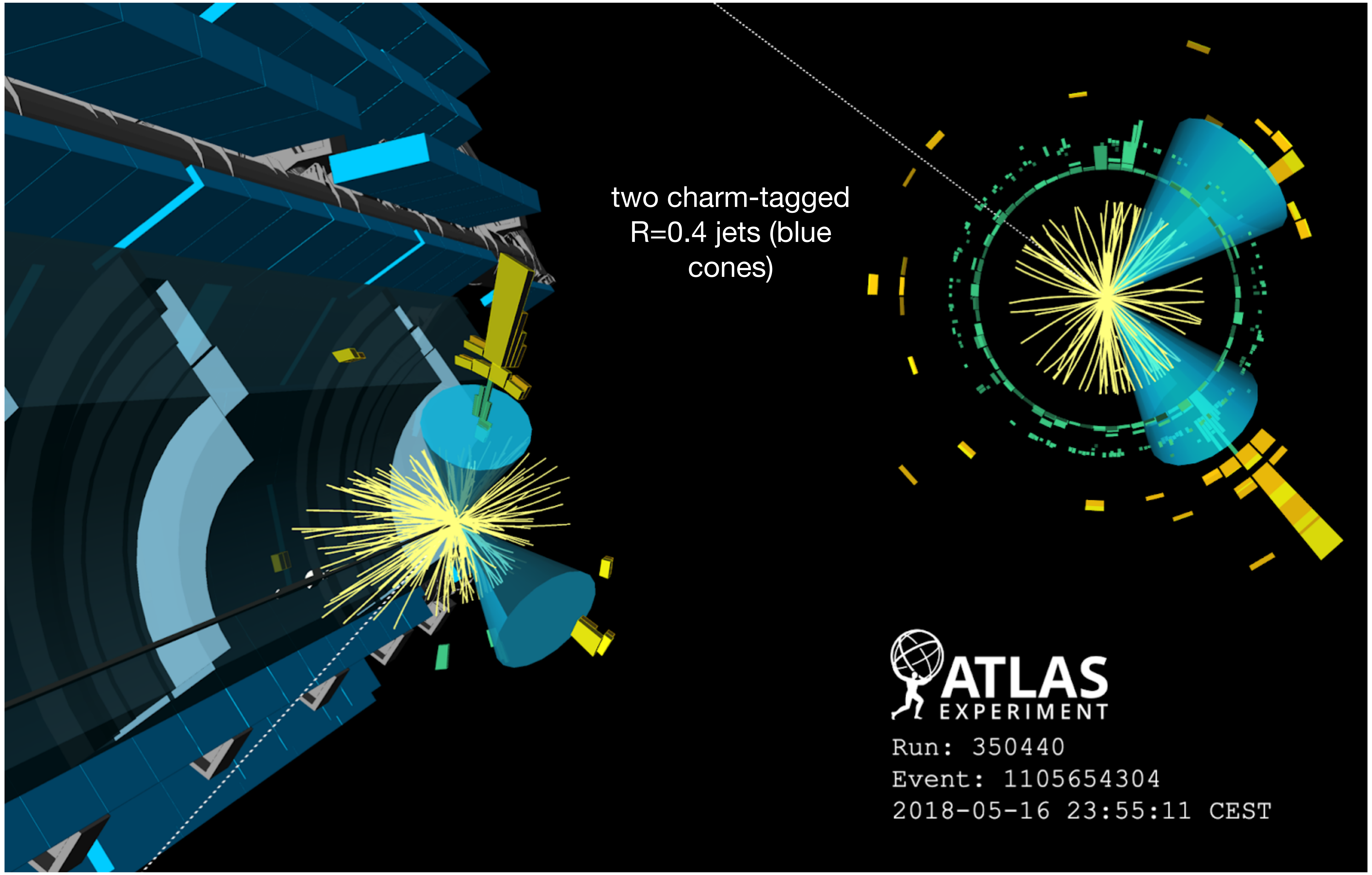

https://atlas.cern/updates/briefing/Higgs-tau-symmetry

CP properties

Full Run-2 dataset

- *H→ττ :* CP properties of the Hττ interaction from decay kinematics
  - *CP*-sensitive angular observables
  - Pure *CP*-odd hypothesis excluded at 3.4 σ

HIGG-2019-10

arXiv:2212.05833

- *H→γγ:* CP properties of the HVV interaction in VBF production
  - Optimal Observable method to probe the CP structure of interactions between Higgs boson and electroweak gauge bosons
    - event-based information from a multidimensional phase space combined into a single CP-sensitive observable
  - Most stringent constraints on CP violation in the coupling between Higgs and weak bosons

HIGG-2020-08

arXiv:2208.02338

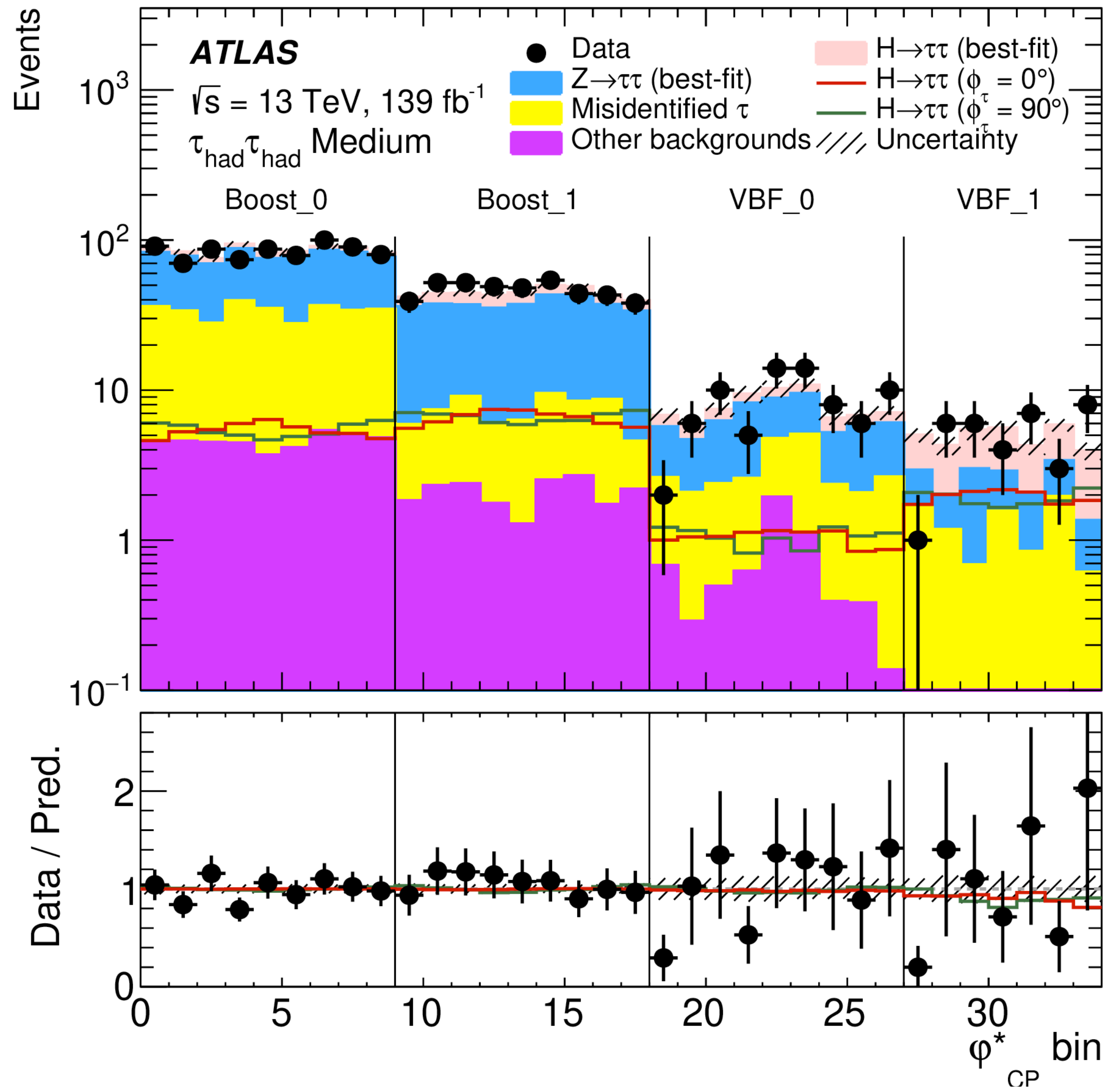

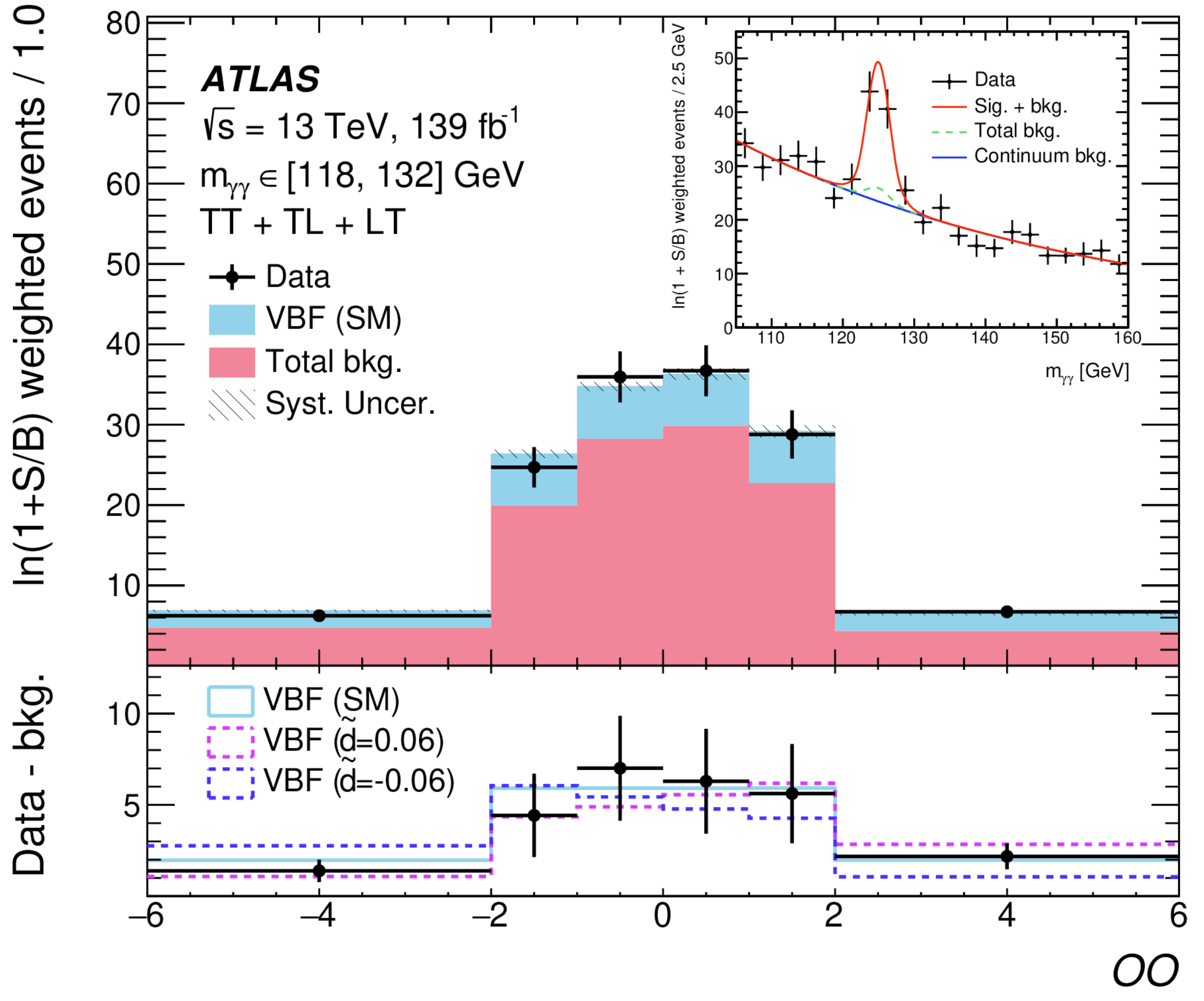

UPPSALA UNIVERSITET

Higgs self-interaction

HDBS-2022-03 arXiv:2211.01216

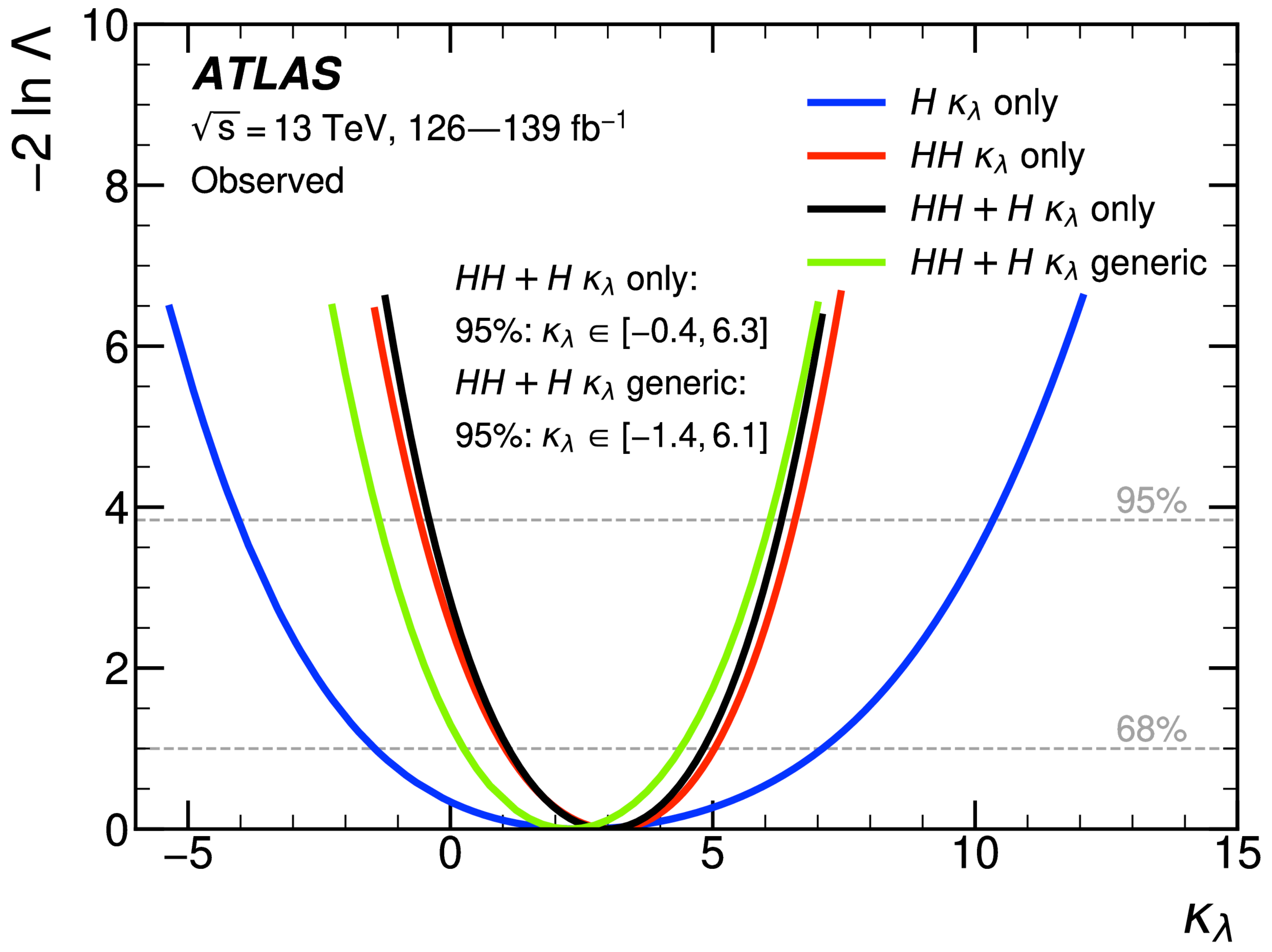

- Largely unconstrained
- Higgs boson self-coupling → direct insight into the structure of the Higgs potential (sensitive to BSM and electroweak phase transition)
- HH Very small cross-section: 32.7 fb (0.1% of single H)
- Negative interference between main contributions
- Full Run-2 dataset: H and HH
- HH: *bbbb*, *bbττ* and *bbγγ* decay channels
  - $-0.4 < \kappa_\lambda < 6.3$

The LHC is still a top factory

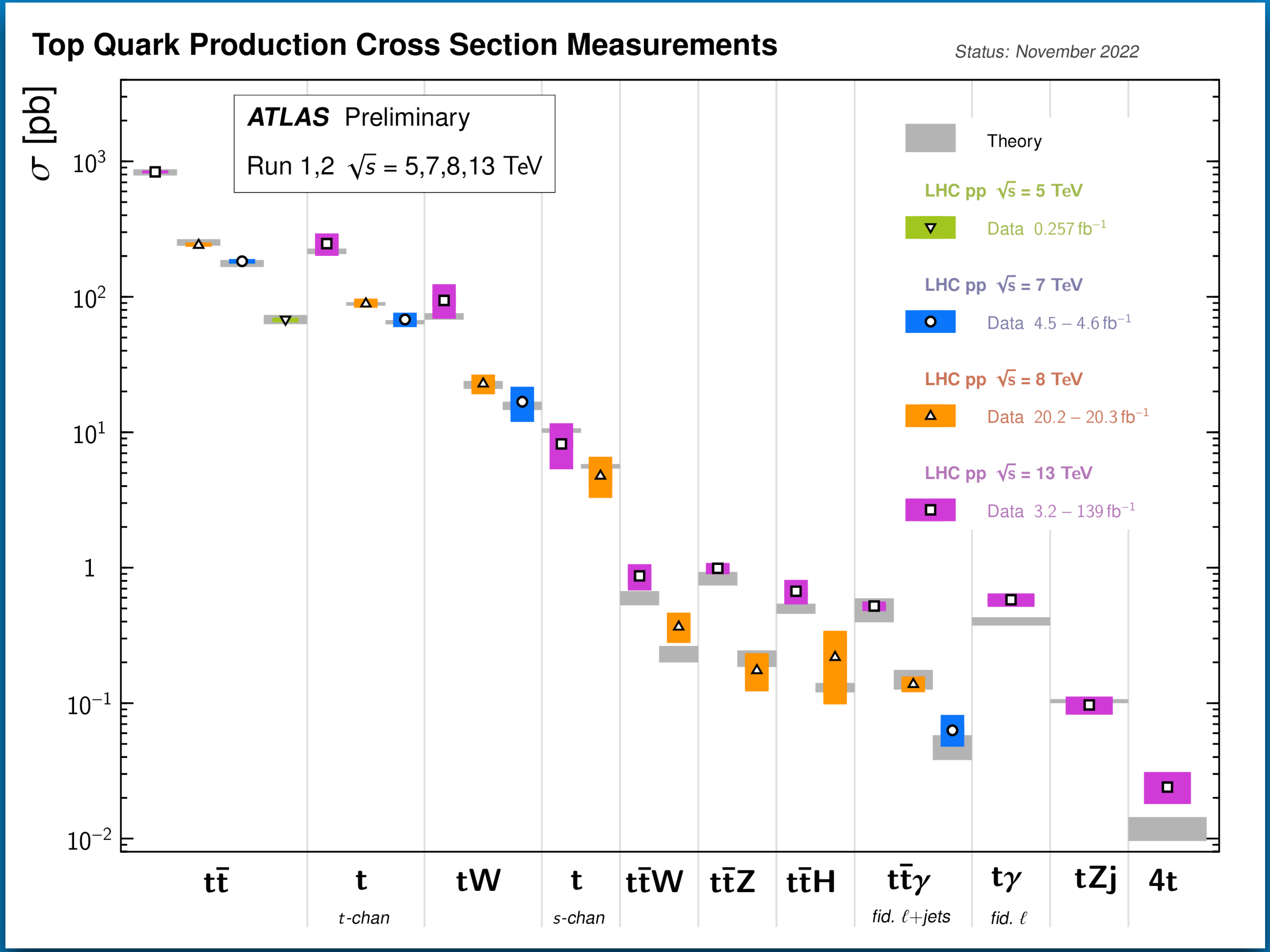

https://atlas.cern/Updates/Briefing/First-Run3-Measurements

ATLAS EXPERIMENT

The first ATLAS 13.6 TeV result

- 1.2fb^{-1} of 13.6 TeV data
- Measurement of the tt cross section

$$\sigma = 830 \pm 12(\text{stat.}) \pm 27(\text{syst.}) \pm 86(\text{lumi.})\ \text{pb}$$

$$\sigma_{theory} = 924^{+32}_{-40}\ (\text{scale+PDF})\ \text{pb}$$

- Measurement of the *tt/Z* boson production cross-section ratio

$$\boldsymbol{R = 0.400 \pm 0.006(\text{stat.}) \pm 0.017(\text{syst.}) \pm 0.005(\text{lumi.})}$$

$$R_{theory} = 0.423 \pm 0.015\ (\text{scale+PDF})$$

- Sensitivity to the gluon-to-quark PDF ratio
- Consistent with the Standard Model prediction using the PDF4LHC21 PDF set

ATLAS-CONF-2022-070

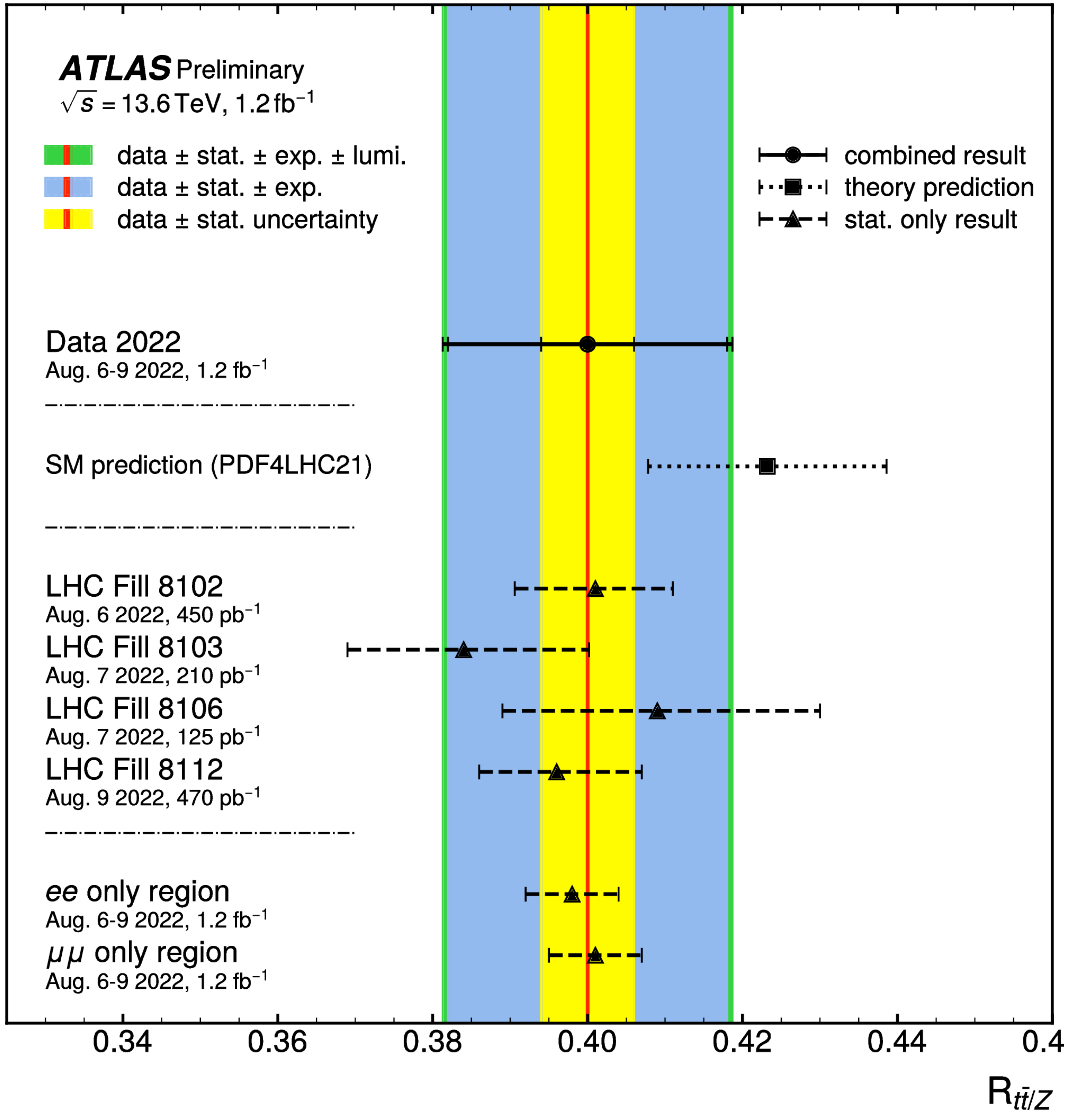

Cross sections

ATLAS-CONF-2022-061

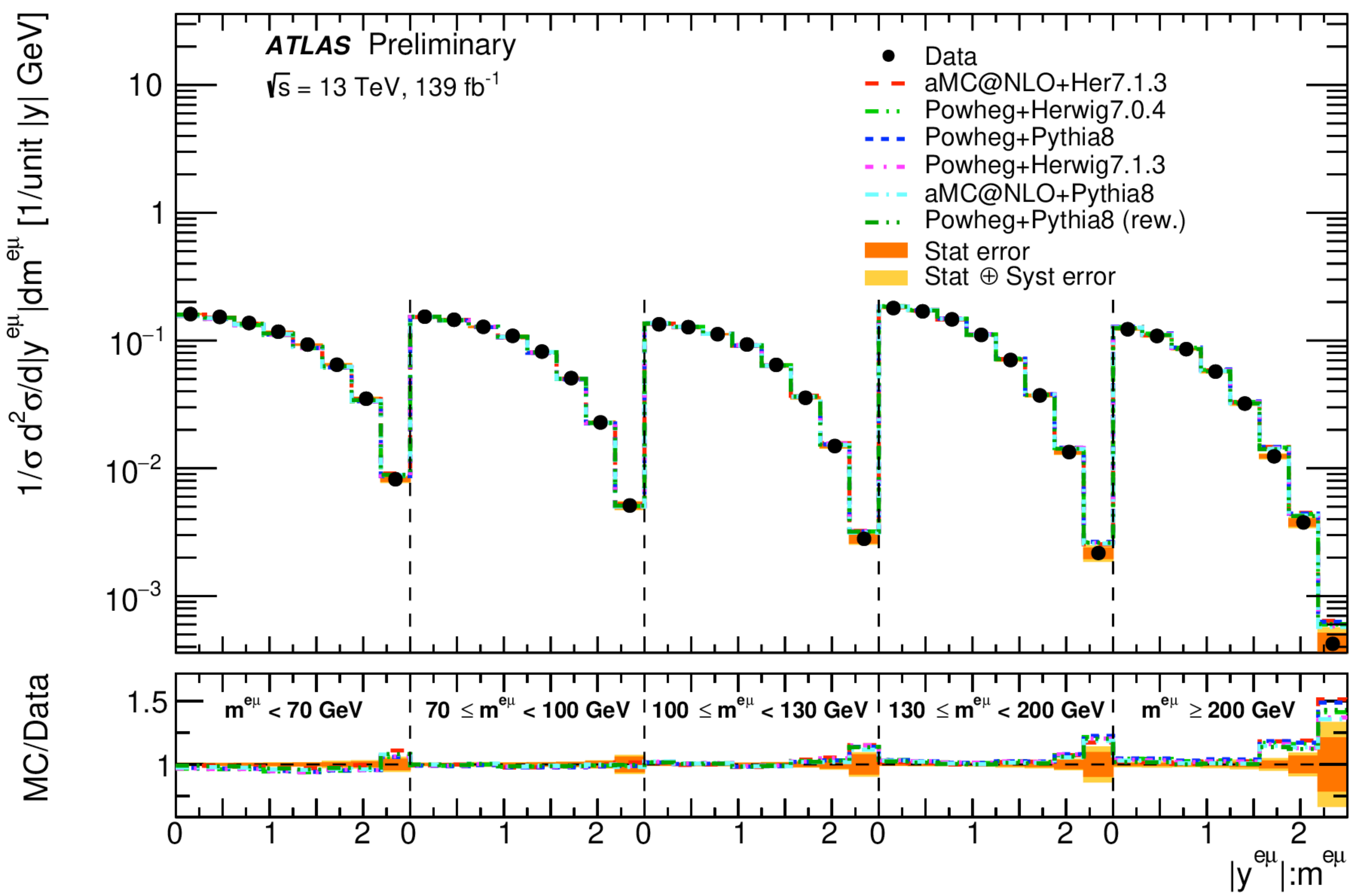

- **Differential and double differential distributions**
- Full Run-2, eμ final state
- Inclusive production cross section
  - σtt =836±1(stat)±12(syst)±16(lumi)±2(beam)pb

arXiv:2207.01354 TOPQ-2018-40

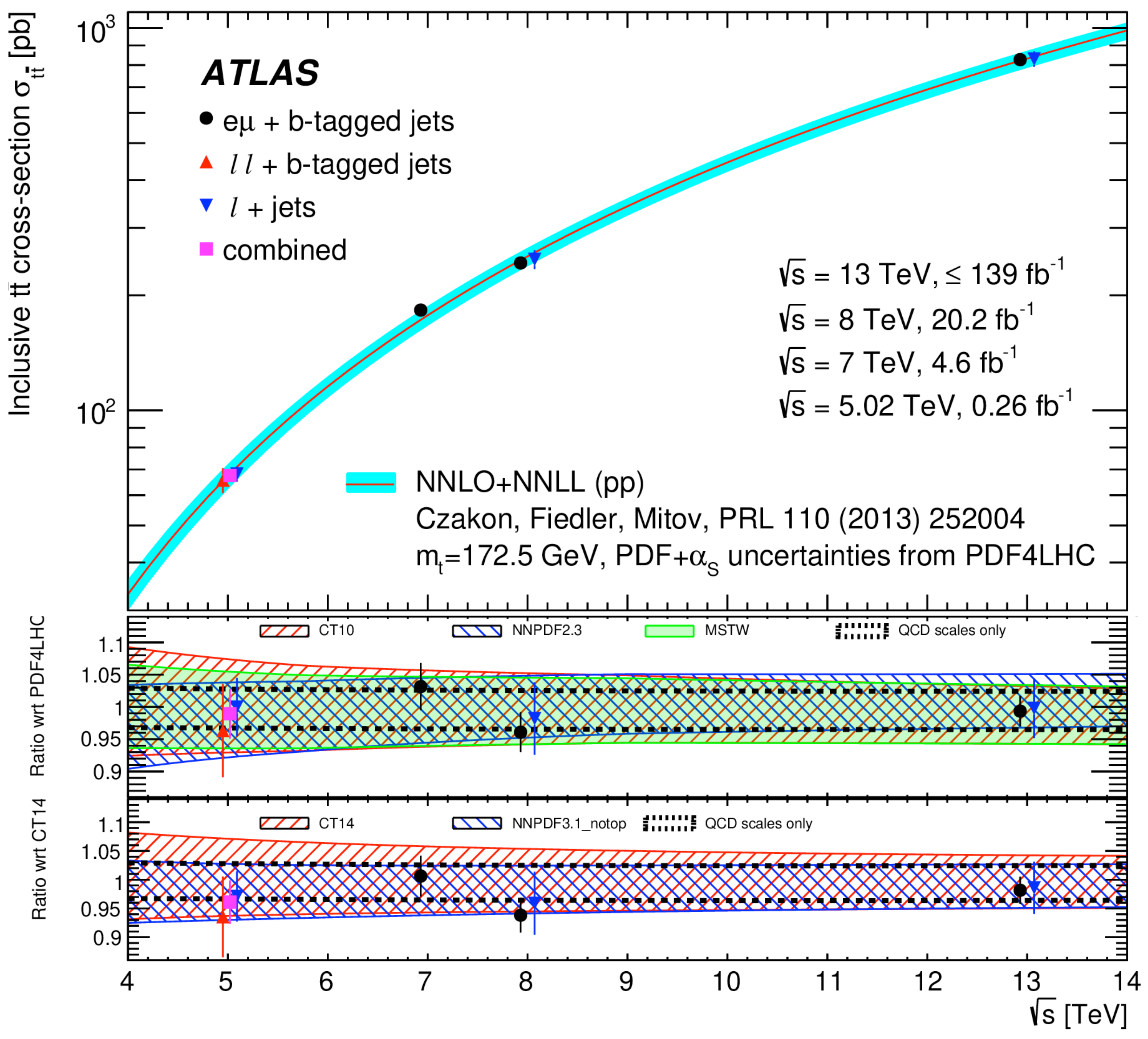

- **5.02 TeV**
- dilepton and single-lepton
- *σtt*=67.5±0.9(stat.)±2.3(syst.) ±1.1(lumi.)±0.2(beam) pb
- Relative uncertainty~3.9%
- In agreement with theoretical QCD calculations at NNLO
- Constrains proton parton distribution functions at large Bjorken-*x*

- **Run-1, 7 TeV *l*+jets**
- Multidimensional event classifier based on support vector machines
- *σtt*=168.5±0.7 (stat.)+6.2−5.9 (syst.)+3.4−3.2 (lumi.) pb

TOPQ-2017-08
arXiv:2212.00571

Mass, charge asymmetry

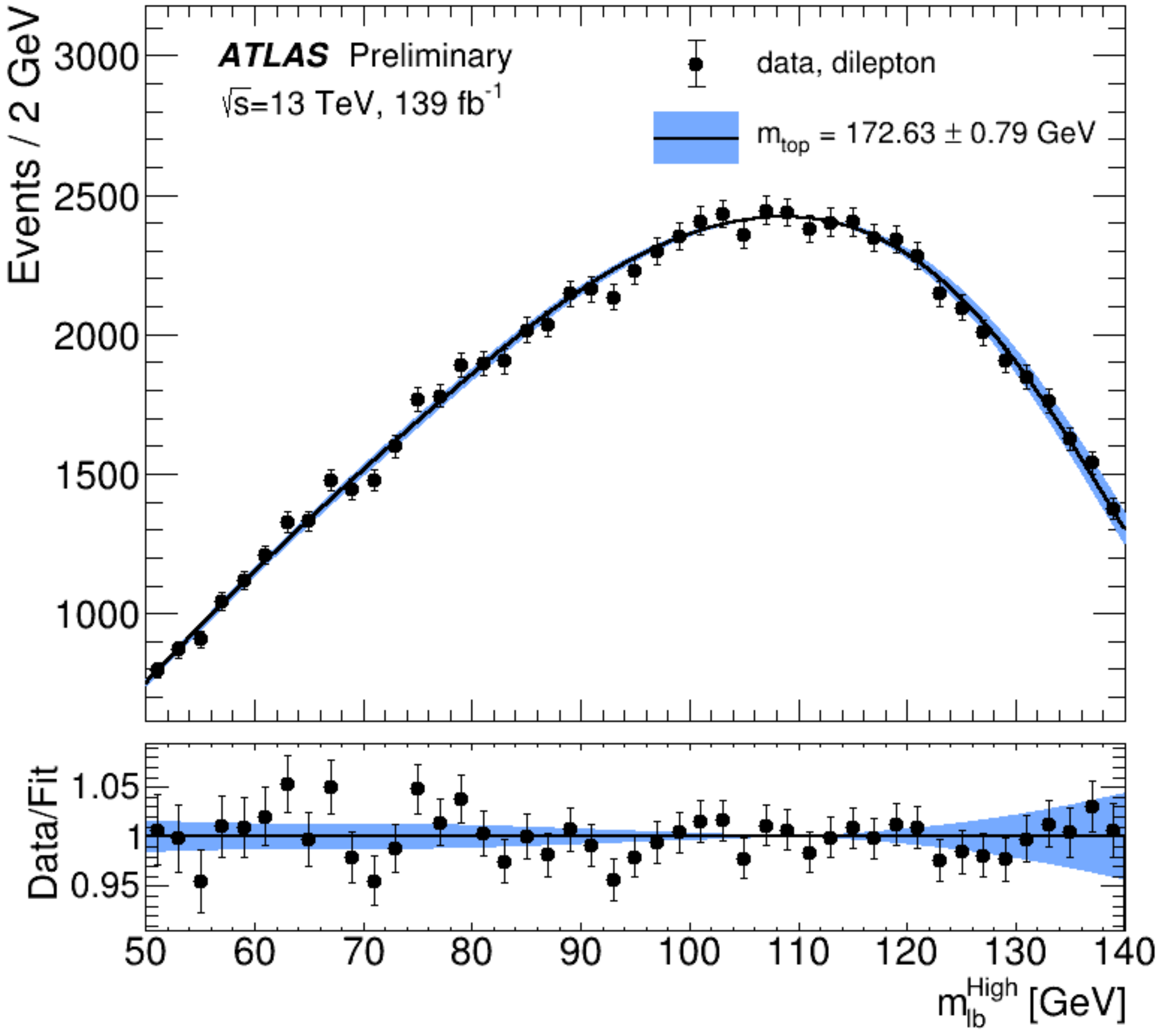

- Top quark mass in dilepton channel.
- Fit to invariant mass distribution of one lepton and a *b*-tagged jet
- **mtop=172.63±0.20(stat)±0.67(syst) ±0.37(recoil) GeV**

ATLAS-CONF-2022-058

TOPQ-2020-06 arXiv:2208.12095

- Inclusive and differential tt charge asymmetry
- single- and dilepton, resolved and boosted
- **Ac: 0.0068±0.0015 (4.7σ from 0)**
  - Ac: NLO effect
- Agreement at NNLO (Ac = 0.0064)
- EFT interpretation

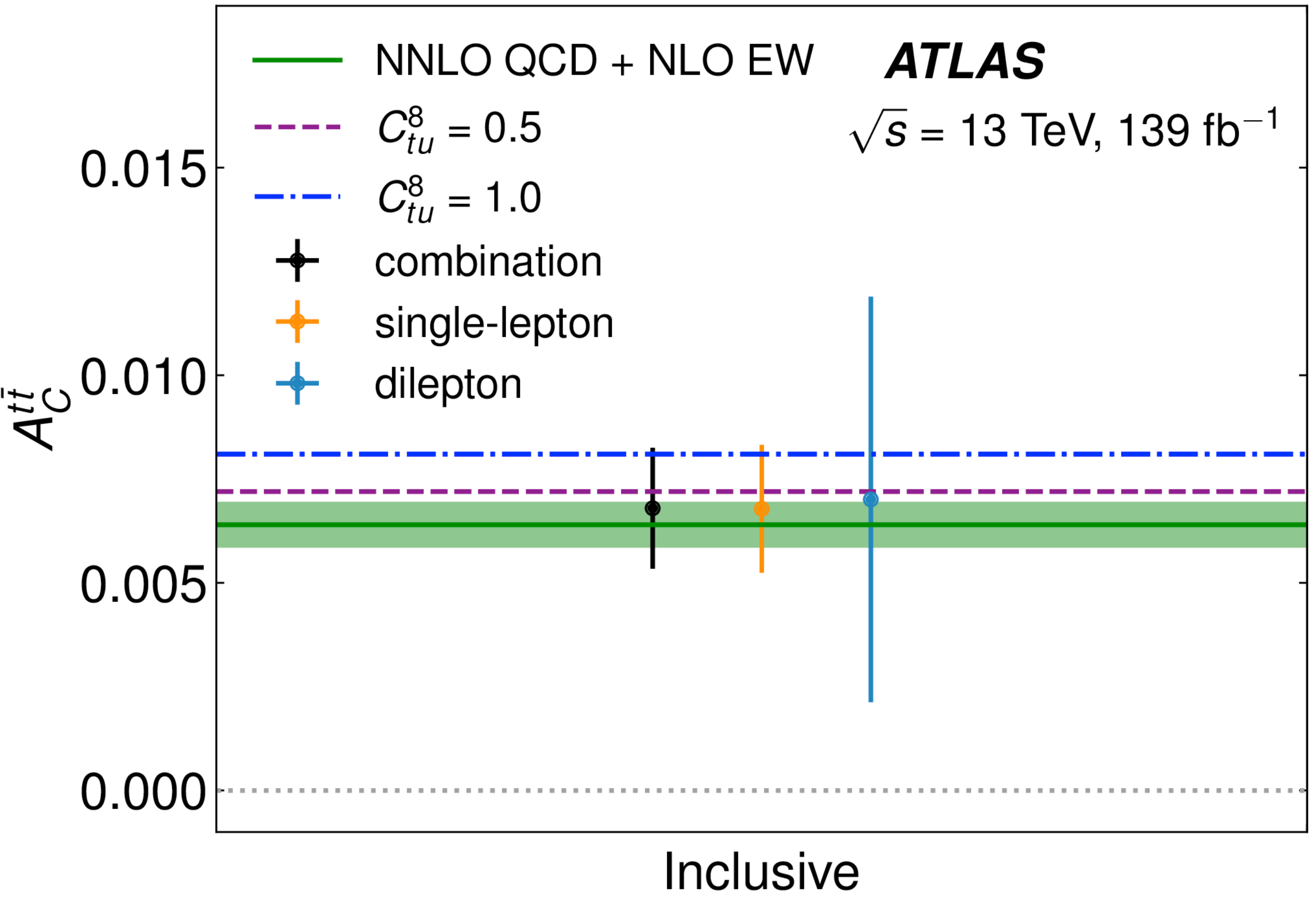

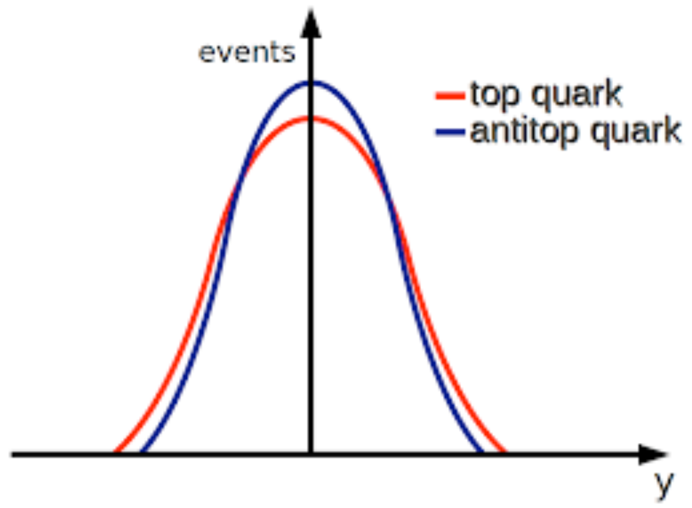

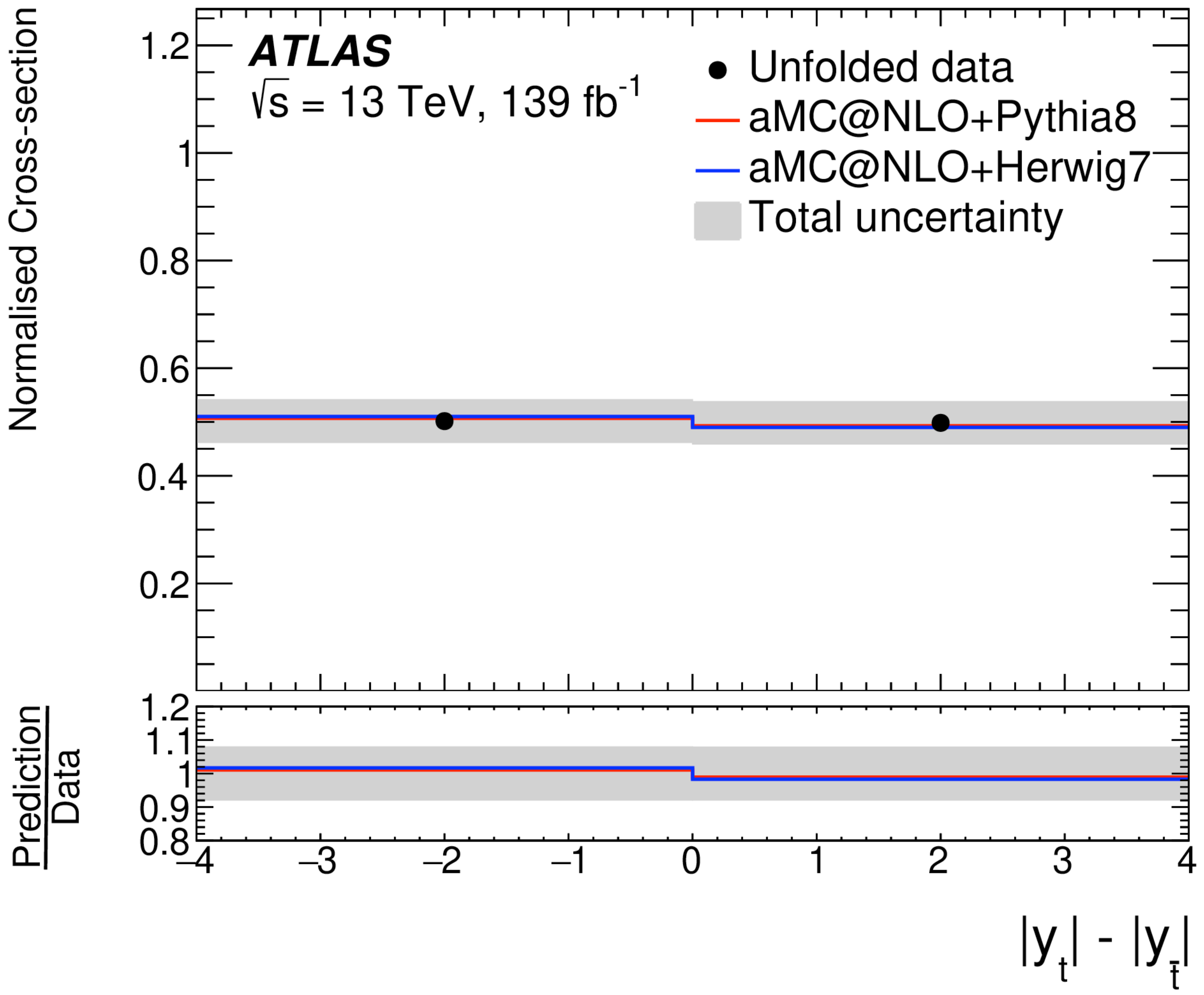

- tt+photon
- **Ac=−0.003±0.029**
- Statistically limited

TOPQ-2021-29

arXiv:2212.10552

Full Run-2 dataset

https://atlas.cern/updates/briefing/single-top-photon-observation

Rare single top processes

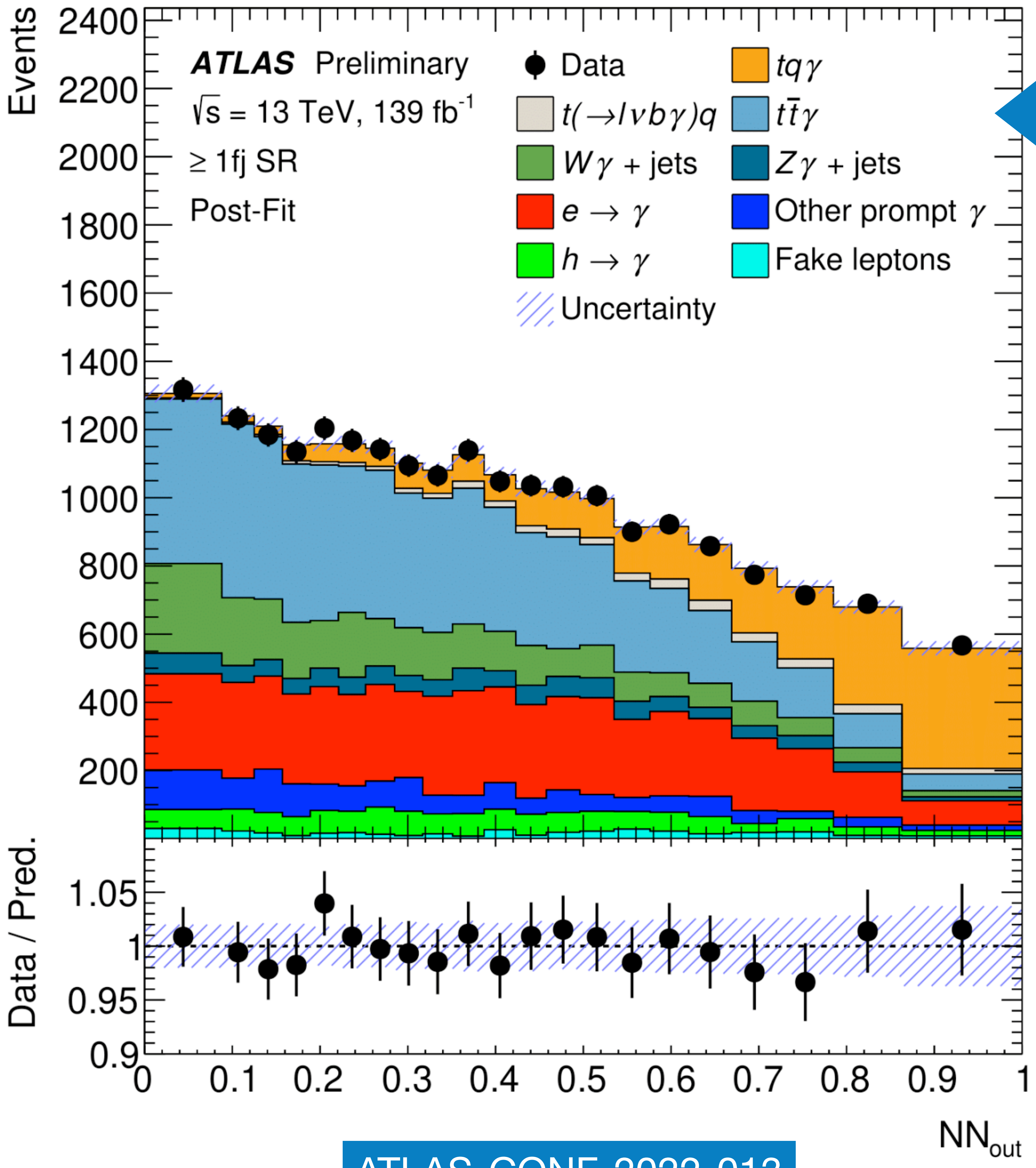

ATLAS-CONF-2022-013

- **First observation of single top quarks produced together with a photon**
  - fiducial cross section:
    - 580 ± 19 (stat.) ± 63 (syst.) (SM prediction: 406+25–32fb)
  - Probe of top-EW coupling (constrains BSM)
- **Evidence for s-channel at 13TeV: 3.3 (3.9) σ**
  - 7TeV was best at LHC, 13TeV is very difficult
  - σ = 8.2+3.5–2.9 pb
  - (σ_{SM} = 10.32+0.40–0.36 pb)

Full Run-2 dataset

TOPQ-2018-04

arXiv:2209.08990

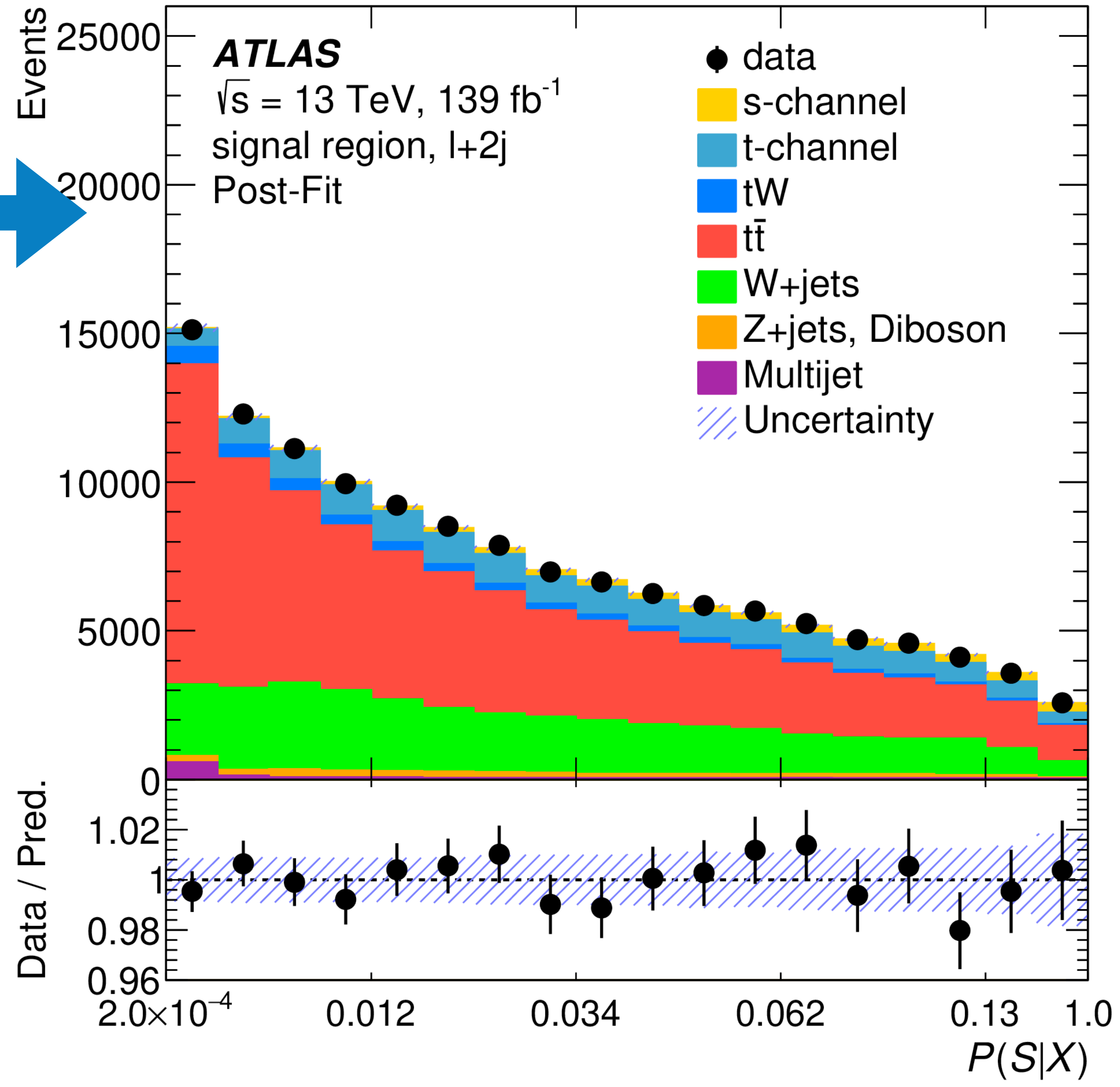

https://atlas.cern/updates/briefing/top-quark-currents

Flavour-changing neutral-currents

TOPQ-2019-19 arXiv:2205.02537

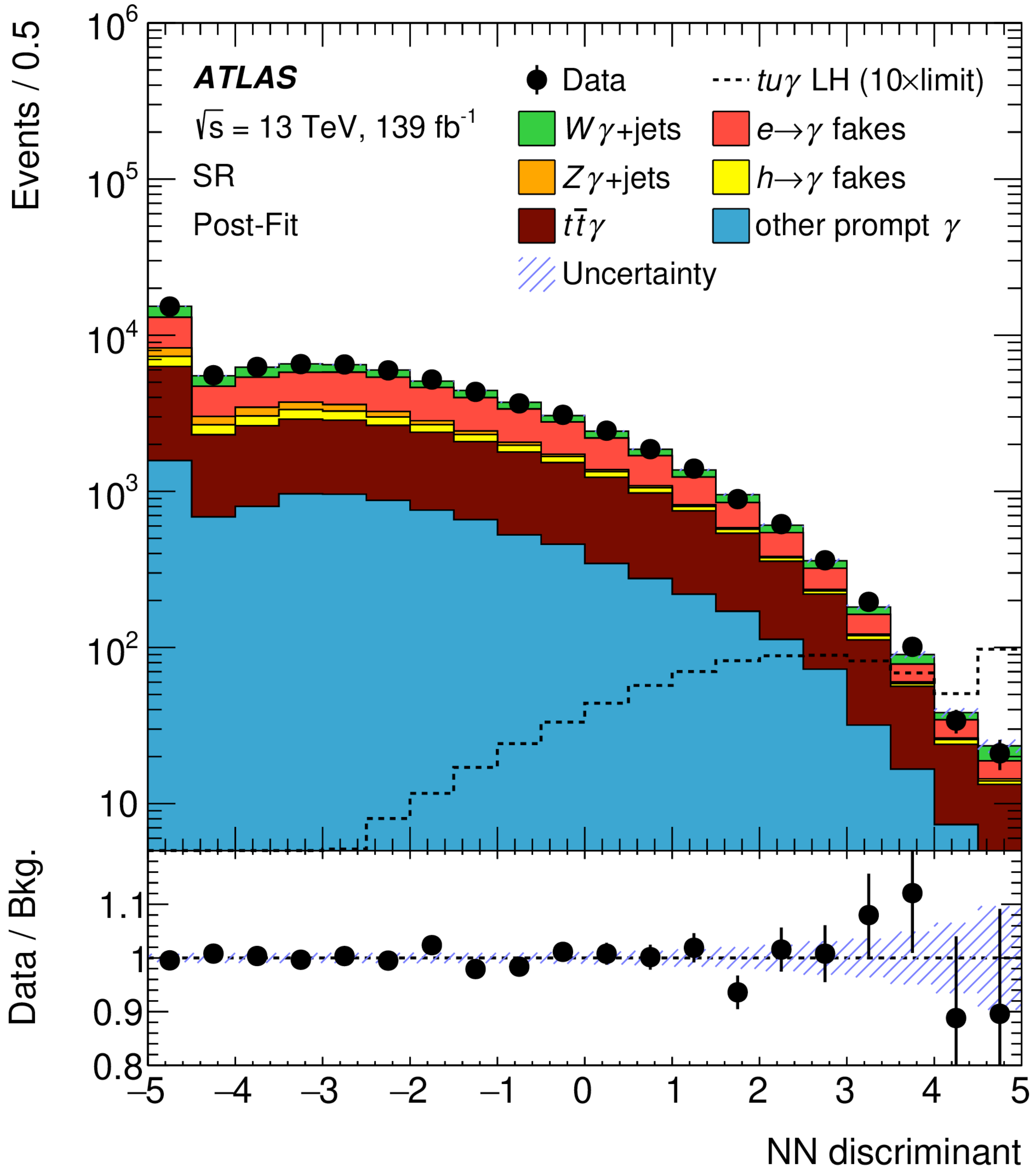

- **Single top + photon**
- FCNC in production and decay
- No significant excess is observed and 95% CL upper limits are placed

TOPQ-2019-17 arXiv:2208.11415

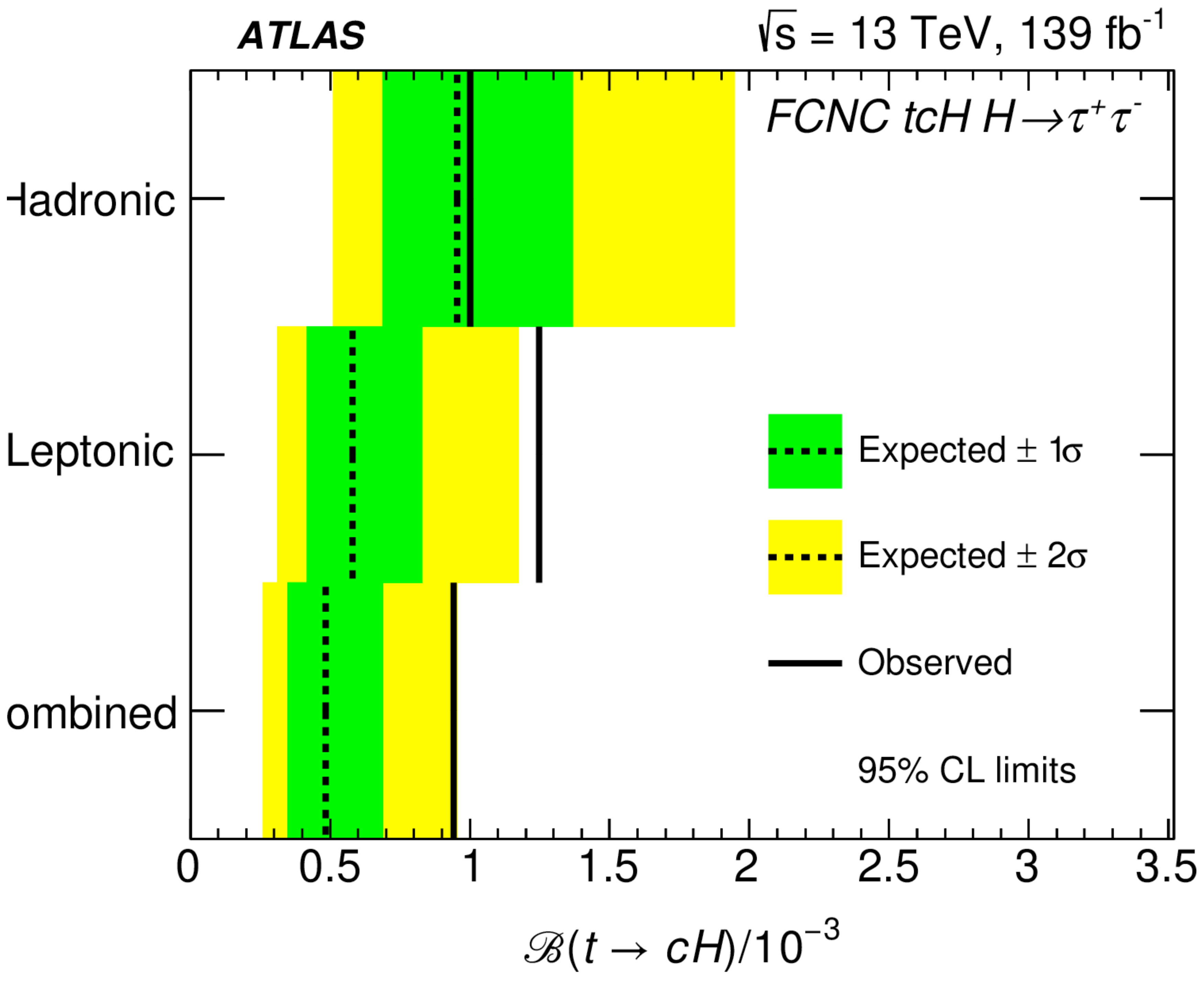

- **tqH: pp→tH and t→ qH**
- slight 2.3σ excess above the expected SM background, and 95% CL upper limits derived.
- Wilson coefficients

ATLAS-CONF-2022-027

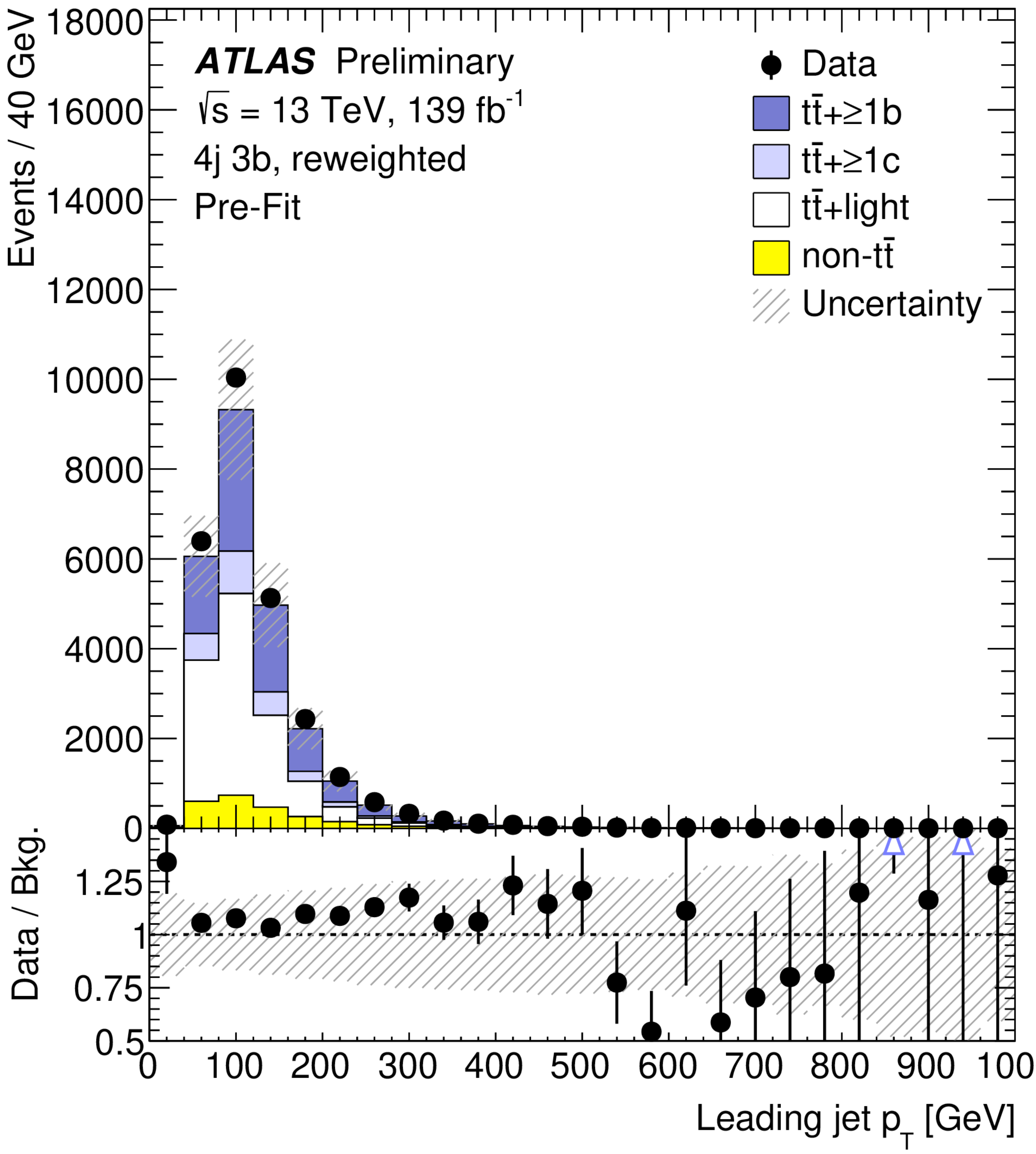

- **top → qX, with $X\to b\bar{b}$**
- 1 lepton channel, complex signatures
- Intermediate new particle search
- $\mathcal{B}(t\to uX)$ $\mathcal{B}(t\to cX)$ limits at 95% CL

Full Run-2 dataset

The SM legacy

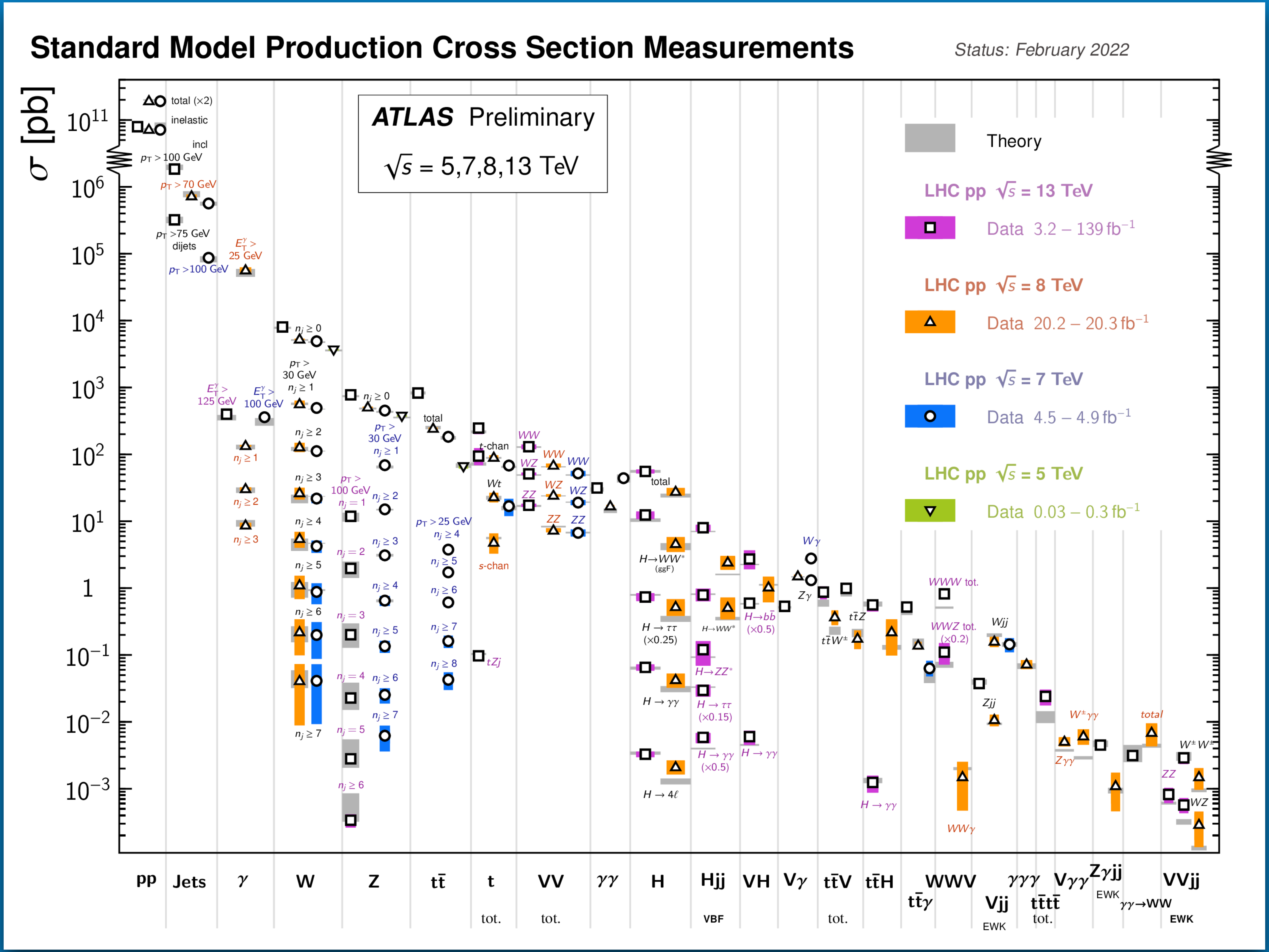

Joint polarisation of W and Z bosons

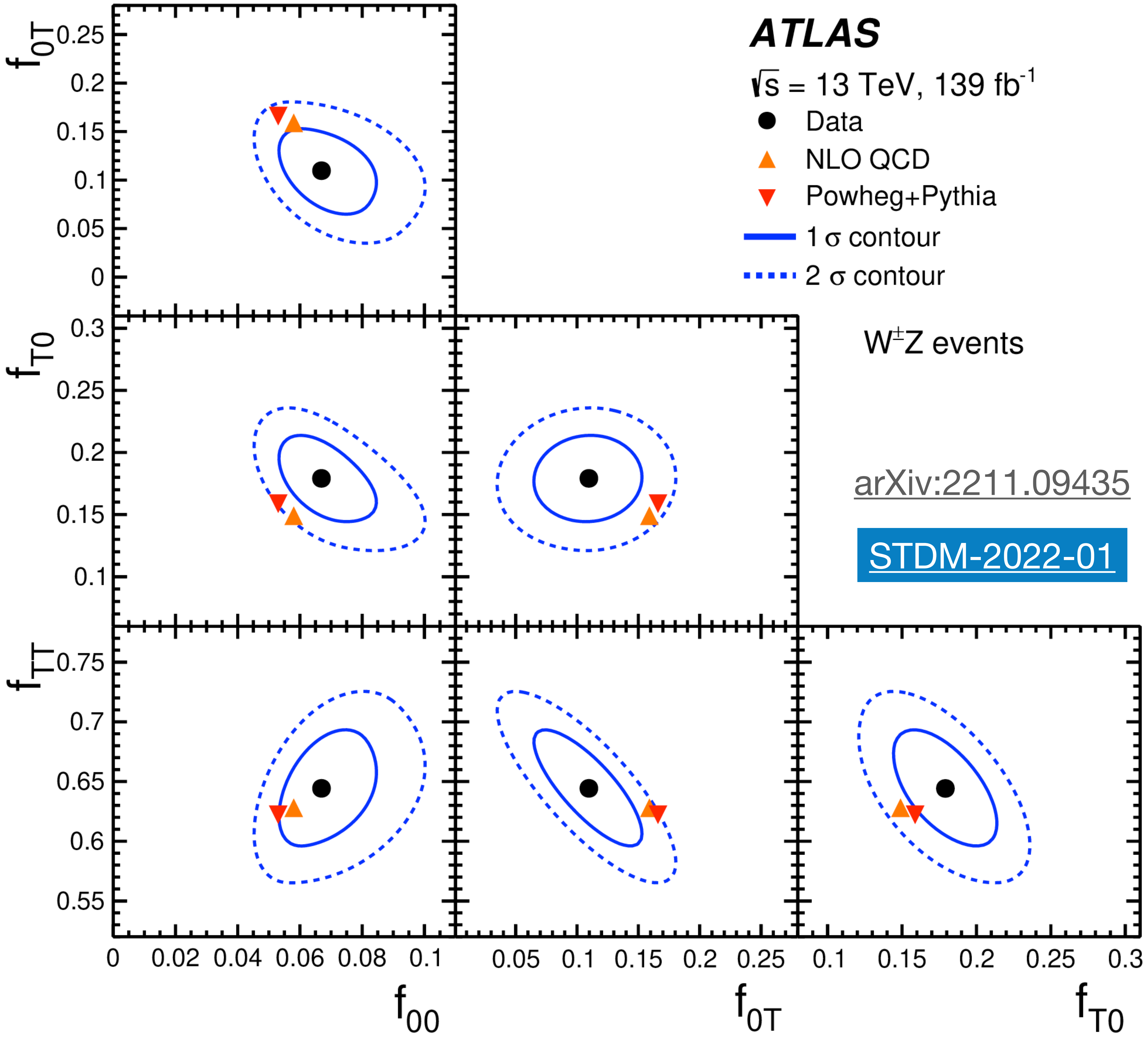

arXiv:2211.09435

STDM-2022-01

- **Full Run-2 dataset**
- 7.1 σ observation of events with both W and Z simultaneously longitudinal polarised
  - both bosons exhibiting a longitudinal polarisation are only ~7% of all WZ events
- WZ production in leptonic decays
- Joint and individual helicity fractions, inclusive and differential cross sections

Z+jets, Zγ+jets, *Zγγ*

STDM-2018-49 arXiv:2205.02597

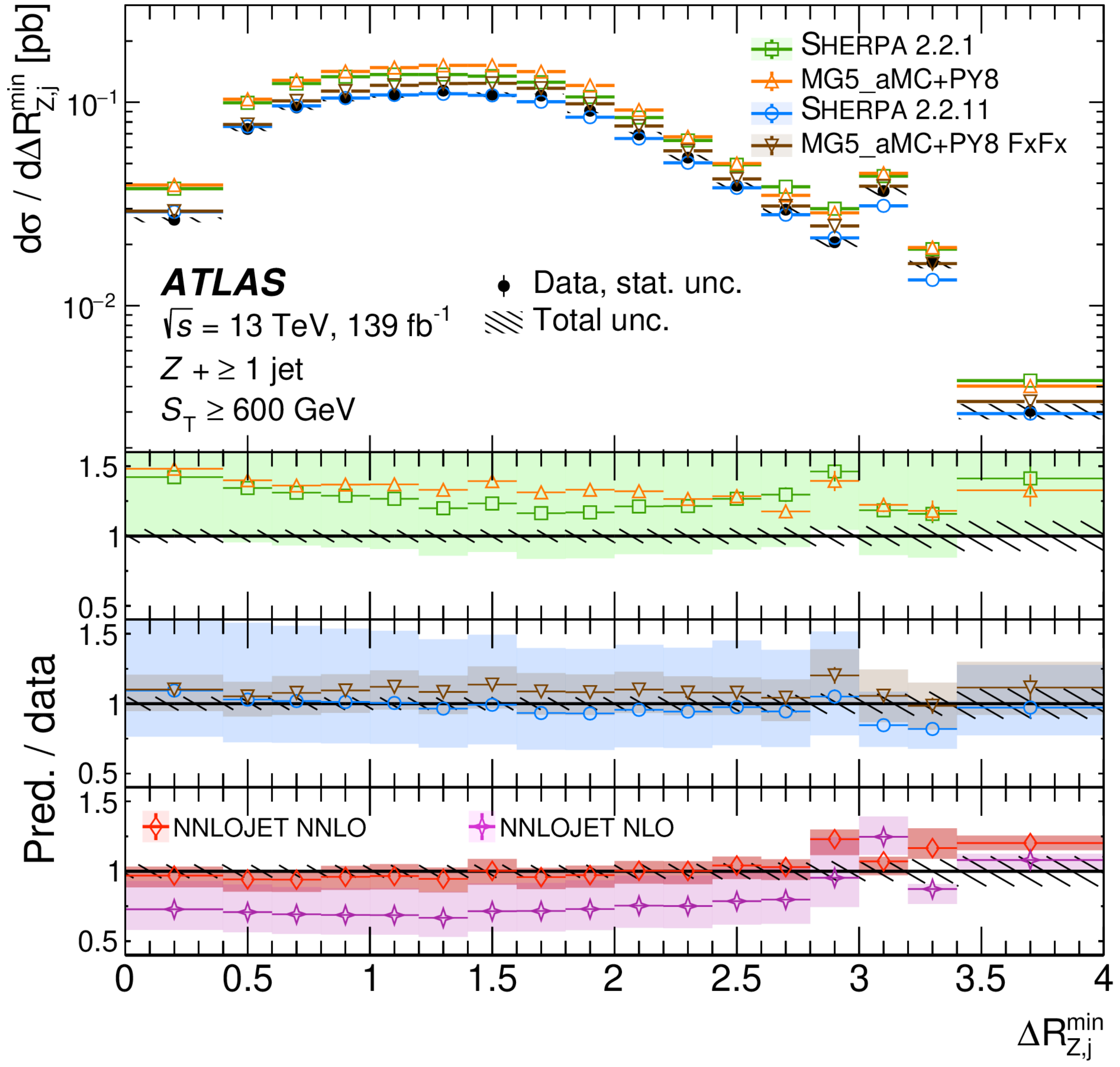

- ***Z*+ high-pT jets (*p*T≥100 GeV)**
- angular correlations between *Z* and closest jet
- Fiducial cross sections
- Agreement with NNLO predictions by NNLOjet, and NLO by MadGraph5_aMC@NLO and Sherpa

STDM-2020-14 arXiv:2212.07184

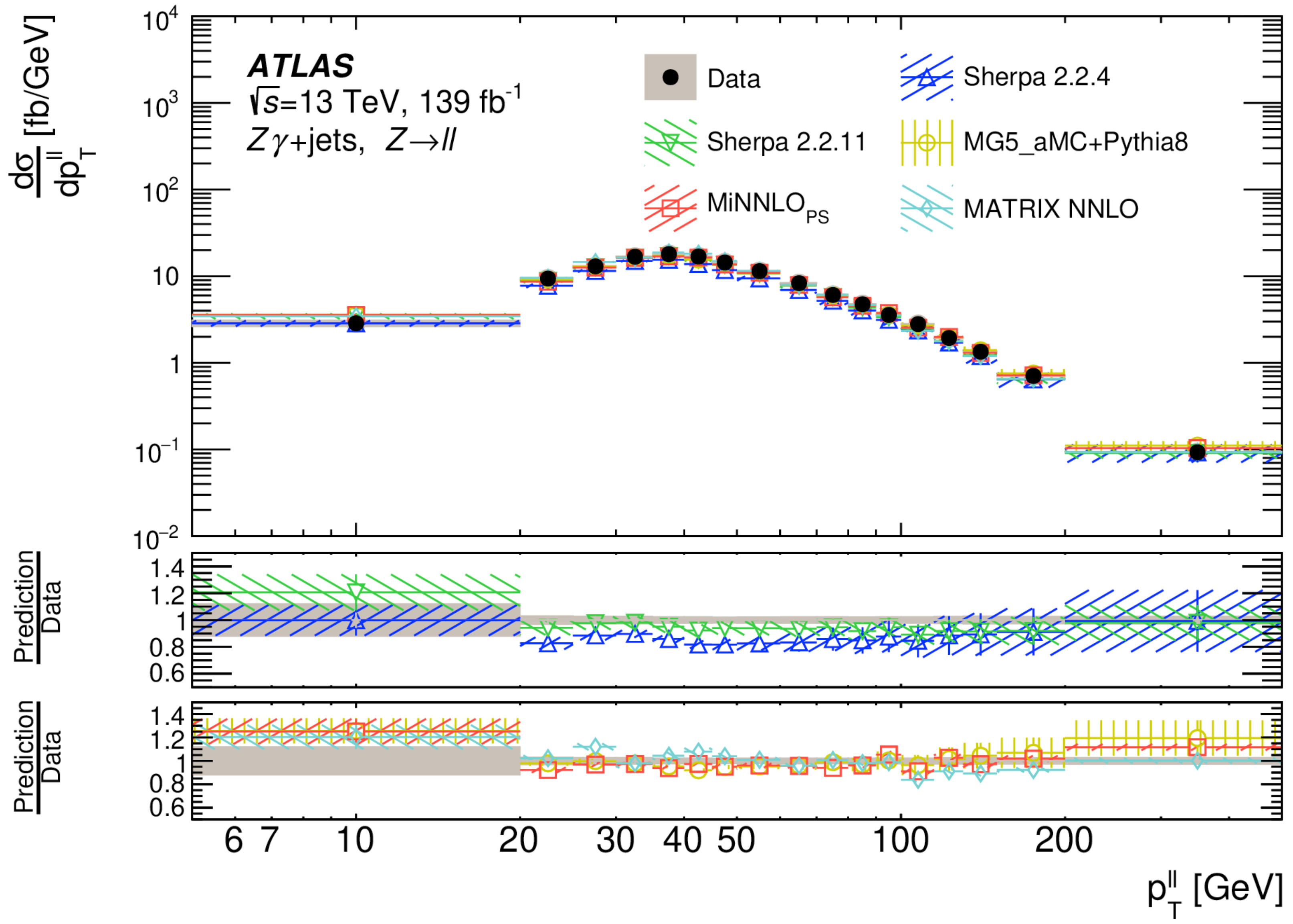

- **Zγ + jets**
- Differential cross-sections
- good agreement with predictions from MATRIX and MiNNLO PS, MadGraph5_aMC@NLO and Sherpa.

STDM-2021-09 arXiv:2211.14171

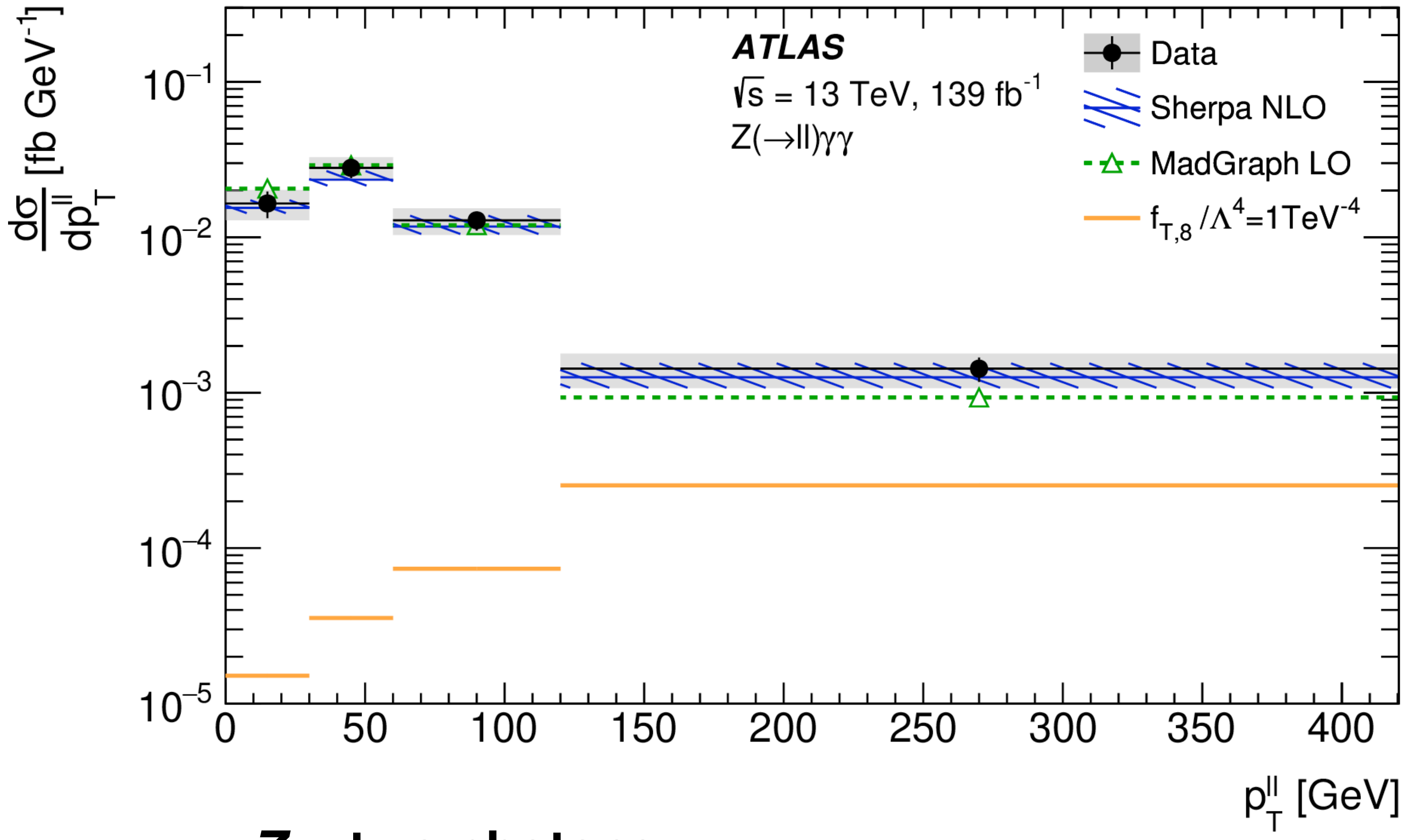

- ***Z* + two photons**
- cross-section measured with 12% precision
- differential cross-sections
- limits on the coupling strengths of dimension-8 operators in the framework of an EFT

Full Run-2 dataset

Forward results

- **Exclusive pion pair production *pp→pp π+π−***
  - 80 μb^{-1} of low-luminosity data at 7TeV
  - Pion pairs in the central detector, outgoing protons in the forward ATLAS ALFA detector system.
  - First use of proton tagging to measure an exclusive hadronic final state at the LHC

STDM-2017-07 arXiv:2212.00664

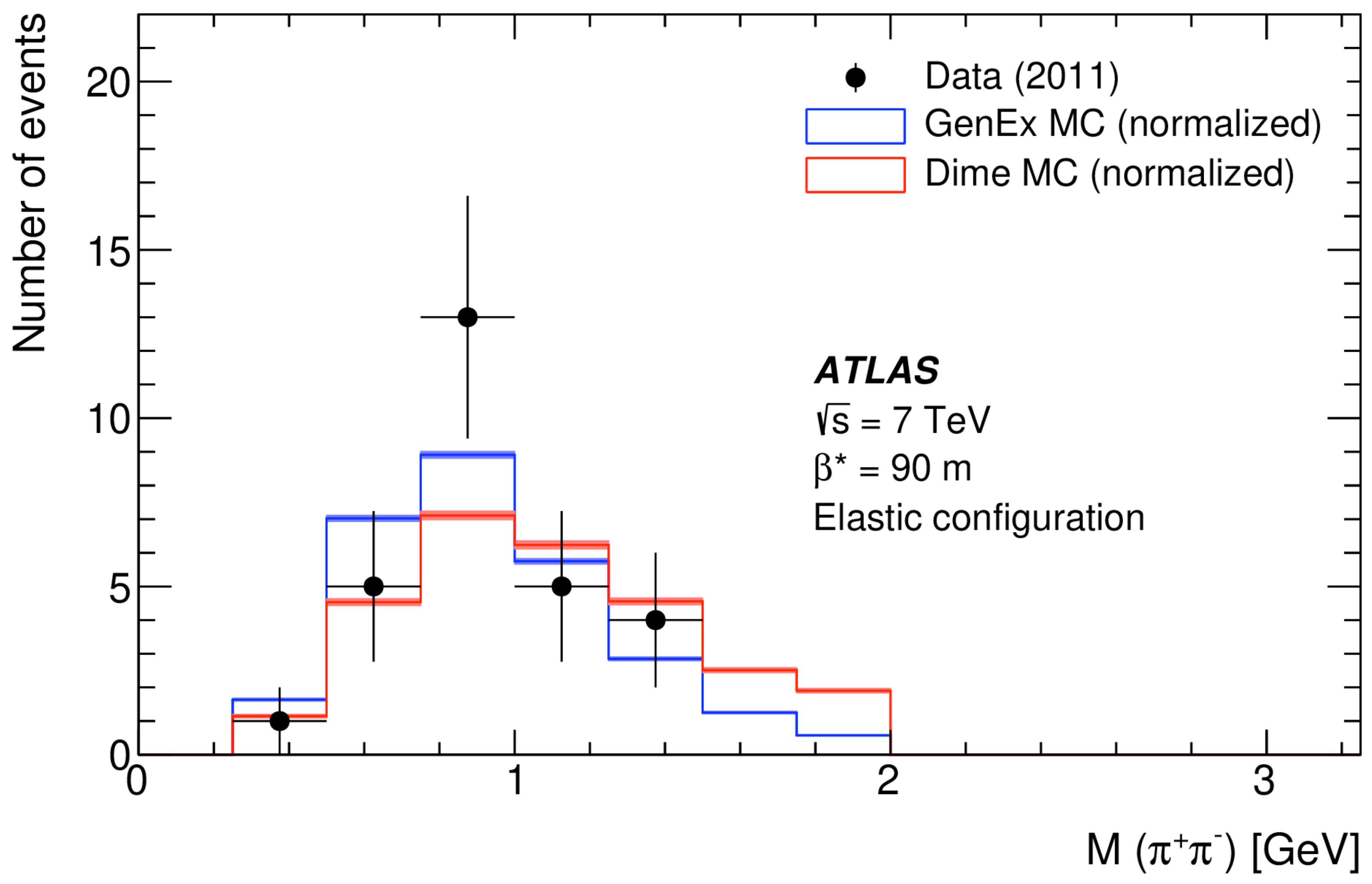

STDM-2018-08 arXiv:2207.12246

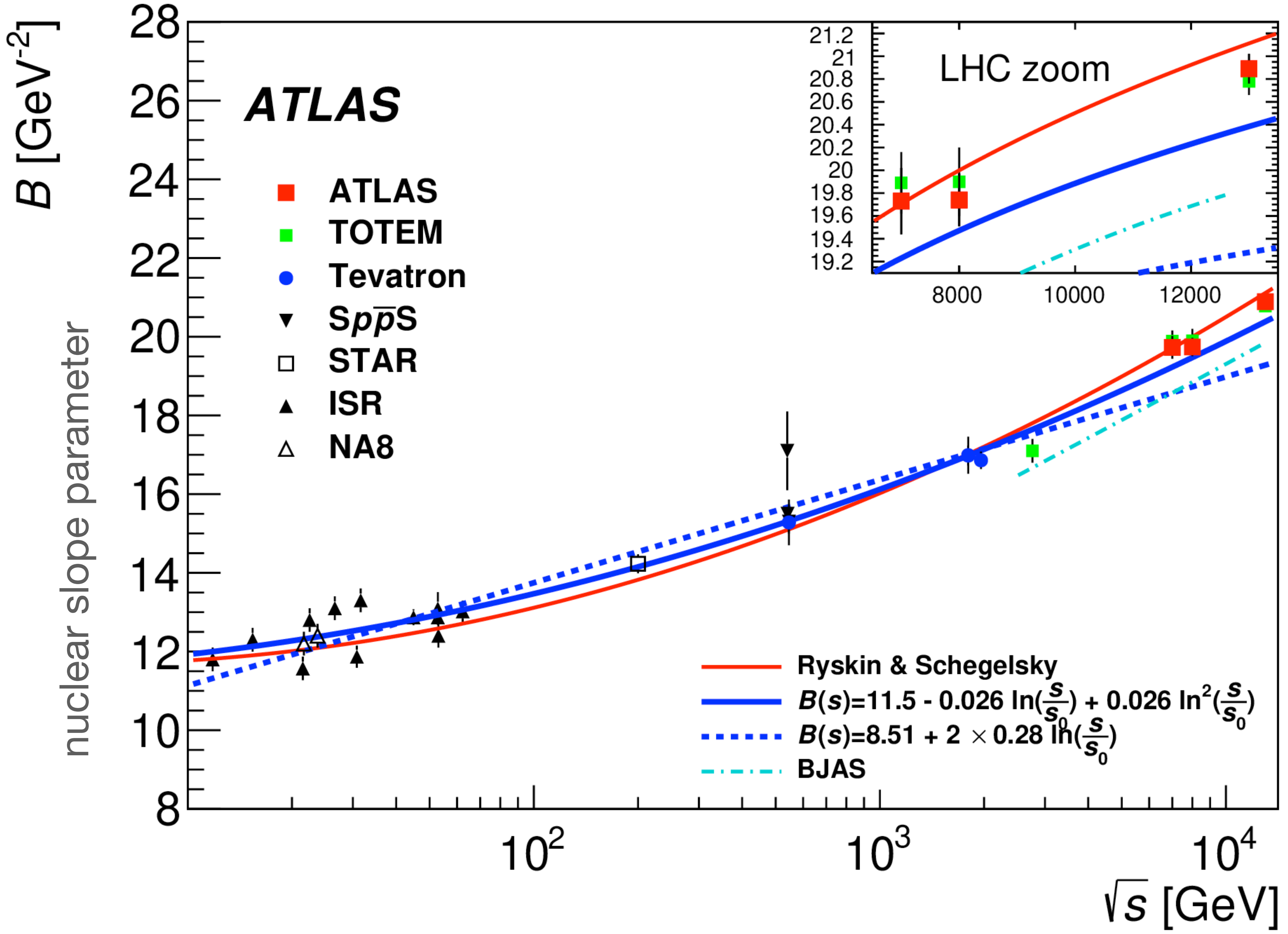

- **pp elastic-scattering measurements**
  - can help revealing complex dynamics that govern proton interactions
  - special LHC run with β⋆=2.5km, 13TeV, 340μb^{-1}
  - Total and differential elastic cross section

A discovery machine

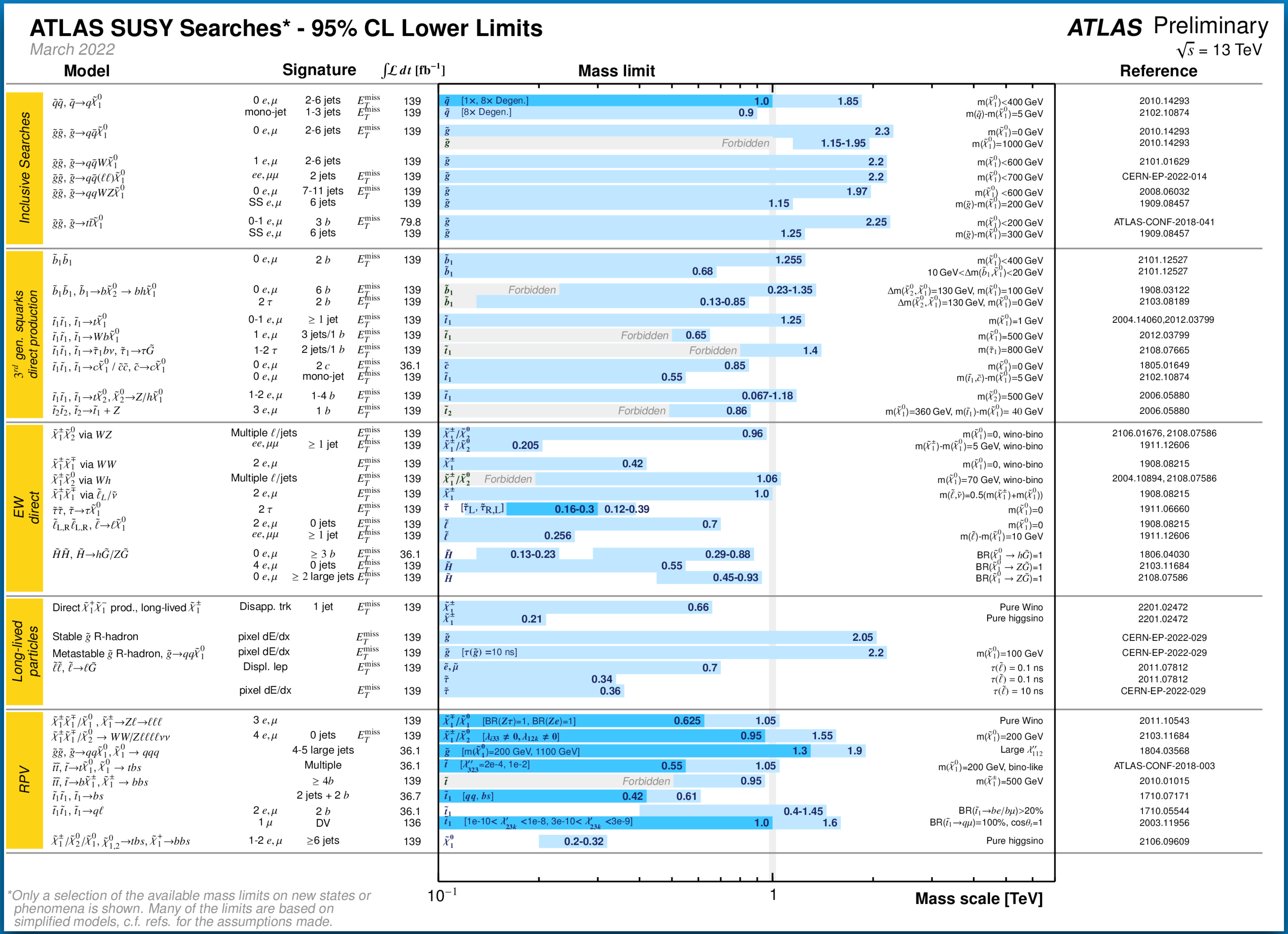

ATLAS SUSY Searches* - 95% CL Lower Limits

March 2022

ATLAS Preliminary

$\sqrt{s}$ = 13 TeV

	Model	Signature			$\int\mathcal{L}\,dt$ [fb^{-1}]	Mass limit		Reference
Inclusive Searches	$\tilde{q}\tilde{q}, \tilde{q}\to q\tilde{\chi}^0_1$	0 e,μ	2-6 jets	$E_T^{\rm miss}$	139	$\tilde{q}$ [1×, 8× Degen.] 1.0 1.85	m($\tilde{\chi}^0_1$)<400 GeV	2010.14293
		mono-jet	1-3 jets	$E_T^{\rm miss}$	139	$\tilde{q}$ [8× Degen.] 0.9	m($\tilde{q}$)-m($\tilde{\chi}^0_1$)=5 GeV	2102.10874
	$\tilde{g}\tilde{g}, \tilde{g}\to q\bar{q}\tilde{\chi}^0_1$	0 e,μ	2-6 jets	$E_T^{\rm miss}$	139	$\tilde{g}$ 2.3	m($\tilde{\chi}^0_1$)=0 GeV	2010.14293
						$\tilde{g}$ Forbidden 1.15-1.95	m($\tilde{\chi}^0_1$)=1000 GeV	2010.14293
	$\tilde{g}\tilde{g}, \tilde{g}\to q\bar{q}W\tilde{\chi}^0_1$	1 e,μ	2-6 jets		139	$\tilde{g}$ 2.2	m($\tilde{\chi}^0_1$)<600 GeV	2101.01629
	$\tilde{g}\tilde{g}, \tilde{g}\to q\bar{q}(\ell\ell)\tilde{\chi}^0_1$	$ee,\mu\mu$	2 jets	$E_T^{\rm miss}$	139	$\tilde{g}$ 2.2	m($\tilde{\chi}^0_1$)<700 GeV	CERN-EP-2022-014
	$\tilde{g}\tilde{g}, \tilde{g}\to qqWZ\tilde{\chi}^0_1$	0 e,μ	7-11 jets	$E_T^{\rm miss}$	139	$\tilde{g}$ 1.97	m($\tilde{\chi}^0_1$) <600 GeV	2008.06032
		SS e,μ	6 jets		139	$\tilde{g}$ 1.15	m($\tilde{g}$)-m($\tilde{\chi}^0_1$)=200 GeV	1909.08457
	$\tilde{g}\tilde{g}, \tilde{g}\to t\bar{t}\tilde{\chi}^0_1$	0-1 e,μ	3 b	$E_T^{\rm miss}$	79.8	$\tilde{g}$ 2.25	m($\tilde{\chi}^0_1$)<200 GeV	ATLAS-CONF-2018-041
		SS e,μ	6 jets		139	$\tilde{g}$ 1.25	m($\tilde{g}$)-m($\tilde{\chi}^0_1$)=300 GeV	1909.08457
3^{rd} gen. squarks direct production	$\tilde{b}_1\tilde{b}_1$	0 e,μ	2 b	$E_T^{\rm miss}$	139	$\tilde{b}_1$ 1.255	m($\tilde{\chi}^0_1$)<400 GeV	2101.12527
						$\tilde{b}_1$ 0.68	10 GeV<Δm($\tilde{b}_1$,$\tilde{\chi}^0_1$)<20 GeV	2101.12527
	$\tilde{b}_1\tilde{b}_1, \tilde{b}_1\to b\tilde{\chi}^0_2\to bh\tilde{\chi}^0_1$	0 e,μ	6 b	$E_T^{\rm miss}$	139	$\tilde{b}_1$ Forbidden 0.23-1.35	Δm($\tilde{\chi}^0_2$,$\tilde{\chi}^0_1$)=130 GeV, m($\tilde{\chi}^0_1$)=100 GeV	1908.03122
		2 τ	2 b	$E_T^{\rm miss}$	139	$\tilde{b}_1$ 0.13-0.85	Δm($\tilde{\chi}^0_2$,$\tilde{\chi}^0_1$)=130 GeV, m($\tilde{\chi}^0_1$)=0 GeV	2103.08189
	$\tilde{t}_1\tilde{t}_1, \tilde{t}_1\to t\tilde{\chi}^0_1$	0-1 e,μ	$\geq$ 1 jet	$E_T^{\rm miss}$	139	$\tilde{t}_1$ 1.25	m($\tilde{\chi}^0_1$)=1 GeV	2004.14060,2012.03799
	$\tilde{t}_1\tilde{t}_1, \tilde{t}_1\to Wb\tilde{\chi}^0_1$	1 e,μ	3 jets/1 b	$E_T^{\rm miss}$	139	$\tilde{t}_1$ Forbidden 0.65	m($\tilde{\chi}^0_1$)=500 GeV	2012.03799
	$\tilde{t}_1\tilde{t}_1, \tilde{t}_1\to\tilde{\tau}_1 b\nu, \tilde{\tau}_1\to\tau\tilde{G}$	1-2 τ	2 jets/1 b	$E_T^{\rm miss}$	139	$\tilde{t}_1$ Forbidden 1.4	m($\tilde{\tau}_1$)=800 GeV	2108.07665
	$\tilde{t}_1\tilde{t}_1, \tilde{t}_1\to c\tilde{\chi}^0_1$ / $\tilde{c}\tilde{c}, \tilde{c}\to c\tilde{\chi}^0_1$	0 e,μ	2 c	$E_T^{\rm miss}$	36.1	$\tilde{c}$ 0.85	m($\tilde{\chi}^0_1$)=0 GeV	1805.01649
		0 e,μ	mono-jet	$E_T^{\rm miss}$	139	$\tilde{t}_1$ 0.55	m($\tilde{t}_1$,$\tilde{c}$)-m($\tilde{\chi}^0_1$)=5 GeV	2102.10874
	$\tilde{t}_1\tilde{t}_1, \tilde{t}_1\to t\tilde{\chi}^0_2, \tilde{\chi}^0_2\to Z/h\tilde{\chi}^0_1$	1-2 e,μ	1-4 b	$E_T^{\rm miss}$	139	$\tilde{t}_1$ 0.067-1.18	m($\tilde{\chi}^0_2$)=500 GeV	2006.05880
	$\tilde{t}_2\tilde{t}_2, \tilde{t}_2\to\tilde{t}_1+Z$	3 e,μ	1 b	$E_T^{\rm miss}$	139	$\tilde{t}_2$ Forbidden 0.86	m($\tilde{\chi}^0_1$)=360 GeV, m($\tilde{t}_1$)-m($\tilde{\chi}^0_1$)= 40 GeV	2006.05880
EW direct	$\tilde{\chi}^\pm_1\tilde{\chi}^0_2$ via WZ	Multiple ℓ/jets		$E_T^{\rm miss}$	139	$\tilde{\chi}^\pm_1/\tilde{\chi}^0_2$ 0.96	m($\tilde{\chi}^0_1$)=0, wino-bino	2106.01676, 2108.07586
		$ee,\mu\mu$	$\geq$ 1 jet	$E_T^{\rm miss}$	139	$\tilde{\chi}^\pm_1/\tilde{\chi}^0_2$ 0.205	m($\tilde{\chi}^\pm_1$)-m($\tilde{\chi}^0_1$)=5 GeV, wino-bino	1911.12606
	$\tilde{\chi}^\pm_1\tilde{\chi}^\mp_1$ via WW	2 e,μ		$E_T^{\rm miss}$	139	$\tilde{\chi}^\pm_1$ 0.42	m($\tilde{\chi}^0_1$)=0, wino-bino	1908.08215
	$\tilde{\chi}^\pm_1\tilde{\chi}^0_2$ via Wh	Multiple ℓ/jets		$E_T^{\rm miss}$	139	$\tilde{\chi}^\pm_1/\tilde{\chi}^0_2$ Forbidden 1.06	m($\tilde{\chi}^0_1$)=70 GeV, wino-bino	2004.10894, 2108.07586
	$\tilde{\chi}^\pm_1\tilde{\chi}^\mp_1$ via $\tilde{\ell}_L/\tilde{\nu}$	2 e,μ		$E_T^{\rm miss}$	139	$\tilde{\chi}^\pm_1$ 1.0	m($\tilde{\ell}$,$\tilde{\nu}$)=0.5(m($\tilde{\chi}^\pm_1$)+m($\tilde{\chi}^0_1$))	1908.08215
	$\tilde{\tau}\tilde{\tau}, \tilde{\tau}\to\tau\tilde{\chi}^0_1$	2 τ		$E_T^{\rm miss}$	139	$\tilde{\tau}$ [$\tilde{\tau}_{\rm L}$, $\tilde{\tau}_{\rm R,L}$] 0.16-0.3 0.12-0.39	m($\tilde{\chi}^0_1$)=0	1911.06660
	$\tilde{\ell}_{\rm L,R}\tilde{\ell}_{\rm L,R}, \tilde{\ell}\to\ell\tilde{\chi}^0_1$	2 e,μ	0 jets	$E_T^{\rm miss}$	139	$\tilde{\ell}$ 0.7	m($\tilde{\chi}^0_1$)=0	1908.08215
		$ee,\mu\mu$	$\geq$ 1 jet	$E_T^{\rm miss}$	139	$\tilde{\ell}$ 0.256	m($\tilde{\ell}$)-m($\tilde{\chi}^0_1$)=10 GeV	1911.12606
	$\tilde{H}\tilde{H}, \tilde{H}\to h\tilde{G}/Z\tilde{G}$	0 e,μ	$\geq$ 3 b	$E_T^{\rm miss}$	36.1	$\tilde{H}$ 0.13-0.23 0.29-0.88	BR($\tilde{\chi}^0_1\to h\tilde{G}$)=1	1806.04030
		4 e,μ	0 jets	$E_T^{\rm miss}$	139	$\tilde{H}$ 0.55	BR($\tilde{\chi}^0_1\to Z\tilde{G}$)=1	2103.11684
		0 e,μ	$\geq$ 2 large jets	$E_T^{\rm miss}$	139	$\tilde{H}$ 0.45-0.93	BR($\tilde{\chi}^0_1\to Z\tilde{G}$)=1	2108.07586
Long-lived particles	Direct $\tilde{\chi}^+_1\tilde{\chi}^-_1$ prod., long-lived $\tilde{\chi}^\pm_1$	Disapp. trk	1 jet	$E_T^{\rm miss}$	139	$\tilde{\chi}^\pm_1$ 0.66	Pure Wino	2201.02472
						$\tilde{\chi}^\pm_1$ 0.21	Pure higgsino	2201.02472
	Stable $\tilde{g}$ R-hadron	pixel dE/dx		$E_T^{\rm miss}$	139	$\tilde{g}$ 2.05		CERN-EP-2022-029
	Metastable $\tilde{g}$ R-hadron, $\tilde{g}\to qq\tilde{\chi}^0_1$	pixel dE/dx		$E_T^{\rm miss}$	139	$\tilde{g}$ [$\tau(\tilde{g})$ =10 ns] 2.2	m($\tilde{\chi}^0_1$)=100 GeV	CERN-EP-2022-029
	$\tilde{\ell}\tilde{\ell}, \tilde{\ell}\to\ell\tilde{G}$	Displ. lep		$E_T^{\rm miss}$	139	$\tilde{e},\tilde{\mu}$ 0.7	$\tau(\tilde{\ell})$ = 0.1 ns	2011.07812
						$\tilde{\tau}$ 0.34	$\tau(\tilde{\ell})$ = 0.1 ns	2011.07812
		pixel dE/dx		$E_T^{\rm miss}$	139	$\tilde{\tau}$ 0.36	$\tau(\tilde{\ell})$ = 10 ns	CERN-EP-2022-029
RPV	$\tilde{\chi}^\pm_1\tilde{\chi}^\mp_1/\tilde{\chi}^0_1$, $\tilde{\chi}^\pm_1\to Z\ell\to\ell\ell\ell$	3 e,μ			139	$\tilde{\chi}^\mp_1/\tilde{\chi}^0_1$ [BR($Z\tau$)=1, BR(Ze)=1] 0.625 1.05	Pure Wino	2011.10543
	$\tilde{\chi}^\pm_1\tilde{\chi}^\mp_1/\tilde{\chi}^0_2\to WW/Z\ell\ell\ell\ell\nu\nu$	4 e,μ	0 jets	$E_T^{\rm miss}$	139	$\tilde{\chi}^\pm_1/\tilde{\chi}^0_2$ [$\lambda_{i33}\neq 0, \lambda_{12k}\neq 0$] 0.95 1.55	m($\tilde{\chi}^0_1$)=200 GeV	2103.11684
	$\tilde{g}\tilde{g}, \tilde{g}\to qq\tilde{\chi}^0_1, \tilde{\chi}^0_1\to qqq$		4-5 large jets		36.1	$\tilde{g}$ [m($\tilde{\chi}^0_1$)=200 GeV, 1100 GeV] 1.3 1.9	Large λ''_{112}	1804.03568
	$\tilde{t}\tilde{t}, \tilde{t}\to t\tilde{\chi}^0_1, \tilde{\chi}^0_1\to tbs$		Multiple		36.1	$\tilde{t}$ [λ''_{323}=2e-4, 1e-2] 0.55 1.05	m($\tilde{\chi}^0_1$)=200 GeV, bino-like	ATLAS-CONF-2018-003
	$\tilde{t}\tilde{t}, \tilde{t}\to b\tilde{\chi}^\pm_1, \tilde{\chi}^\pm_1\to bbs$		$\geq$ 4b		139	$\tilde{t}$ Forbidden 0.95	m($\tilde{\chi}^\pm_1$)=500 GeV	2010.01015
	$\tilde{t}_1\tilde{t}_1, \tilde{t}_1\to bs$		2 jets + 2 b		36.7	$\tilde{t}_1$ [qq, bs] 0.42 0.61		1710.07171
	$\tilde{t}_1\tilde{t}_1, \tilde{t}_1\to q\ell$	2 e,μ	2 b		36.1	$\tilde{t}_1$ 0.4-1.45	BR($\tilde{t}_1\to be/b\mu$)>20%	1710.05544
		1 μ	DV		136	$\tilde{t}_1$ [1e-10< λ'_{23k} <1e-8, 3e-10< λ'_{23k} <3e-9] 1.0 1.6	BR($\tilde{t}_1\to q\mu$)=100%, cosθ_t=1	2003.11956
	$\tilde{\chi}^\pm_1/\tilde{\chi}^0_2/\tilde{\chi}^0_1, \tilde{\chi}^0_{1,2}\to tbs, \tilde{\chi}^+_1\to bbs$	1-2 e,μ	$\geq$6 jets		139	$\tilde{\chi}^0_1$ 0.2-0.32	Pure higgsino	2106.09609

Only a selection of the available mass limits on new states or phenomena is shown. Many of the limits are based on simplified models, c.f. refs. for the assumptions made.

https://atlas.cern/updates/briefing/strengthening-SUSY-searches

Full Run-2 dataset

SUSY searches

Comprehensive 2lepton +MET searches with innovative methods

- Pair production of charginos, neutralinos, and coloured supersymmetric particles (squarks or gluinos) decaying through the next-to-lightest neutralino (strong and electroweak SUSY)

SUSY-2018-05 arXiv:2204.13072

- Electroweak production of pairs of charged sleptons or charginos, extends sensitivity to electroweak SUSY in challenging mass regions

SUSY-2019-02 arXiv:2209.13935

- eμ opposite-sign, in regions inspired by searches for the electroweak production of supersymmetric charginos, first time unfolding of differential distributions used in ATLAS SUSY

SUSY-2021-06 arXiv:2206.15231

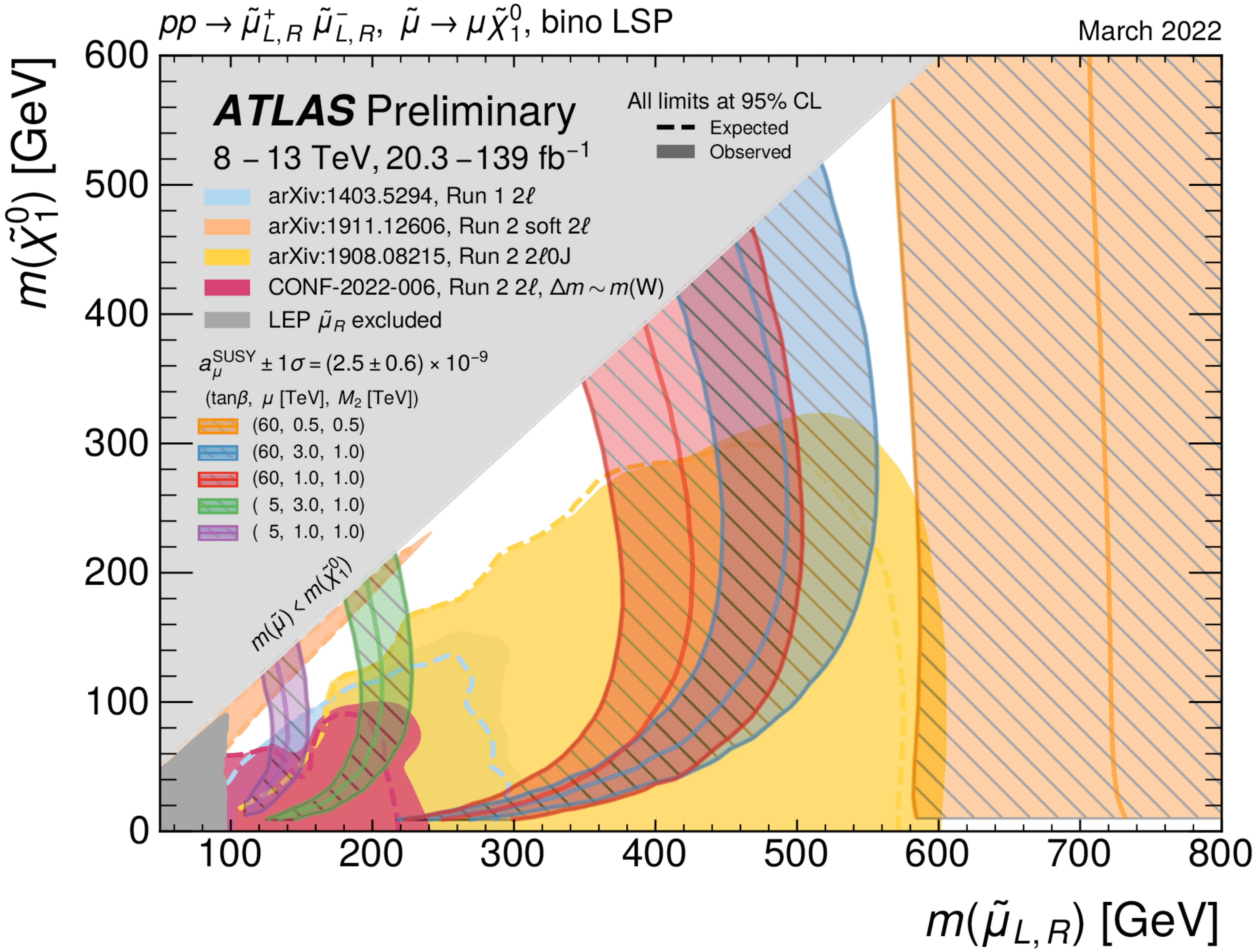

Exclusion limits at 95% CL based on 13 TeV data in the (smuon, lightest neutralino) mass plane for different analyses probing the direct production of smuons with decays to a muon and a bino-like neutralino. Hatched bands indicate regions compatible with the observed muon g-2 anomaly.

https://atlas.cern/updates/briefing/invisible-Higgs-search

Invisible Higgs decays

HIGG-2021-05 EXOT-2020-11

arXiv:2202.07953

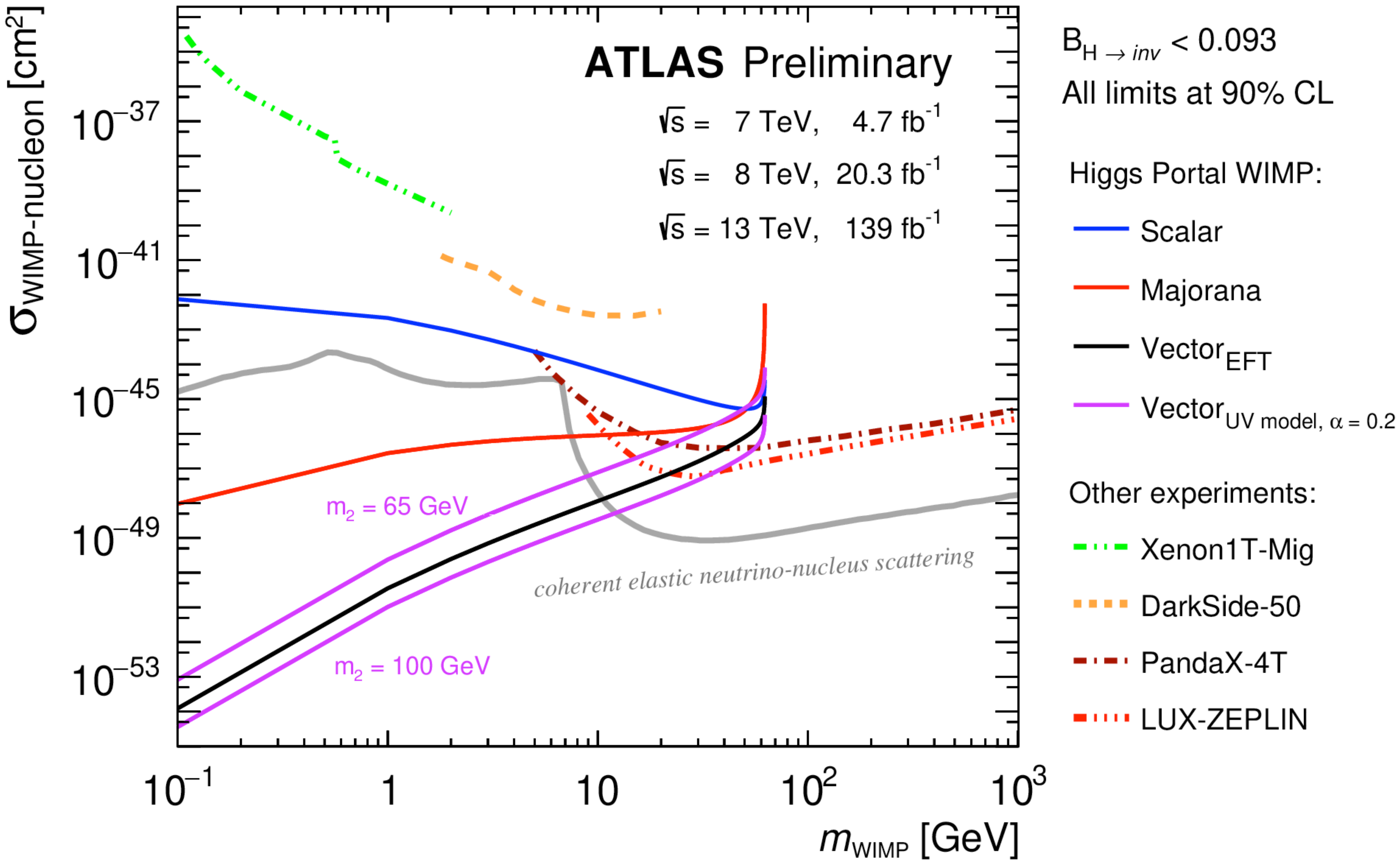

- VBF produced Higgs decaying into dark matter particles
- Higgs to invisible BR >15% excluded at a 95% CL (0.1% in the SM)
- Highly competitive results with other experiments searching for direct evidence of dark matter, especially for dark-matter particles with mass between 1 and 10 GeV

Full Run-2 dataset

https://atlas.cern/Updates/Briefing/Higgs-Dark-Photon

Dark searches

- Dark photons in Higgs decays
  - Higgs produced via ZH, best exclusion limits at the LHC

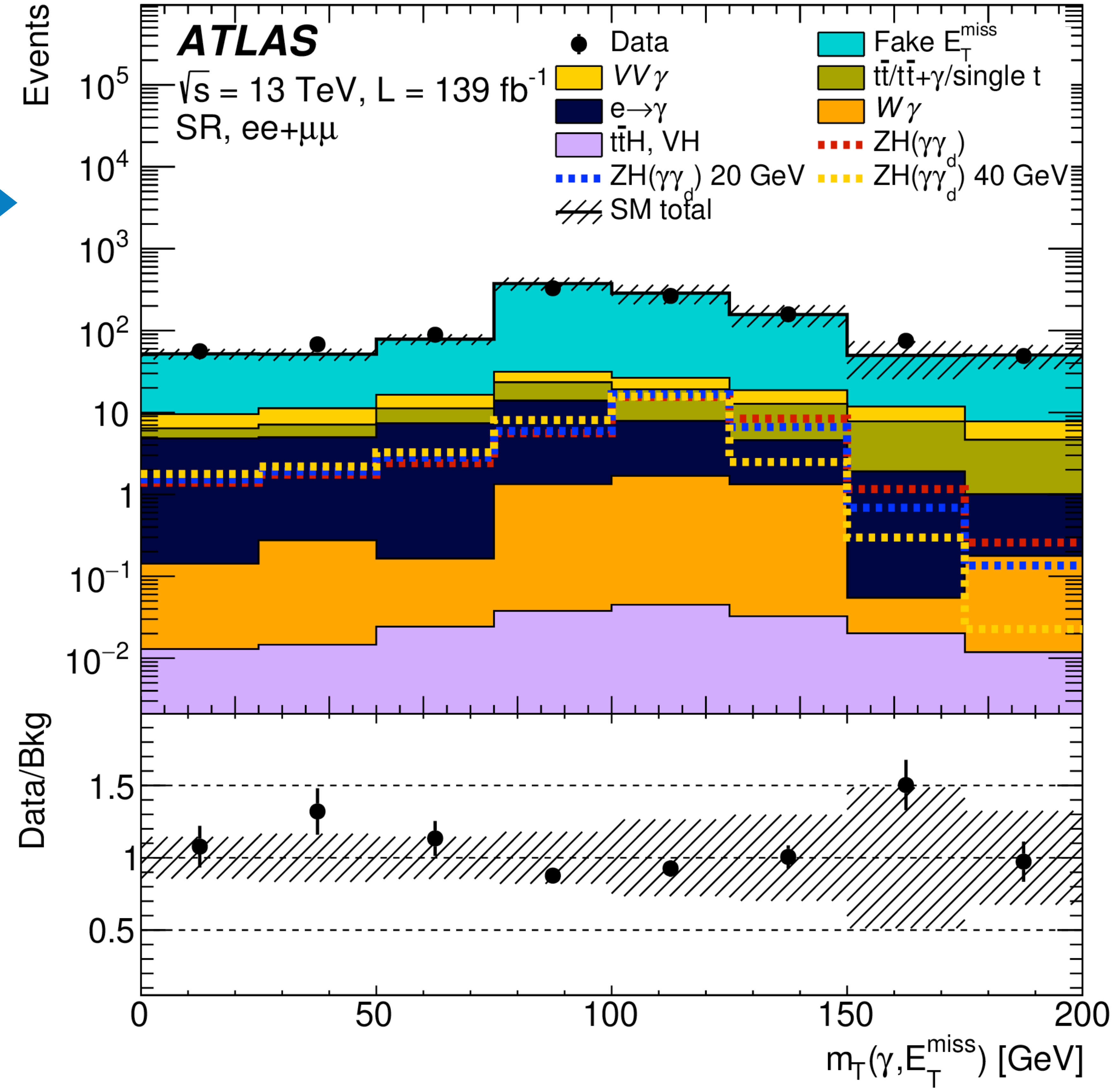

arXiv:2212.09649 HDBS-2019-13

Full Run-2 dataset

- Dark matter produced with a Higgs
  - Final states with τ-leptons + MET

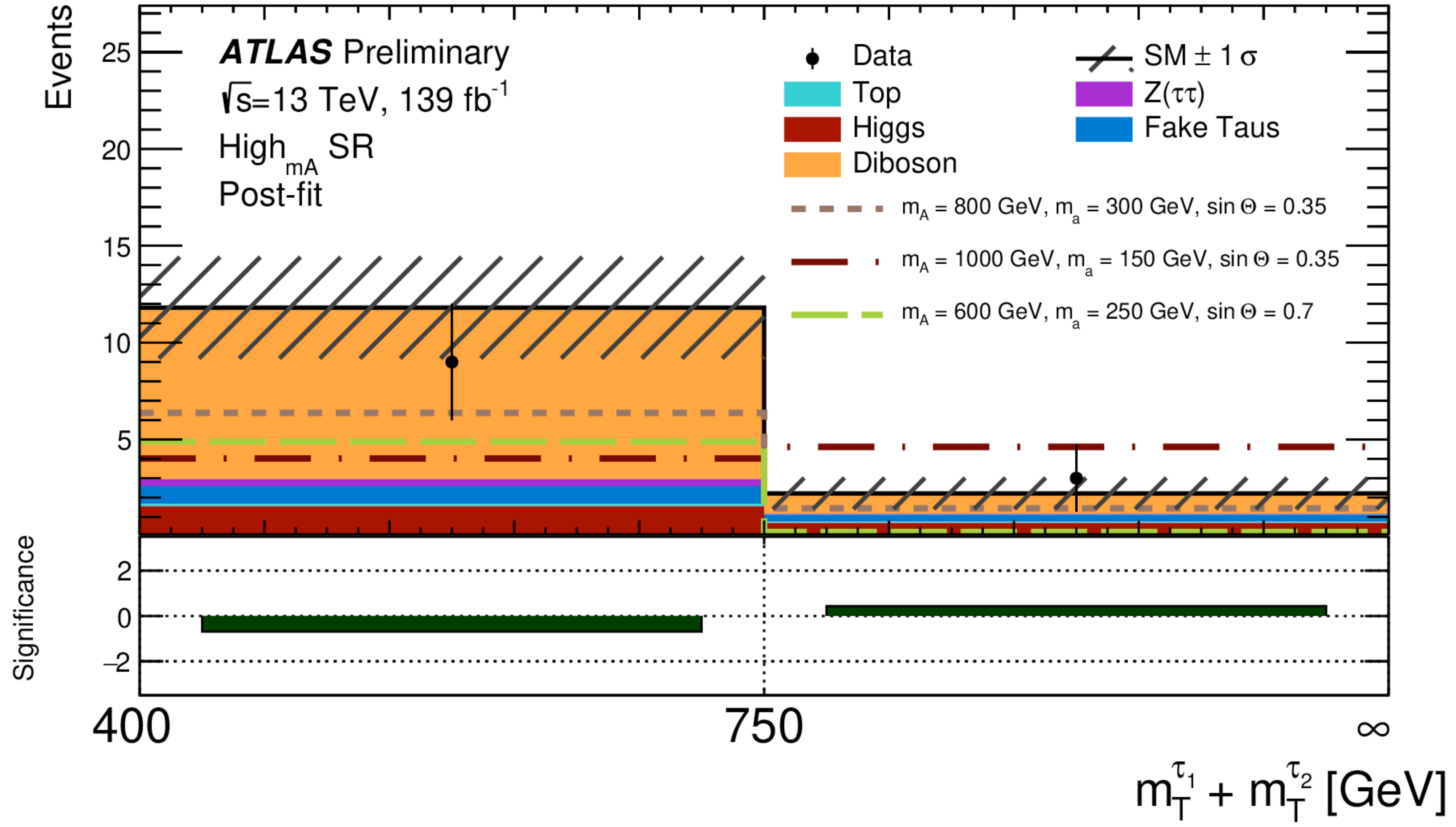

ATLAS-CONF-2022-069

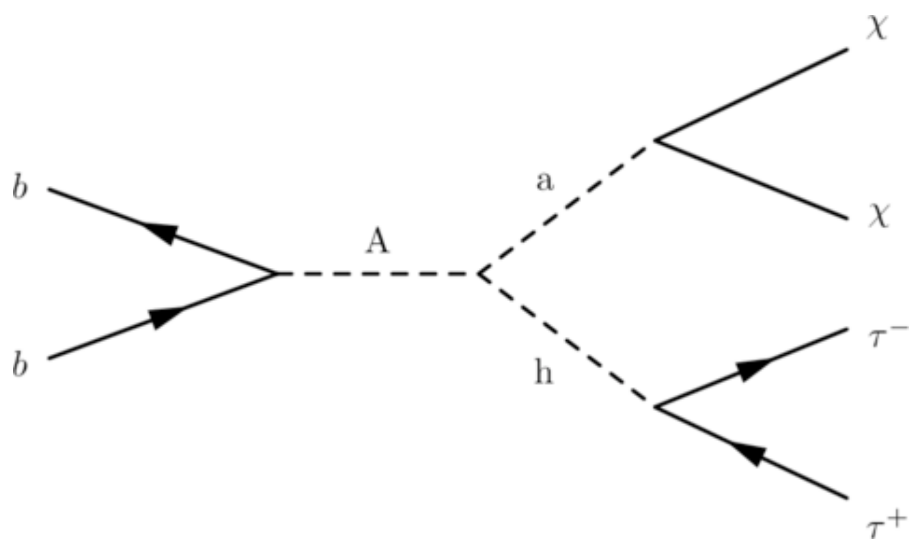

Many new long-lived particle searches

Full Run-2 dataset

- **Exotic Higgs decays** EXOT-2019-05 arXiv:2206.12181
  - (e.g. dark photon), displaced jets
- **Heavy Neutral Leptons** EXOT-2019-23 arXiv:2203.01009 EXOT-2019-29 arXiv:2204.11988
  - displaced vertex
  - limits on HNL masses between 3 and ~15 GeV, first HNL decays to electron-muon pairs
- **Massive, charged, long-lived particles**
  - Slowed-down, high transverse momenta and anomalously large specific ionisation losses,
  - Interpretations for pair-production of R-hadrons, charginos and staus

SUSY-2018-42 arXiv:2205.06013

- **Heavy, multi-charged particles**

ATLAS-CONF-2022-034

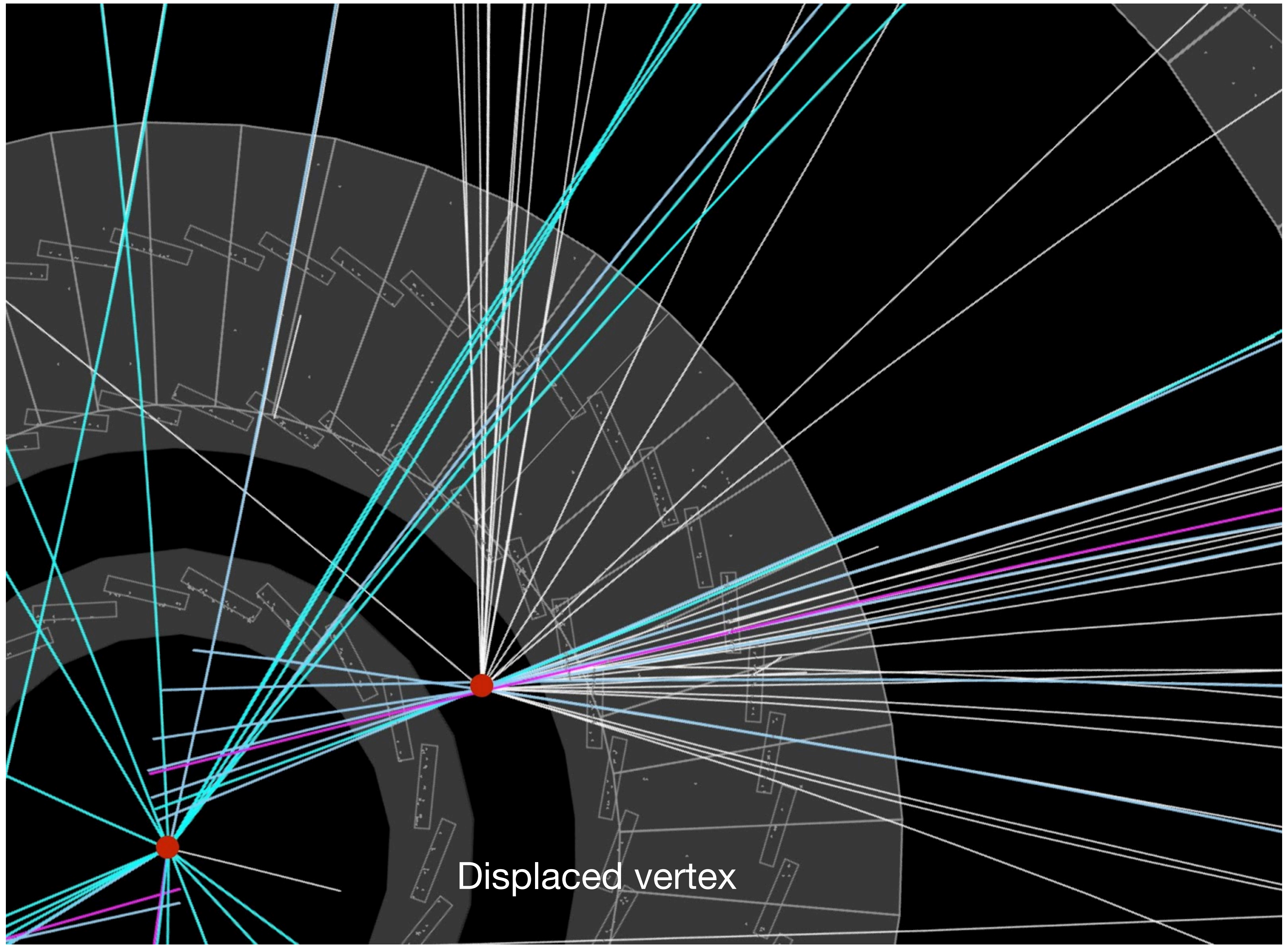

https://atlas.cern/updates/briefing/Higgs-displaced-photons

Long-lived particles

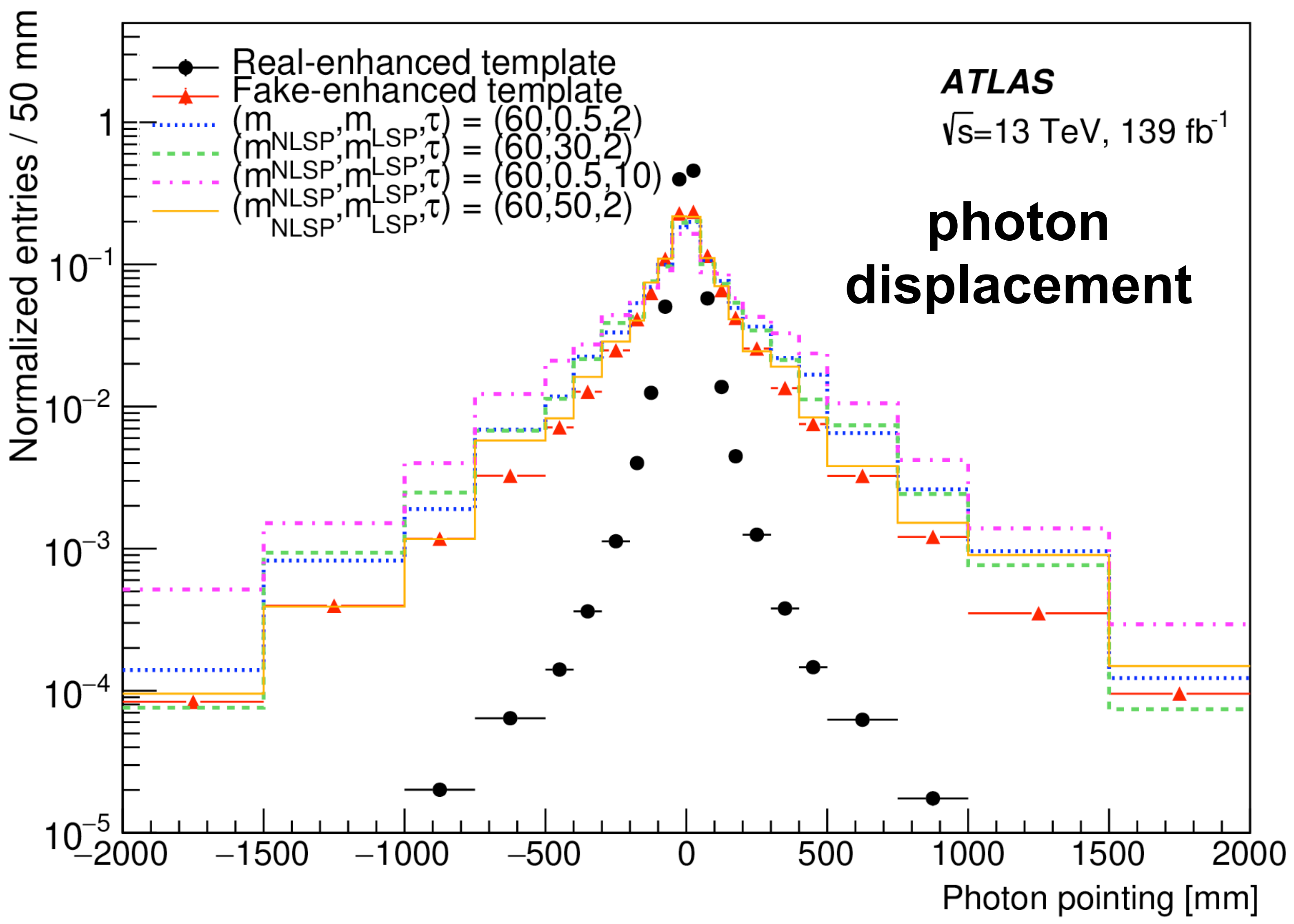

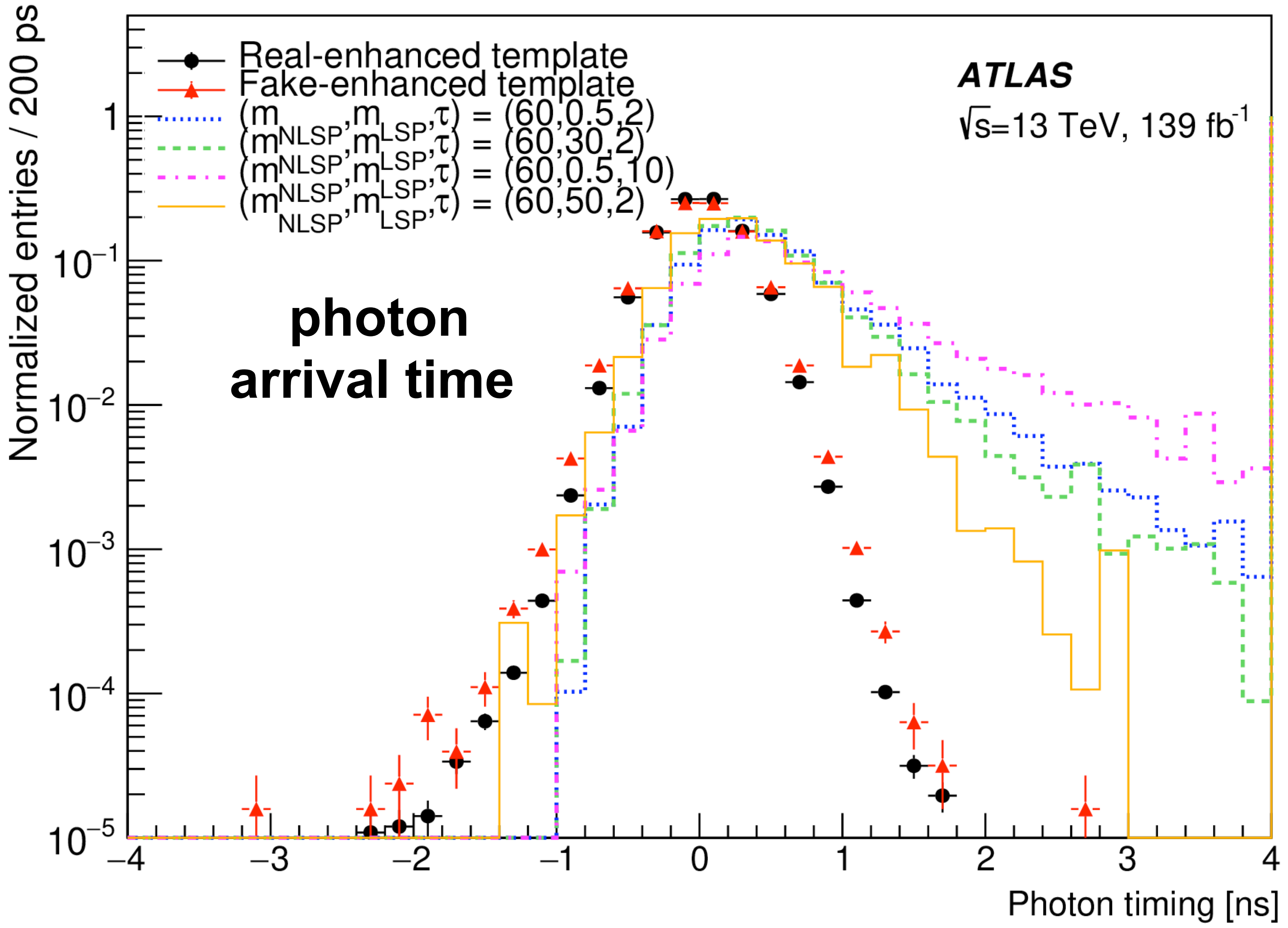

SUSY-2019-14

arXiv:2209.01029

Full Run-2 dataset

- **Delayed and non-pointing photons** from the displaced decay of a neutral long-lived particle (non-resonant)
- LLPs pair-produced in exotic Higgs decays, final states with photons + MET
  - electromagnetic calorimeter: measure the arrival times and trajectories of photons
- No significant excess is observed

Displaced production of H or Z from LLP decays (resonant)

ATLAS-CONF-2022-051

https://atlas.cern/updates/briefing/searches-united https://atlas.cern/updates/briefing/search-charged-Higgs

https://atlas.cern/Updates/Briefing/Search-High-Mass-Particles

Resonances

HDBS-2018-19 arXiv:2207.03925

ATLAS-CONF-2022-028

WW, different models

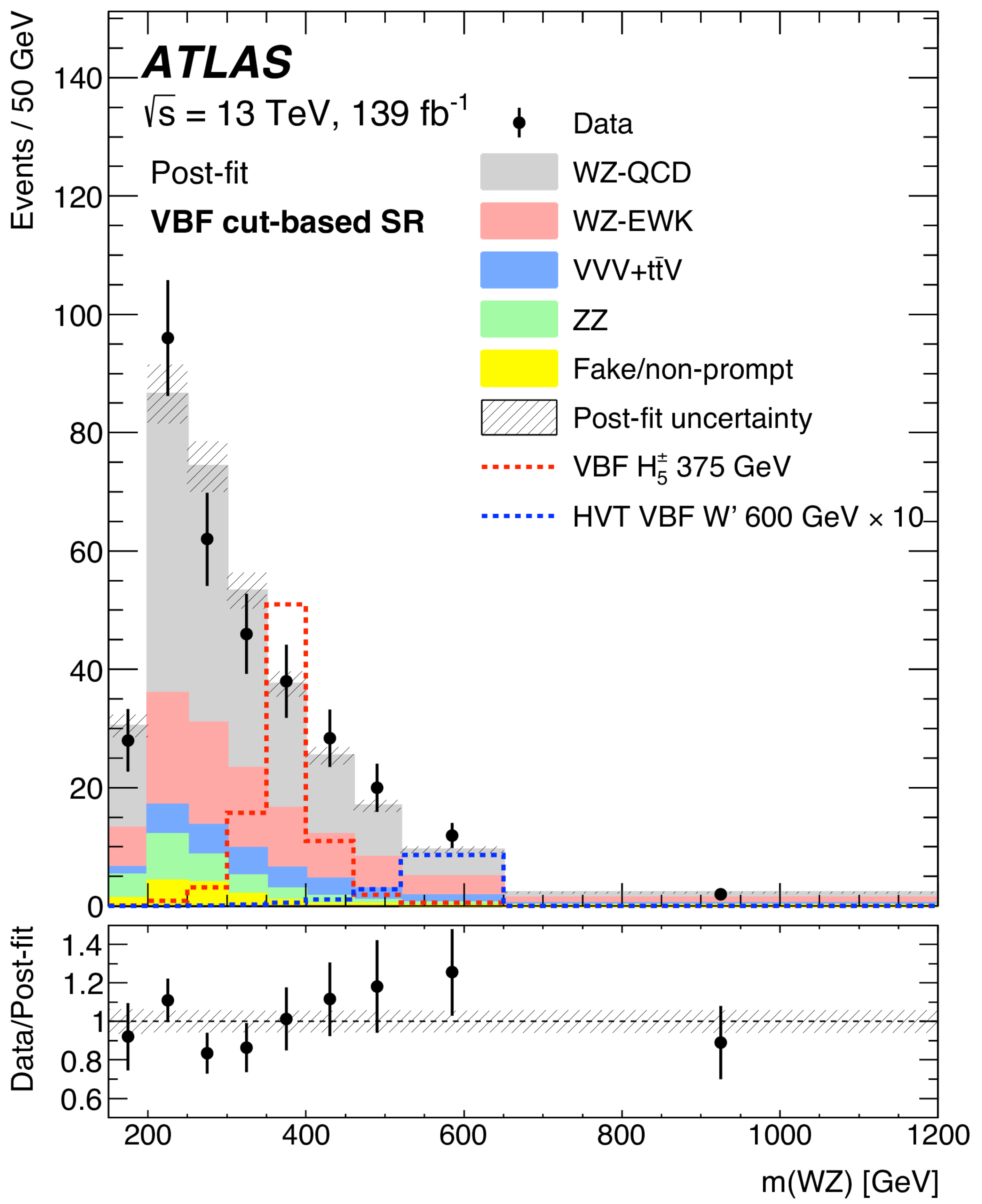

- Combinations of VV (V=W,Z) and VH searches
- 13 individual searches studying different final states

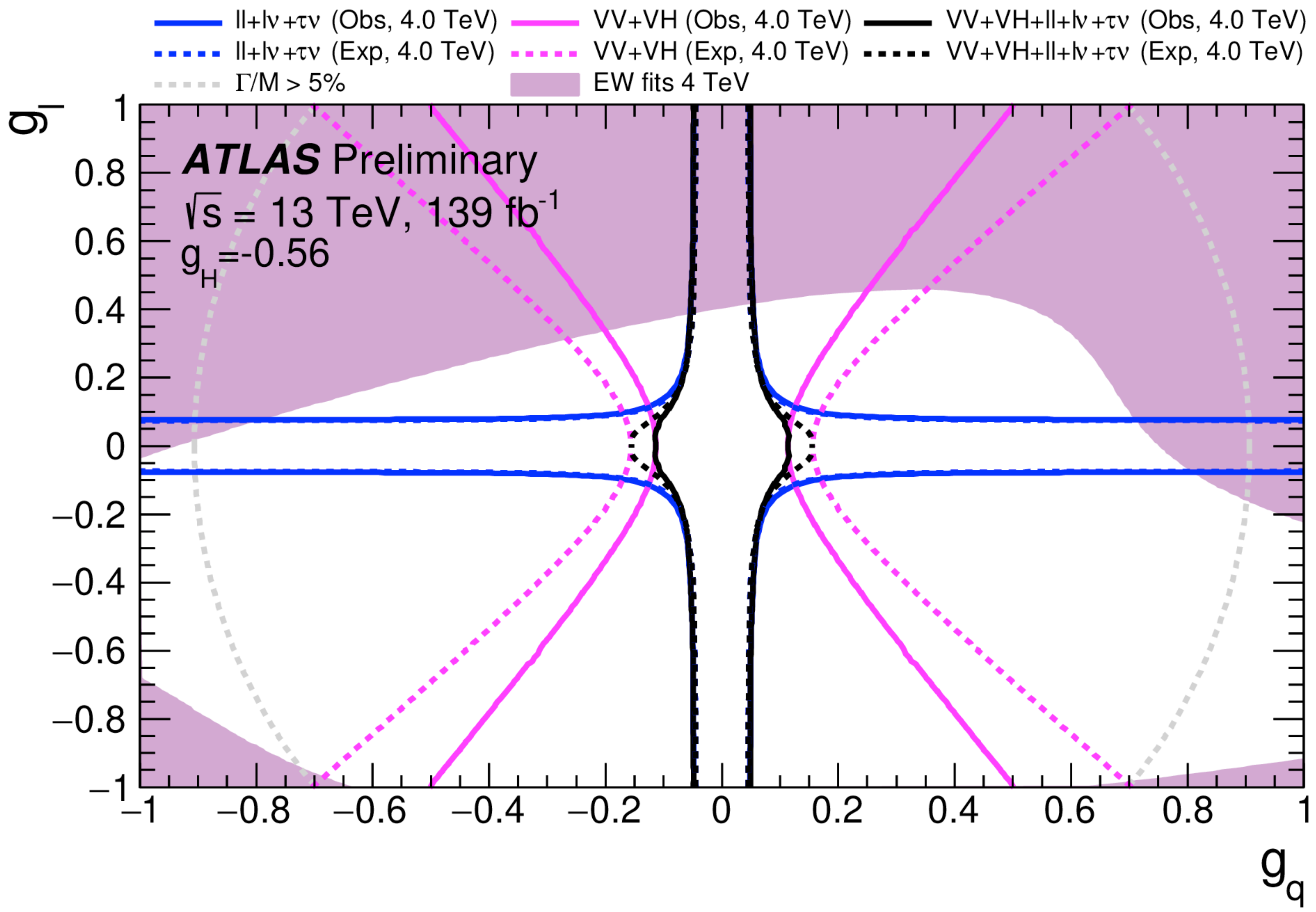

Constraints on the coupling between q and l with a new heavy W/Z boson.

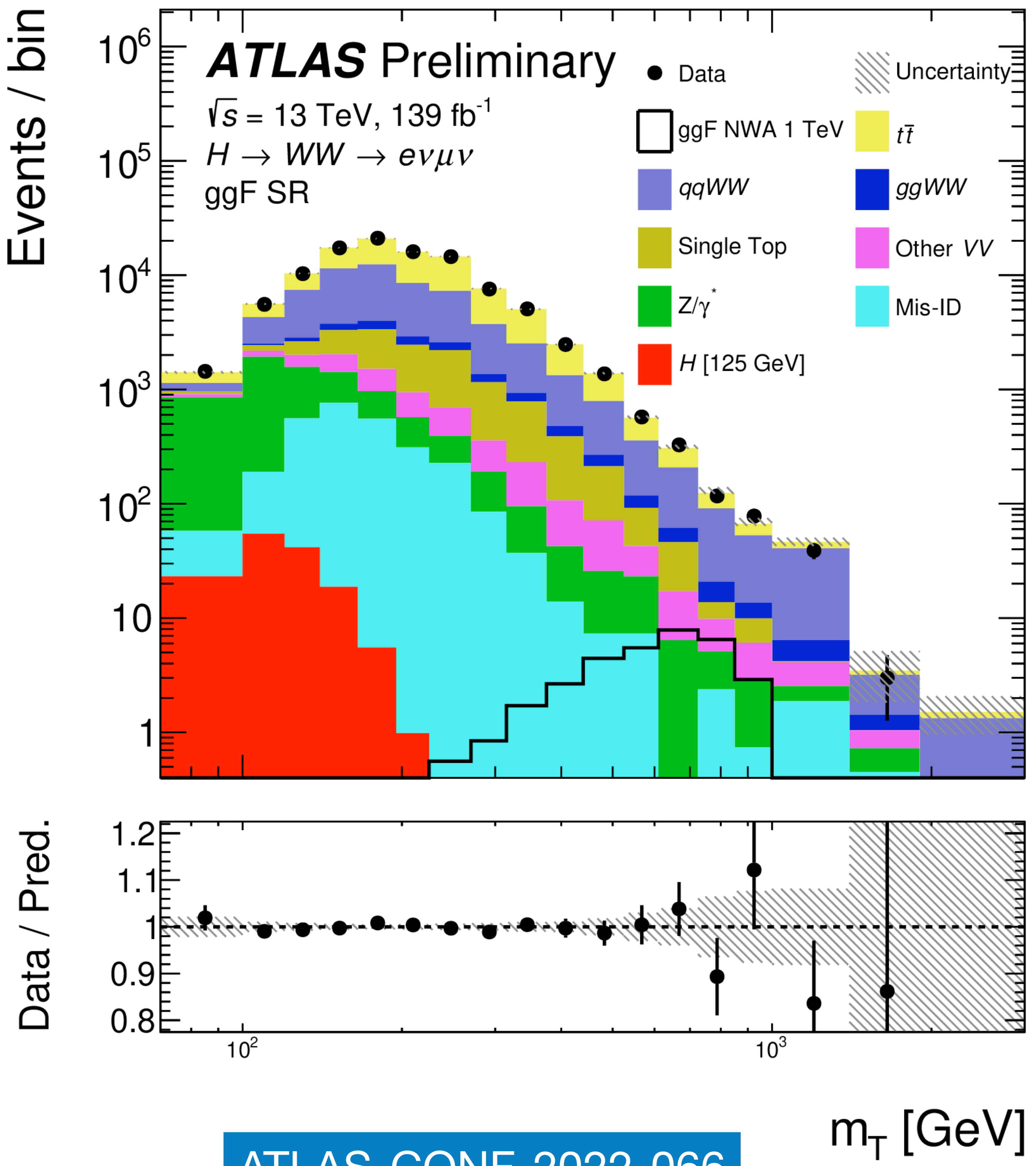

ATLAS-CONF-2022-066

Search for WZ resonances in lνll final states, from Heavy Vector Triplet or a charged Higgs boson.

Full Run-2 dataset

b-physics and heavy ions

Four-charm tetraquark and many new results

ATLAS-CONF-2022-040 **Full Run-2 dataset**

https://atlas.cern/Updates/Briefing/Charm-Tetraquark

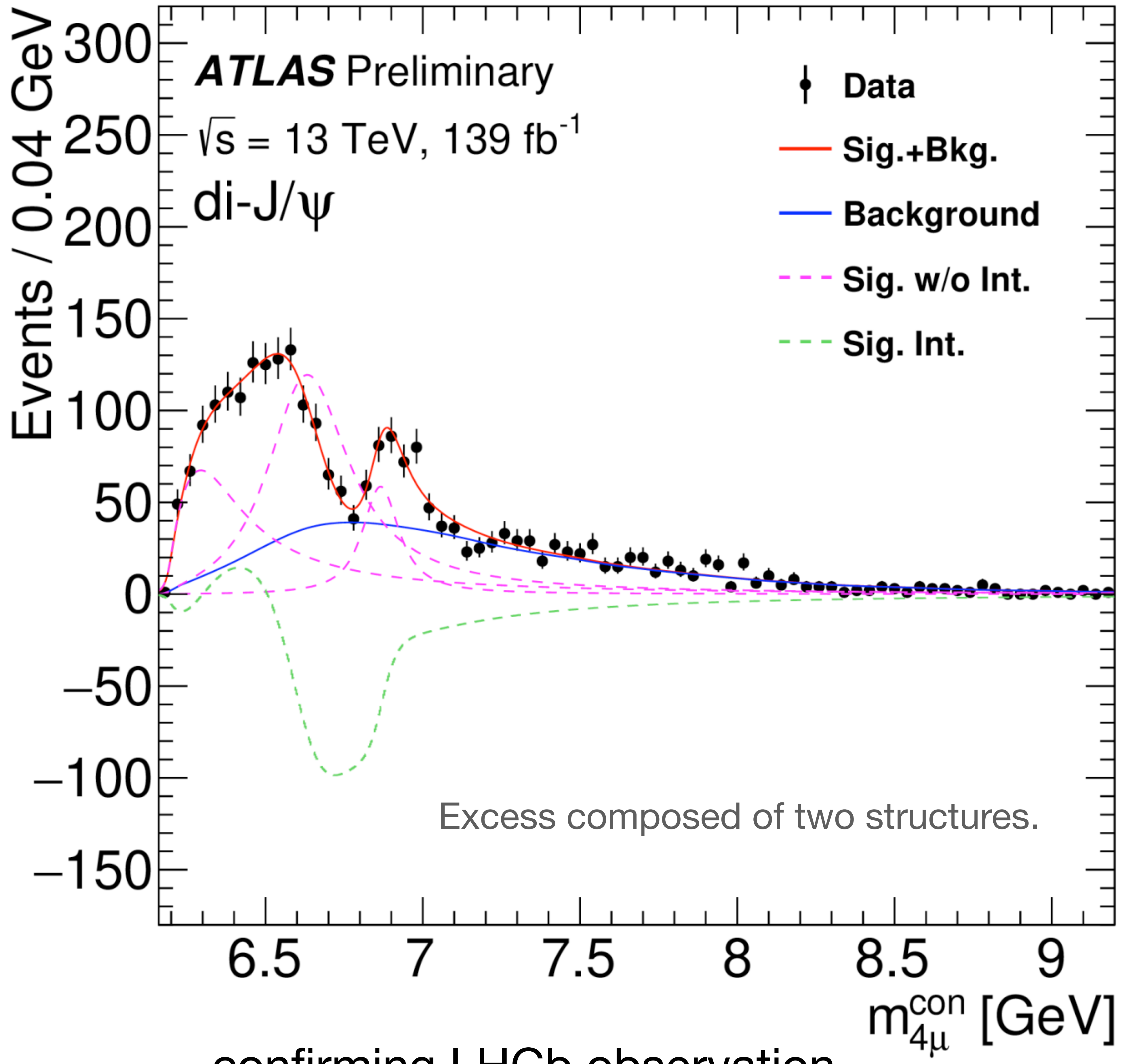

confirming LHCb observation

Many new results on measuring jets in HI, including dijets, gamma-jets, b-jets, and dependence of jet suppression on the substructure

ATL-PHYS-PUB-2022-020

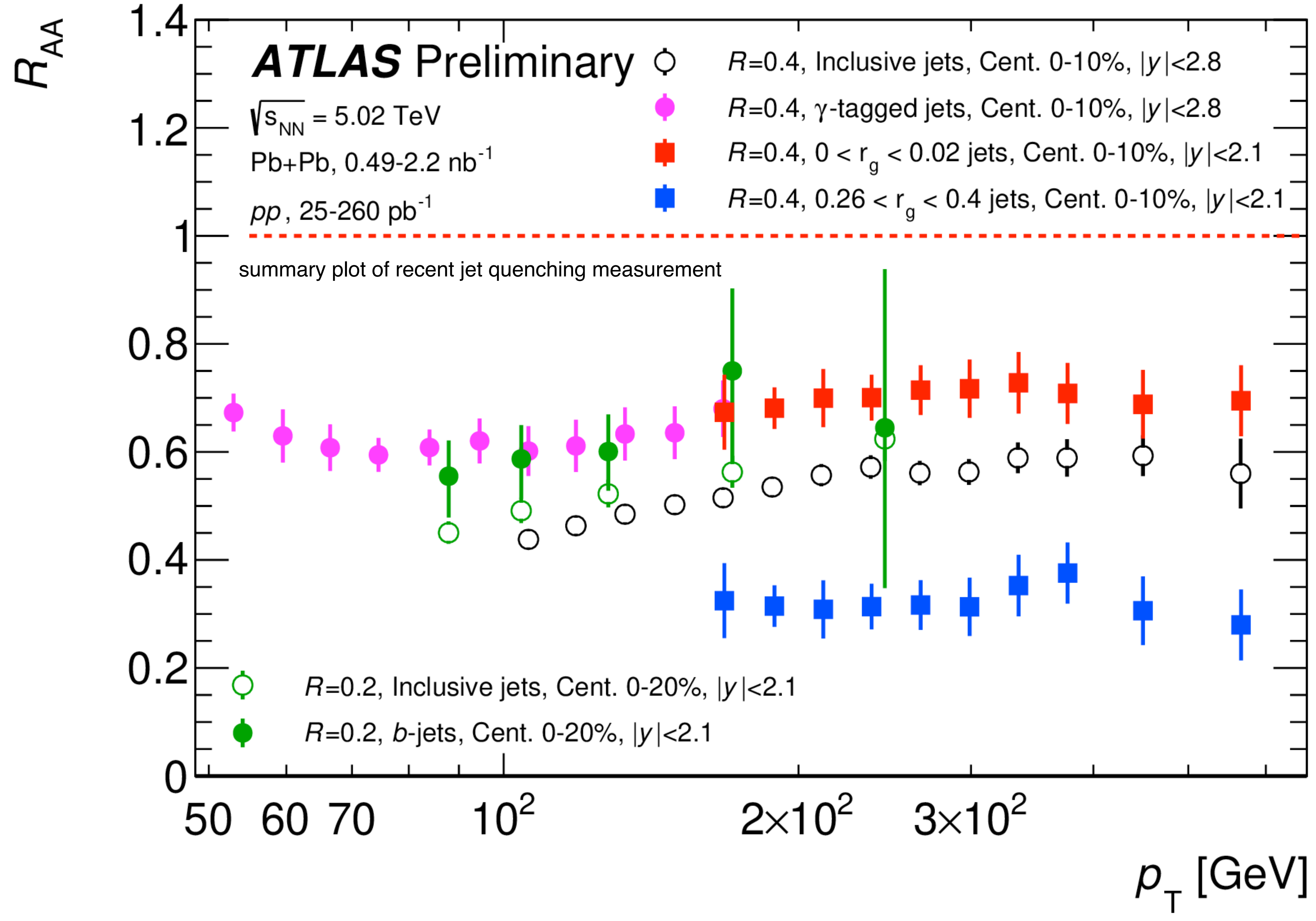

https://atlas.cern/updates/briefing/heavy-ion-energy-loss

https://atlas.cern/updates/briefing/dijet-suppression

https://atlas.cern/updates/briefing/observation-taupair-heavy-ions

In Summary

- ATLAS has an incredibly rich physics program at the high energy frontier
- Exploring the Higgs boson sector, with precision top and SM measurements
- Broad search program at the ~TeV scale
  - Indirect and indirect probes for new physics
- 2022 was a great year for ATLAS: Successful start of Run-3, Higgs 10th anniversary
  - Some key dates: ICHEP 2022 highlights - ICHEP 2022 - Summary - LHCP 2022 Summary - Moriond 2022 Highlights - Winter conferences 2022 - Summary - Lepton-Photon 2022 - Summary

- 2022 also was the 30th anniversary of the Collaboration
- Letter of intent sumitted 1st Oct 1992
  - https://atlas.cern/about#history
  - https://videos.cern.ch/record/2296611

Don’t miss the ATLAS physics talks this week

- ATLAS results in hadron spectroscopy and production - Braden Keim Abbott
- ATLAS results on weak decays of B mesons - Andrew Mark Wharton
- DiHiggs Production Searches with ATLAS In Higgs & Diboson searches - Edson Carquin Lopez
- Highlights on top quark physics with the ATLAS experiment at the LHC - Andreas Kirchhoff
- Improving ATLAS Hadronic Object Performance with ML/AI Algorithms - Reina Coromoto Camacho Toro
- Measurements of Higgs boson production and decay rates and their interpretation with the ATLAS experiment - Mark Andrew Owen
- Measurements of Higgs boson properties with the ATLAS detector - Jose Humberto Ocariz
- Recent ATLAS measurements in heavy-ion collisions - Sebastian Tapia Araya
- Redefining Performance: New Techniques for ATLAS Jet & MET Calibration - Louis Ginabat
- Results from muon reconstruction performance with ATLAS at Run-3 - William Axel Leight
- Searches for BSM physics using challenging and long-lived signatures with the ATLAS detector - Neza Ribaric
- Searches for Dark Matter with the ATLAS Experiment at the LHC - Joseph Haley
- Searches for leptoquarks with the ATLAS detector - Patrick Bauer
- Searches for resonances decaying to pairs of heavy bosons in ATLAS - Alberto Annovi
- Searches for supersymmetric particles with prompt decays with with the ATLAS detector - Tomohiro Yamazaki
- Searching for additional Higgs bosons at ATLAS - Anna Ivina

Backup

ATLAS EXPERIMENT

UPPSALA UNIVERSITET

Lepton-flavour-violating Higgs decays

- Direct $H \to e\tau$ and $H \to \mu\tau$ searches
- Full Run-2 dataset
- No significant excess observed, results are interpreted as upper limits on LFV branching ratios.

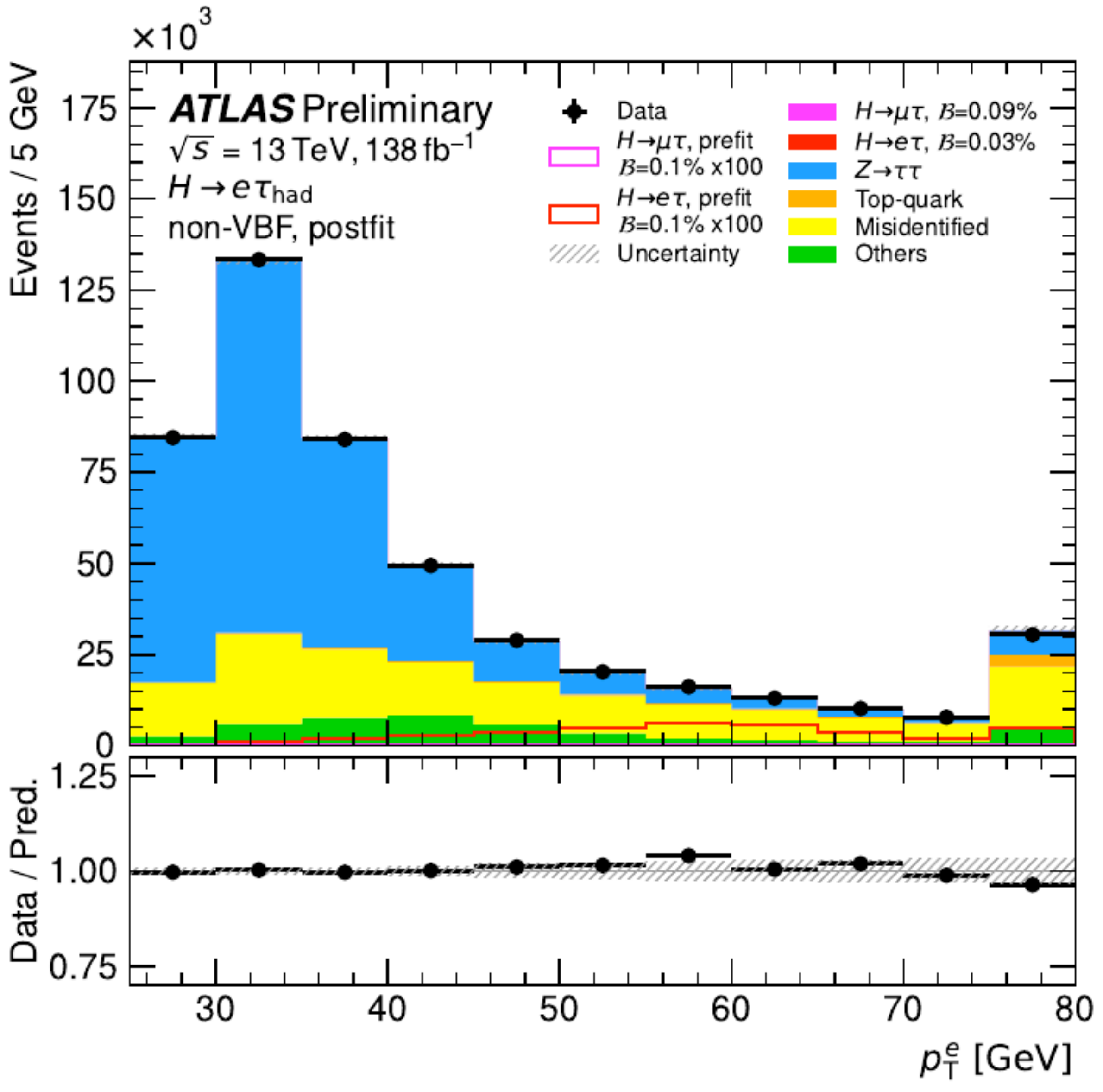

ATLAS-CONF-2022-060

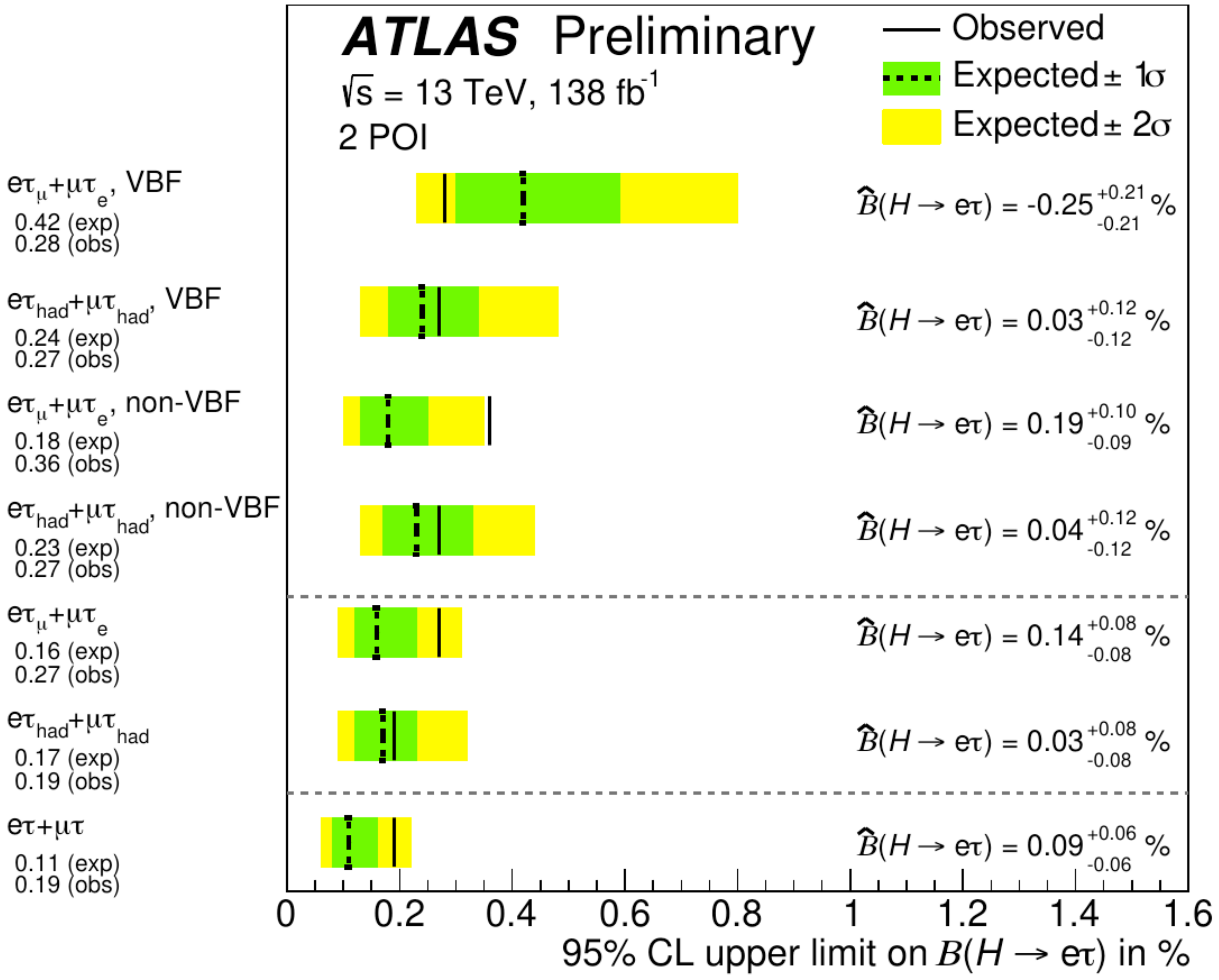

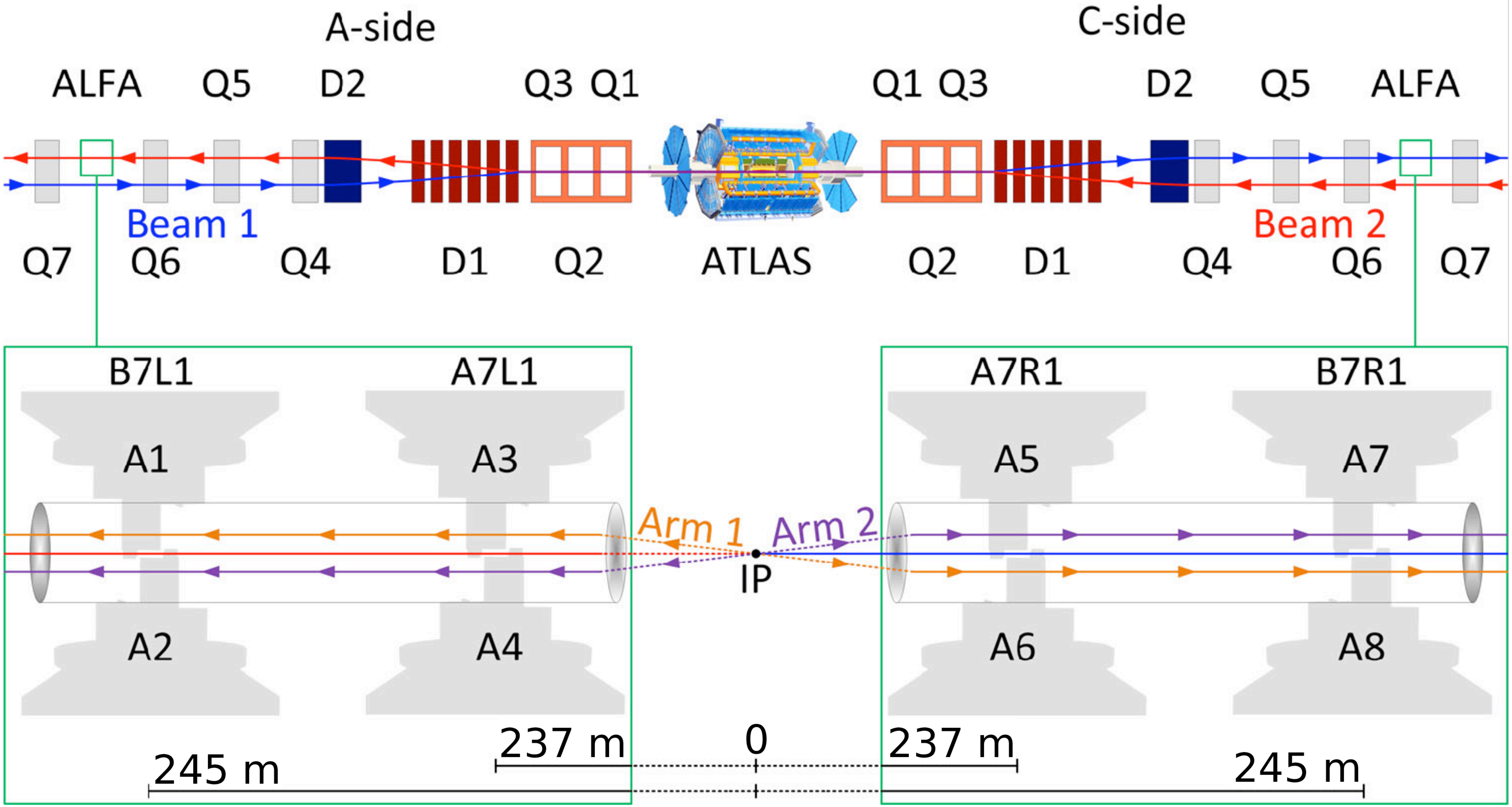
A-side
C-side
ALFA
Q5
D2
Q3
Q1
Q1
Q3
D2
Q5
ALFA
Beam 1
Beam 2
Q7
Q6
Q4
D1
Q2
ATLAS
Q2
D1
Q4
Q6
Q7
B7L1
A7L1
A7R1
B7R1
A1
A3
A5
A7
Arm 1
Arm 2
IP
A2
A4
A6
A8
237 m
0
237 m
245 m
245 m

https://atlas.cern/updates/briefing/search-long-lived-particles

Long-lived particles

EXOT-2019-05 arXiv:2206.12181

- Higgs decays to dark photons with m O(MeV-GeV)
- Branching fractions > 1% excluded at 95% CL for a Higgs decaying into two dark photons for dark-photon mean proper decay lengths between 10 mm and 250 mm and masses between 0.4 GeV and 2 GeV.

EXOT-2019-23 arXiv:2203.01009

- Neutral, pair-produced, displaced jets in the hadronic calorimeter.
- Long-lived Higgs decays
- branching ratios for SM Higgs > 10% are at 95% CL for LLPs with proper lifetime between 20 mm and 10 m depending on the model.
- Upper limits on the cross-section xBR for scalars with a mass of 60 GeV and between 200 GeV and 1 TeV.

EXOT-2019-29 arXiv:2204.11988

- Heavy neutral leptons, displaced vertex
- limits are given for single-flavor and multiflavor mixing scenarios for both normal and inverted neutrino-mass hierarchies.

SUSY-2018-42 arXiv:2205.06013

- massive, charged, long-lived particles
- Slowed-down, high transverse momenta and anomalously large specific ionisation losses,
- Interpretations for pair-production of *R*-hadrons, charginos and staus

Measurement of the properties of Higgs boson production at $\sqrt{s}$=13 TeV in the $H\to\gamma\gamma$ channel using 139 fb-1 of pp collision data with the ATLAS experiment

- https://atlas.web.cern.ch/Atlas/GROUPS/PHYSICS/PAPERS/HIGG-2020-16/
- Measurements of Higgs boson production cross-sections are carried out in the diphoton decay channel using 139 fb−1 of *pp* collision data at 13 TeV collected by the ATLAS experiment at the LHC. The analysis is based on the definition of 101 distinct signal regions using machine-learning techniques. The inclusive Higgs boson signal strength in the diphoton channel is measured to be 1.04+0.10−0.09. Cross-sections for gluon-gluon fusion, vector-boson fusion, associated production with a *W* or *Z* boson, and top associated production processes are reported. An upper limit of 10 times the Standard Model prediction is set for the associated production process of a Higgs boson with a single top quark, which has a unique sensitivity to the sign of the top quark Yukawa coupling. Higgs boson production is further characterized through measurements of Simplified Template Cross-Sections (STXS). In total, cross-sections of 28 STXS regions are measured. The measured STXS cross-sections are compatible with their Standard Model predictions, with a *p*-value of 93 %. The measurements are also used to set constraints on Higgs boson coupling strengths, as well as on new interactions beyond the Standard Model in an effective field theory approach. No significant deviations from the Standard Model predictions are observed in these measurements, which provide significant sensitivity improvements compared to the previous ATLAS results.

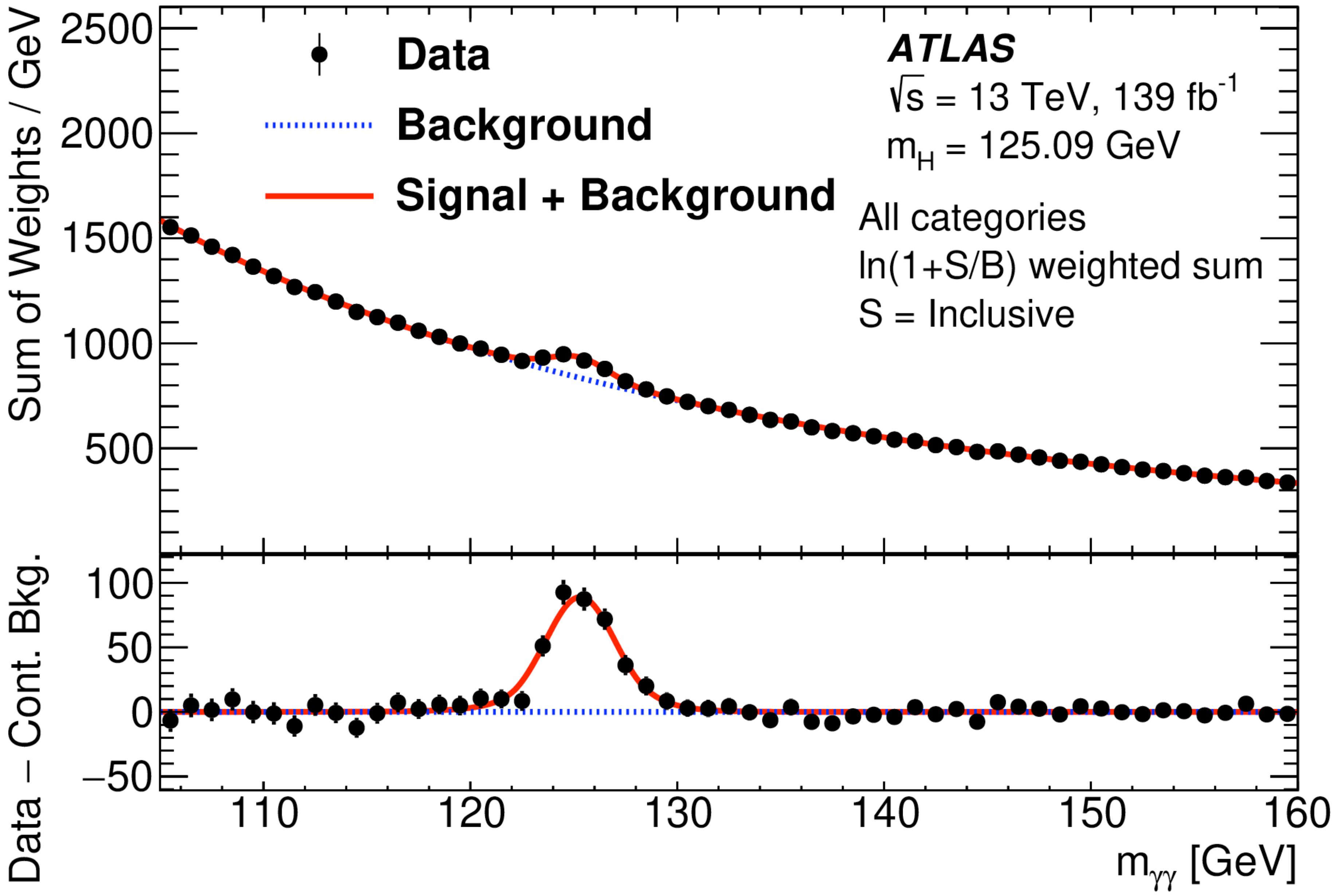

Inclusive-photon production and its dependence on photon isolation in pp collisions at 13 TeV using 139 fb–1 of ATLAS data

- https://atlas.web.cern.ch/Atlas/GROUPS/PHYSICS/CONFNOTES/ATLAS-CONF-2022-065/
- Measurements of differential cross sections for inclusive isolated-photon production in *pp* collisions at a centre-of-mass energy of 13 TeV provided by the LHC and using an integrated luminosity of 139 fb–1 of ATLAS data are presented. The cross sections are measured as functions of the photon transverse energy in different regions of photon pseudorapidity. The photons are required to be isolated by means of a fixed-cone method with two different cone radii, 0.2 and 0.4. The dependence of the inclusive-photon production on the photon isolation is investigated by measuring the fiducial cross sections as functions of the isolation-cone radius and the ratios of the differential cross sections with different radii in different regions of photon pseudorapidity. The measurements presented here, with a more granular segmentation in photon pseudorapidity leading to a more detailed experimental input to fits of the proton parton distribution functions and with different isolation radii, constitute an improvement with respect to those published by ATLAS earlier. These improvements provide a more in-depth test of the theoretical predictions. Next-to-leading-order QCD predictions from JETPHOX and SHERPA and next-to-next-to-leading-order QCD predictions from NNLOJET are compared to the measurements, using several parameterisations of the proton parton distribution functions. The measured cross sections are well described by the fixed-order QCD predictions within the experimental and theoretical uncertainties in most of the investigated phase-space region.

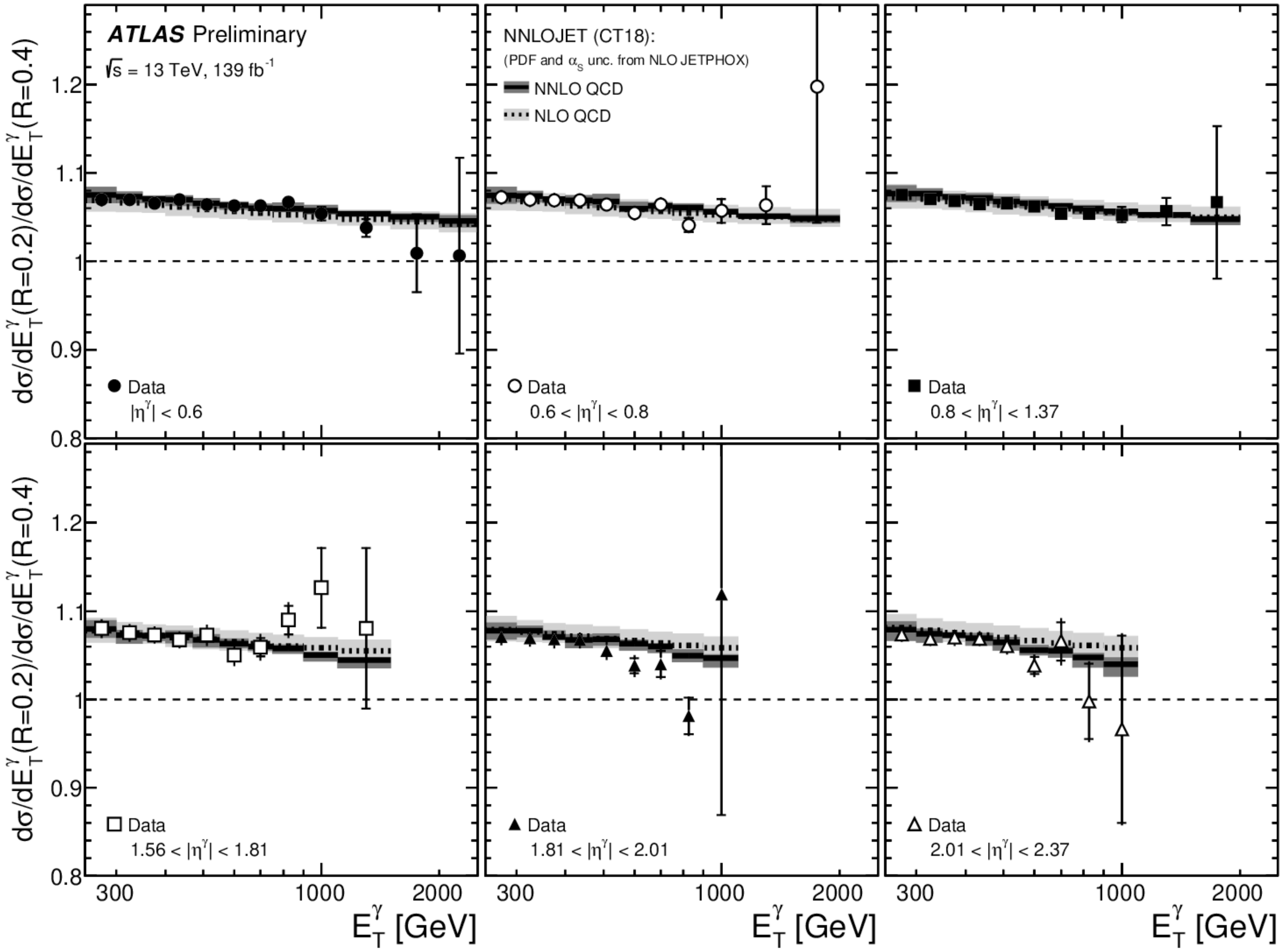

Search for pair-produced vector-like top and bottom partners in events with large missing transverse momentum in pp collisions with the ATLAS detector

- https://atlas.web.cern.ch/Atlas/GROUPS/PHYSICS/PAPERS/EXOT-2019-08/
- A search for pair-produced vector-like quarks using events with exactly one lepton (*e* or *μ*), at least four jets including at least one *b*-tagged jet, and large missing transverse momentum is presented. Data from proton-proton collisions at a centre-of-mass energy of 13 TeV, recorded by the ATLAS detector at the LHC from 2015 to 2018 and corresponding to an integrated luminosity of 139 fb−1, are analysed. Vector-like partners *T* and *B* of the top and bottom quarks are considered, as is a vector-like *X* with charge +5/3, assuming their decay into a *W*, *Z*, or Higgs boson and a third-generation quark. No significant deviations from the Standard Model expectation are observed. Upper limits on the production cross-section of *T* and *B* quark pairs as a function of their mass are derived for various decay branching ratio scenarios. The strongest lower limits on the masses are 1.59 TeV assuming mass-degenerate VLQs and branching ratios corresponding to the weak-isospin doublet model, and 1.47 TeV (1.46 TeV) for exclusive *T*→*Zt* (*B*/*X*→*Wt*) decays. In addition, lower limits on the *T* and *B* quark masses are derived for all possible branching ratios.

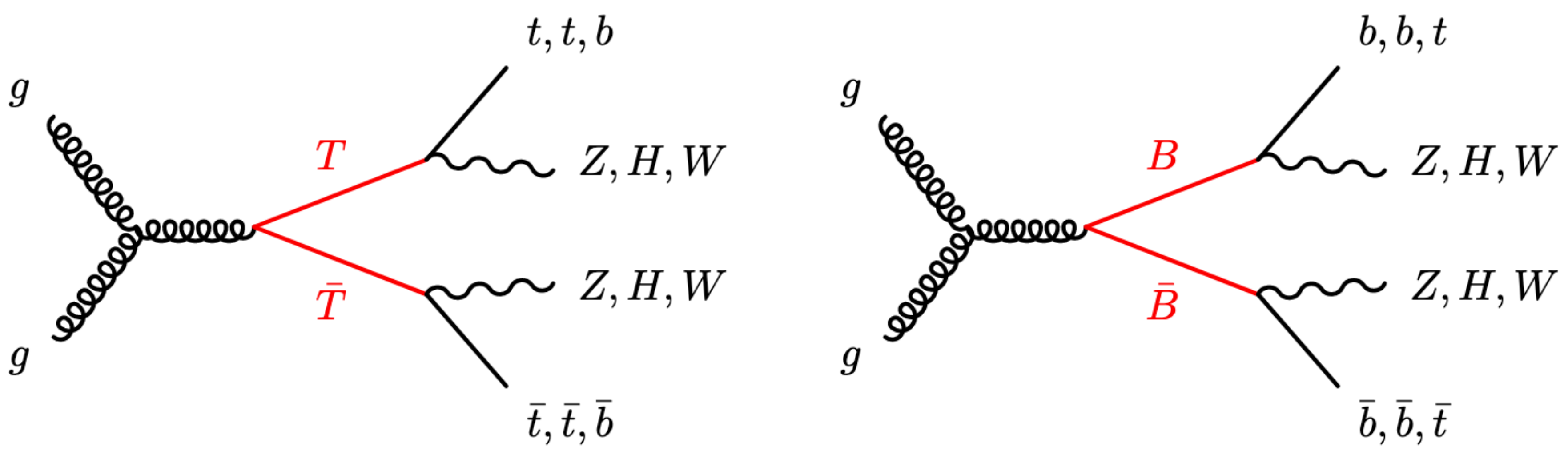

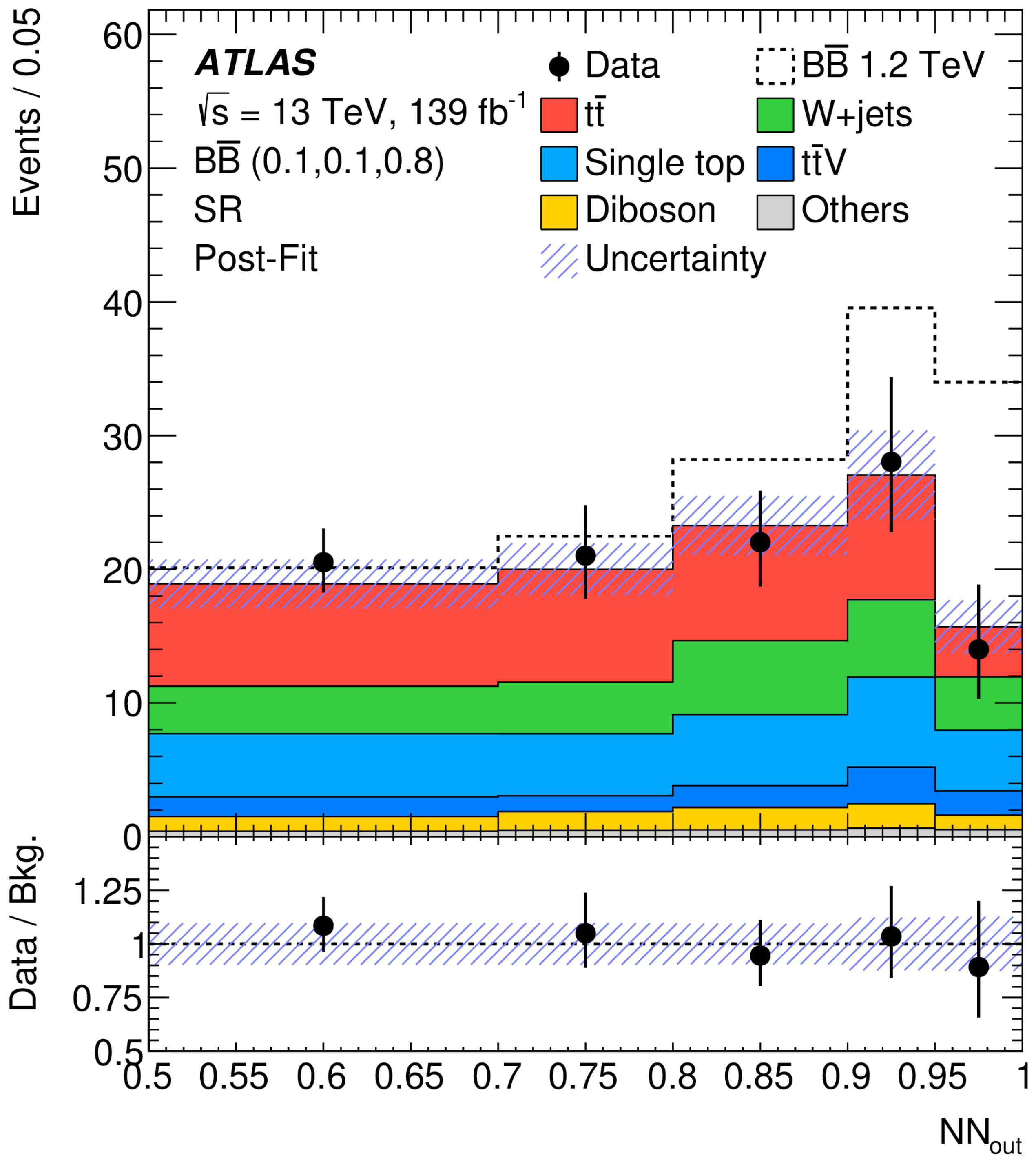

Search for heavy Higgs bosons from a g2HDM in multilepton plus b-jets final states in pp collisions at 13 TeV with the ATLAS detector

- https://atlas.web.cern.ch/Atlas/GROUPS/PHYSICS/CONFNOTES/ATLAS-CONF-2022-039/

- A search for new heavy scalars with flavour-violating decays in final states with multiple leptons and *b*-tagged jets is presented. The results are interpreted in terms of a general two-Higgs-doublet-model involving an additional scalar with couplings to the top-quark and the three up-type quarks (*ρ tt*,*ρtc*, and*ρtu*). The targeted signals lead to final states with either a same-sign top-quark pair, three top-quarks, or four top-quarks. The search is based on a dataset of proton-proton collisions at 13 TeV recorded with the ATLAS detector during Run 2 of the Large Hadron Collider, corresponding to an integrated luminosity of 139 fb−1. Events are categorised depending on the multiplicity of light charged leptons (electrons or muons), total lepton charge, and a deep-neural-network-based categorisation to enhance the purity of each of the signals. A mild excess is observed over the Standard Model expectation corresponding to a local significance of 2.81 standard deviations for a signal with *mH*=1000GeV and *ρtt* =0.32,*ρtc*=0.05, and*ρtu*=0.85. Exclusion limits at 95% confidence are set on the mass and couplings of the heavy Higgs boson. Masses of an additional scalar boson *mH* between 200-630 (200-840) GeV with couplings *ρ tt*=0.4,*ρ tc* =0.2, and *ρtu*=0.2 are observed (expected) to be excluded at 95% confidence level. Additional interpretations are provided in models of *R*-parity violating supersymmetry, motivated by the recent flavour and (*g*–2)*μ* anomalies.

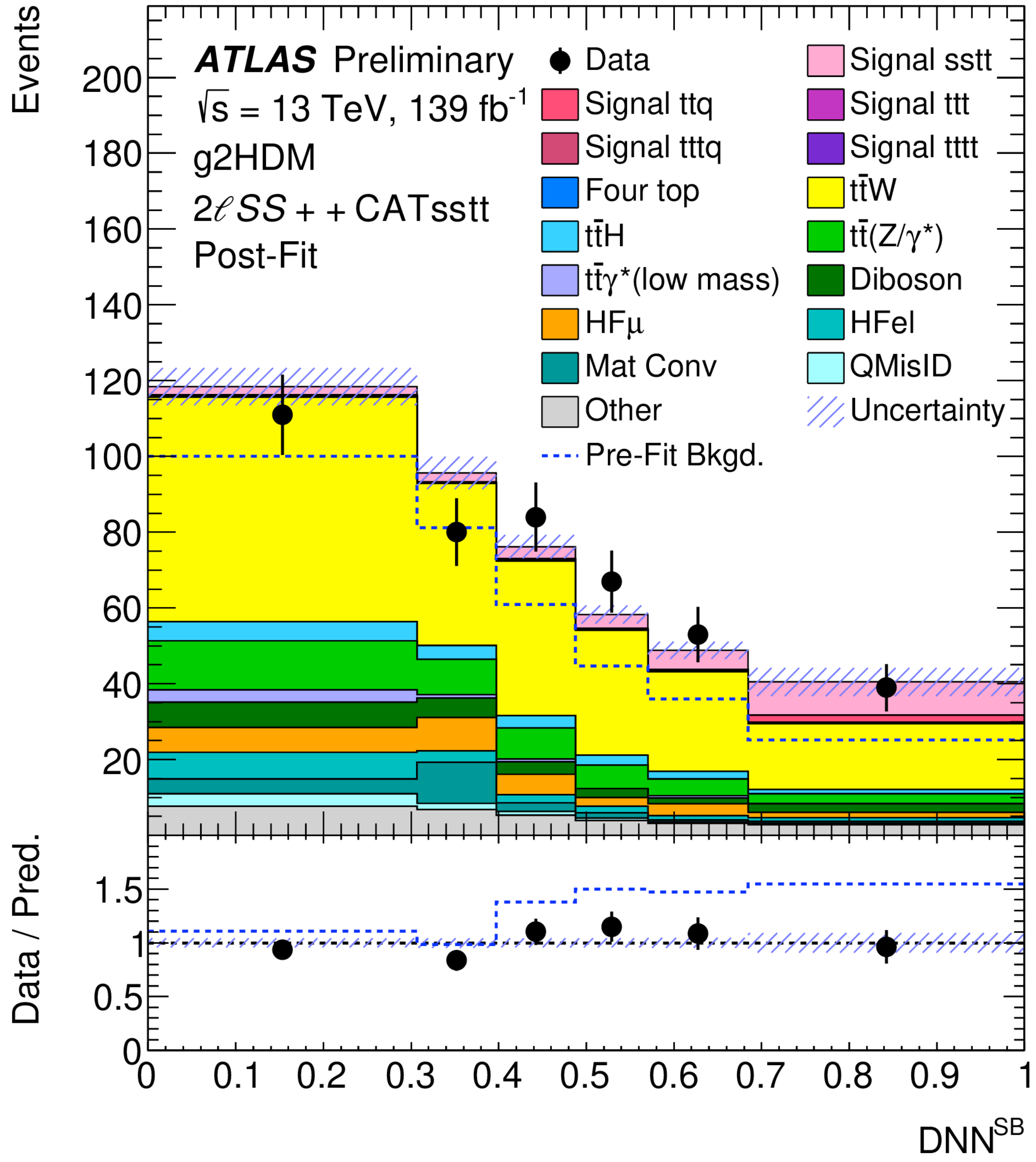

Search for scalar leptoquarks in the b *ττ* final state in *pp* collisions at 13 TeV with the ATLAS detector

- https://atlas.web.cern.ch/Atlas/GROUPS/PHYSICS/CONFNOTES/ATLAS-CONF-2022-037/
- ~1.3 TeV mass reach low b-jet pT selection sensitivity to t-channel LQ production
- A search for singly-produced scalar leptoquarks decaying to *bτ* in proton-proton collisions is performed using Run 2 data from the Large Hadron Collider corresponding to an integrated luminosity of 139 fb−1 at 13 TeV recorded by the ATLAS detector. The signal benchmark model considered is a scalar leptoquark with an electric charge of 4/3*e* and quantum numbers 3*B*+*L*=−2, which decays exclusively into a b-quark and a *τ*-lepton. The mass range explored is from 0.4 TeV to 2.5 TeV. No significant excess above the Standard Model prediction is observed, and 95\% confidence-level upper limits are set on the production cross-section times branching fraction of leptoquarks decaying to *bτ*. Considering both single and pair leptoquark production processes, under the assumption of exclusive decays of scalar leptoquarks to *bτ*, leptoquark masses below 1.26 TeV, 1.30 TeV and 1.41 TeV are excluded for a scalar leptoquark Yukawa coupling to *b*-quark and *τ*-lepton of 1.0, 1.7 and 2.5, respectively.

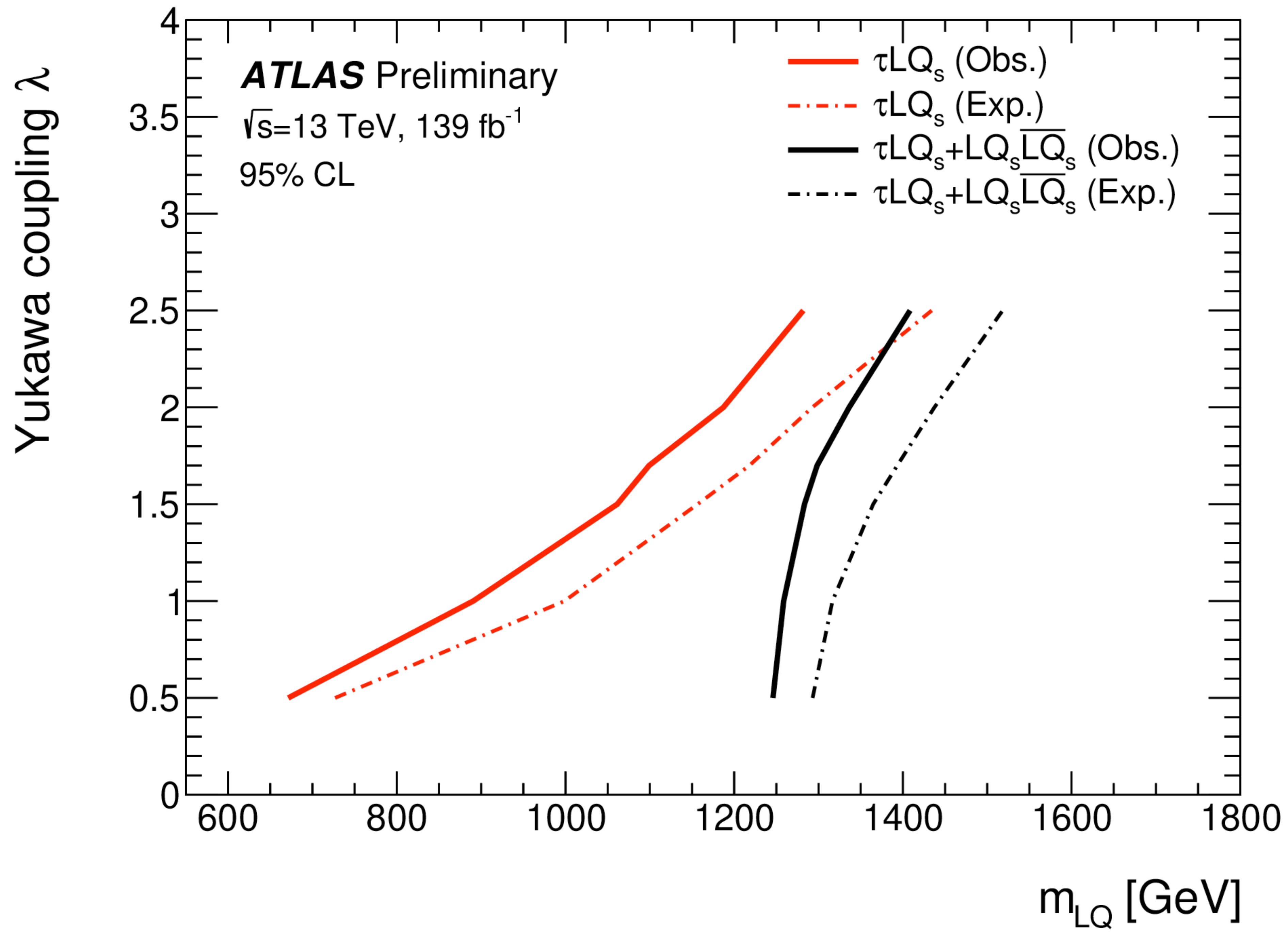

Search for invisible particles produced in association with single top quarks in proton-proton collisions at 13 TeV with the ATLAS detector

- https://atlas.web.cern.ch/Atlas/GROUPS/PHYSICS/CONFNOTES/ATLAS-CONF-2022-036/
- A search for events with one top quark and missing transverse momentum in the final state is presented. The fully hadronic decay of the top quark is explored by selecting events with a reconstructed boosted top quark topology produced in association with large missing transverse momentum. The analysis uses 139 fb−1 of proton--proton collision data at a centre-of-mass energy of 13 TeV recorded during 2015-2018 by the ATLAS detector at the Large Hadron Collider. The results are interpreted in terms of simplified models for Dark Matter particle production and the single production of a vector-like *T* quark. In the absence of a significant excess with respect to the Standard Model expectations, 95% confidence-level upper limits on the corresponding cross-sections are obtained. The production of Dark Matter particles in association with a single top quark is excluded for masses of a scalar (vector) mediator up to 5.0 (2.8) TeV assuming a resonant (non-resonant) model, extending the previous mediator mass limits by 1.5 (0.9) TeV. The production of a single vector-like *T* quark is excluded for masses *mT*<2.2 TeV assuming a coupling to the top quark *κT* =0.5 and a branching ratio for *T*→*Zt* of 25%, representing an improvement with respect to previous mass limits of approximately 500 GeV.

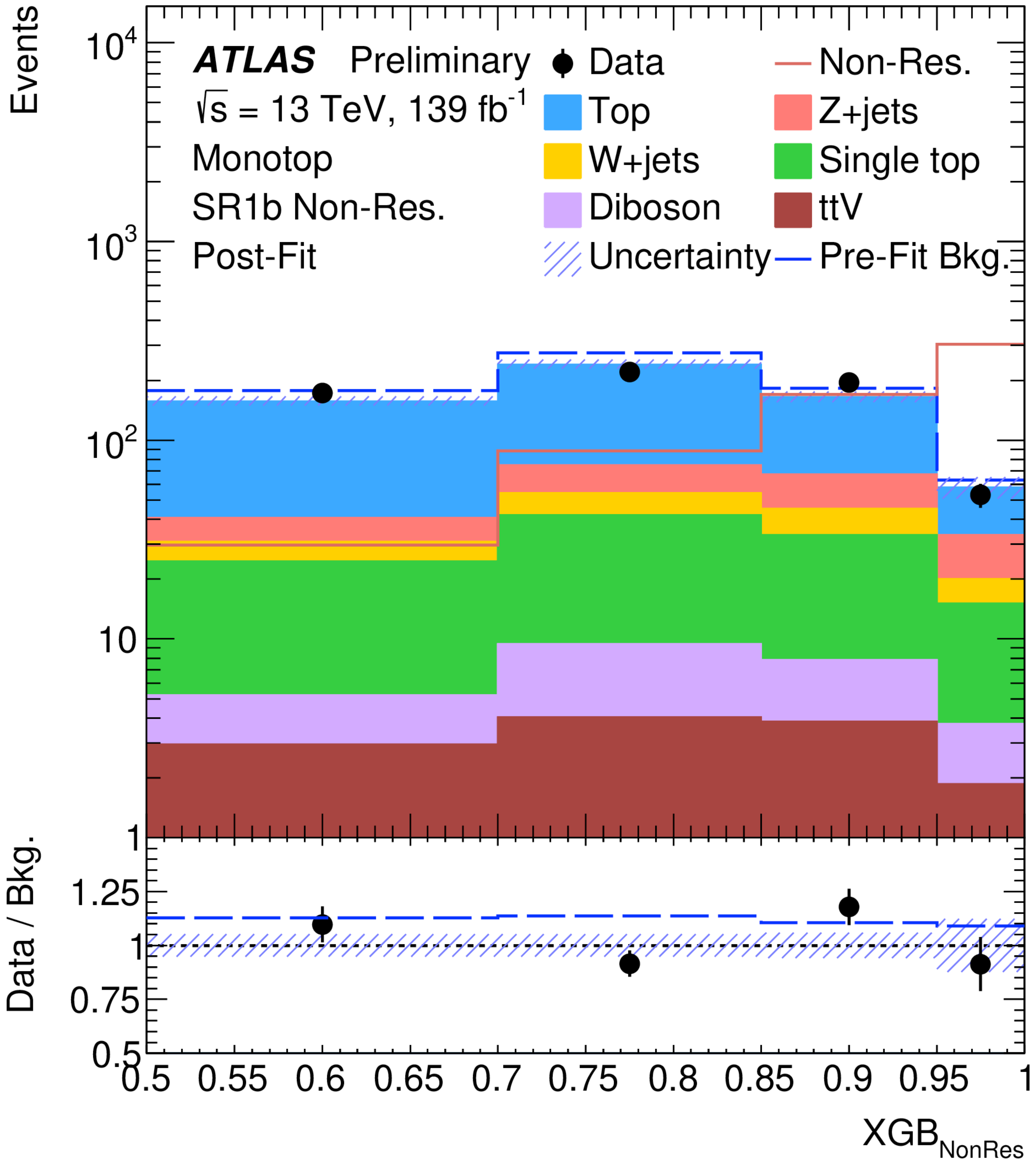

Search for leptoquark pair production decaying into tℓ–t̄ ℓ+ in multilepton final states in pp collisions at 13 TeV with the ATLAS detector

- https://atlas.web.cern.ch/Atlas/GROUPS/PHYSICS/CONFNOTES/ATLAS-CONF-2022-052/
- A search for leptoquark pair production decaying to tℓ–t̄ ℓ+ in final states with multiple leptons is presented. The search is based on a dataset of *pp* collisions at 13 TeV recorded with the ATLAS detector during Run 2 of the Large Hadron Collider, corresponding to an integrated luminosity of 139 fb–1. Events are selected with two or more light leptons (electron or muon) and at least two jets out of which at least one jet identified as coming from *b*-hadron. Four signal regions, with the requirement of at least three light leptons, are considered based on the number of predominant lepton flavour. The main background processes are estimated using dedicated control regions in a simultaneous fit with the signal regions to data. No excess above the Standard Model background prediction is observed and 95\% confidence level limits on the production cross section times branching ratio are derived as a function of the leptoquark mass. Under the assumption of exclusive decays into *te* (*tμ*), the corresponding lower limit on the scalar mixed-generation leptoquark mass *mL Q d* mix is at 1.61 (1.64) TeV and on the vector leptoquark mass *m Ũ*1 at 1.71 (1.73) TeV in minimal coupling scenario and at 2.0 (2.0) TeV in Yang-Mills scenario.

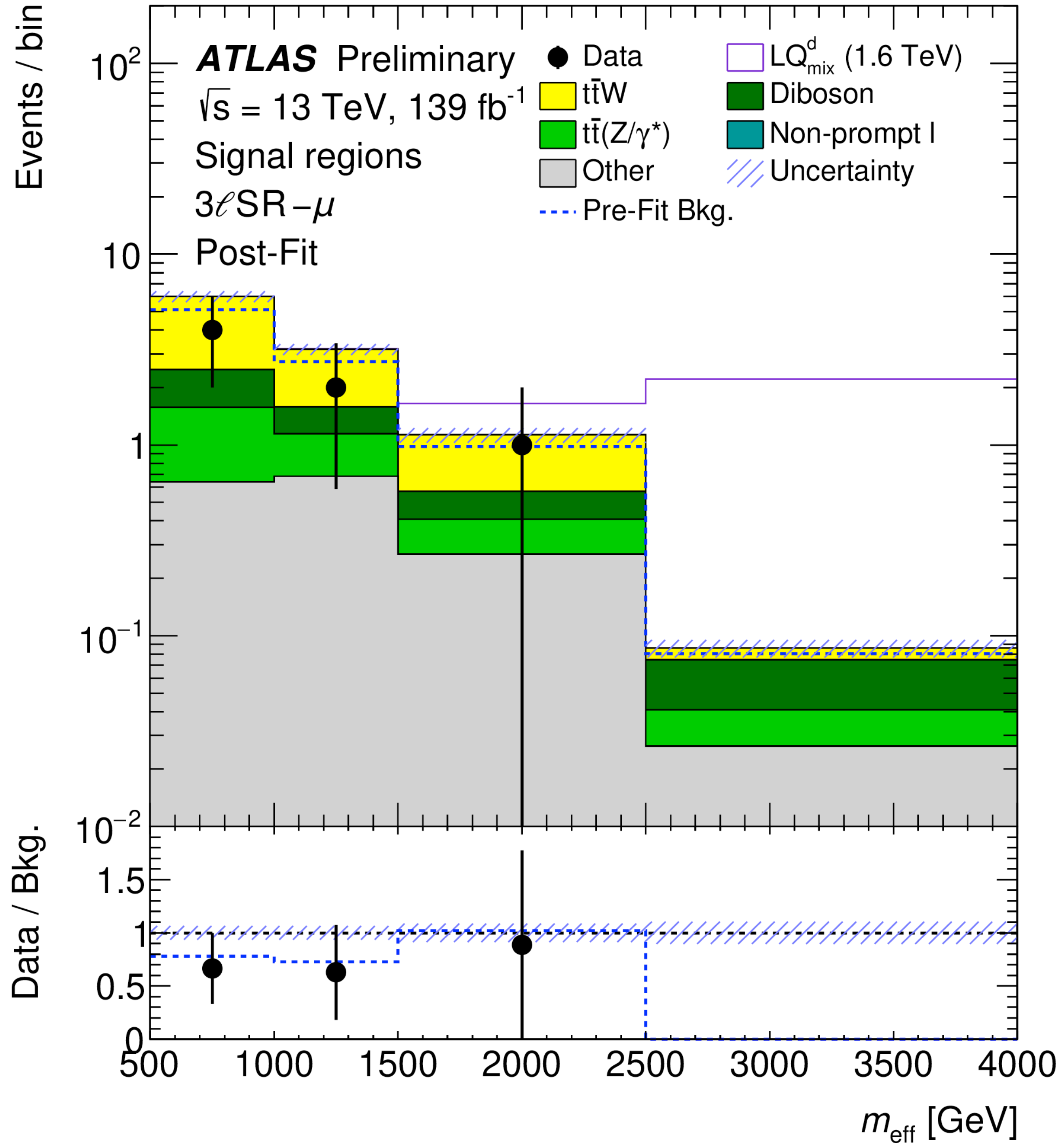

Combined effective field theory interpretation of Higgs boson and weak boson production and decay with ATLAS data and electroweak precision observables

- https://atlas.web.cern.ch/Atlas/GROUPS/PHYSICS/PUBNOTES/ATL-PHYS-PUB-2022-037/

- Wilson coefficients of the Standard Model Effective Field Theory (SMEFT) are constrained in a combined fit of measurements of Higgs boson production and decay in the framework of Simplified Template Cross Sections and differential cross-section measurements of weak boson production at the ATLAS experiment as well as electroweak precision observables measured at the LEP and SLC colliders. The ATLAS measurements are based on 36-139 fb−1 of proton-proton collision data collected at the LHC at 13 TeV. The SMEFT interpretation is performed using a combined likelihood function that takes into account experimental uncertainties and their correlation as well as theoretical uncertainties on Standard Model predictions. Constraints on 28 Wilson coefficients and their mutually orthogonal linear combinations are determined. No new deviations from the SM are observed.

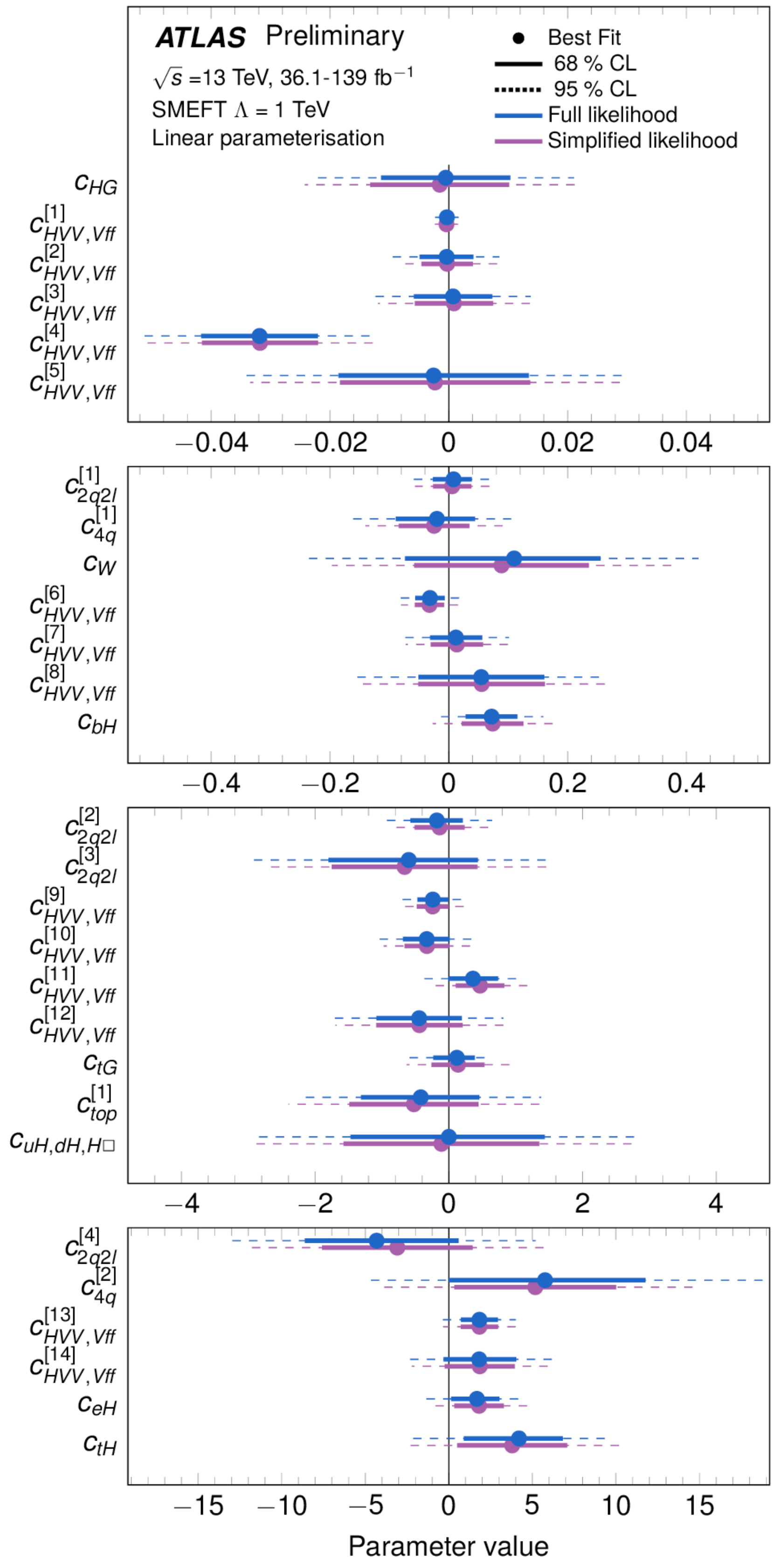

Search for non-resonant pair production of Higgs bosons in the $b\bar{b}b\bar{b}$ final state in *pp* collisions at 13 TeV with the ATLAS detector

- https://atlas.web.cern.ch/Atlas/GROUPS/PHYSICS/CONFNOTES/ATLAS-CONF-2022-035/
- "A search for non-resonant Higgs boson pair production in the $b\bar{b}\,b\bar{b}$ final state is presented. The analysis uses 126 fb −1 of *pp* collision data at 13 TeV collected with the ATLAS detector at the Large Hadron Collider, and targets both the gluon-gluon fusion and vector-boson fusion production modes. No evidence for signal is found and the observed (expected) upper limit on the cross section for non-resonant Higgs boson pair production is determined to be 5.4 (8.1) times the Standard Model predicted cross-section at 95% confidence level. Constraints are placed upon modifiers to the *HHH* and*HHVV* couplings. The observed (expected) constraints on the *HHH* coupling modifier, *κλ*, are determined to be [-3.9, 11.1] ([-4.6, 10.8]) at 95% confidence level, while the corresponding constraints for the *HHVV* coupling modifier, *κ2V*, are [-0.03, 2.11] ([-0.05, 2.12])."

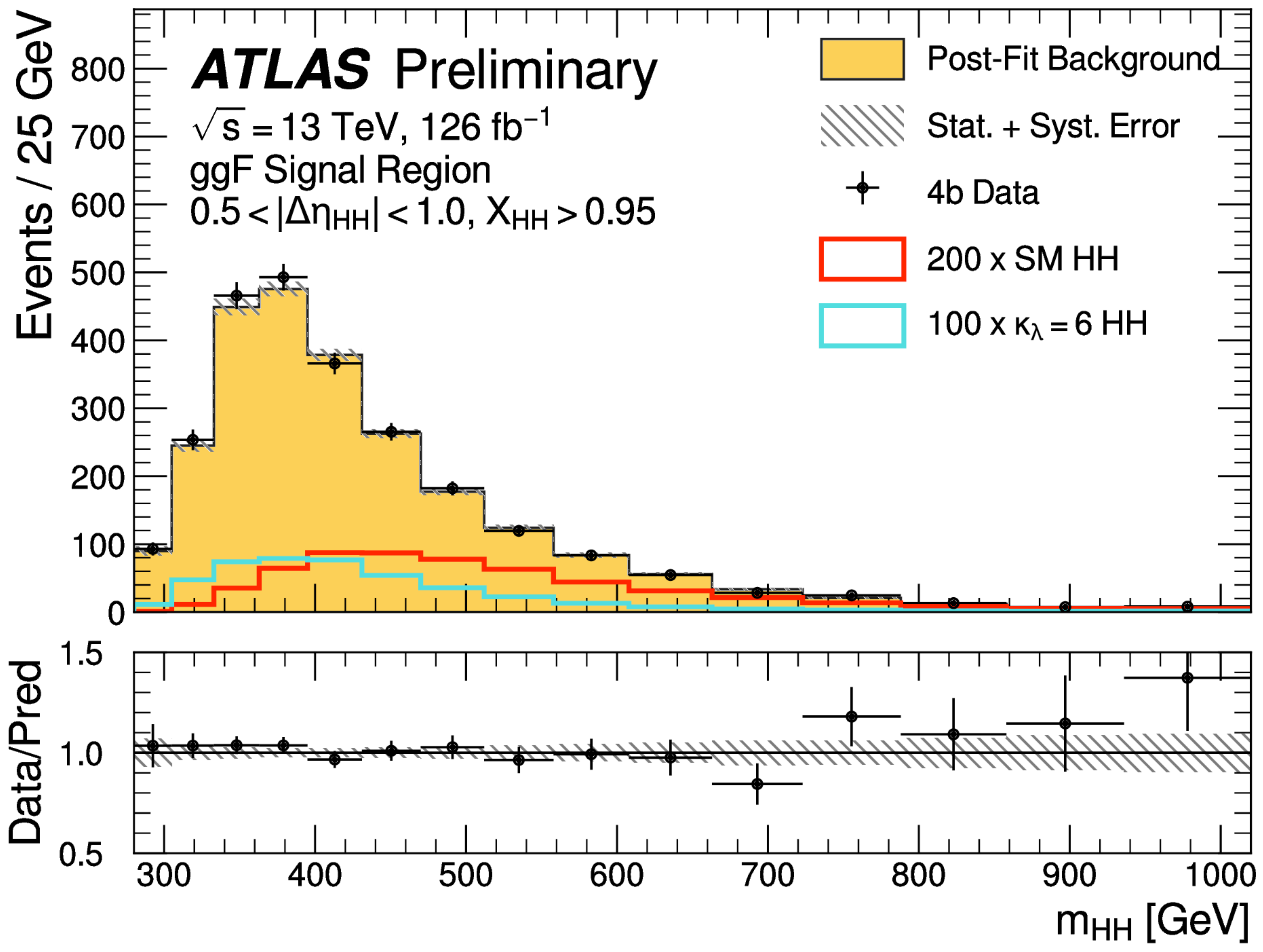

Studies of the muon momentum calibration and performance of the ATLAS detector with pp collisions at 13TeV

- https://atlas.web.cern.ch/Atlas/GROUPS/PHYSICS/PAPERS/MUON-2022-01/

- This paper presents the muon momentum calibration and performance studies for the ATLAS detector based on the *pp* collisions data sample produced at 13 TeV at the LHC during Run 2 and corresponding to an integrated luminosity of 139 fb–1 An innovative approach is used to correct for potential charge-dependent momentum biases related to the knowledge of the detector geometry, using the $Z \rightarrow \mu\mu$ resonance. The muon momentum scale and resolution are measured using samples of $J/\psi \rightarrow \mu\mu$ and $Z \rightarrow \mu\mu$ events. A calibration procedure is defined and applied to simulated data to match the performance measured in real data. The calibration is validated using an independent sample of $\Upsilon \rightarrow \mu\mu$ events. At the Z (J/ψ) peak, the momentum scale is measured with an uncertainty at the 0.05% (0.1%) level, and the resolution is measured with an uncertainty at the 1.5% (2%) level. The charge-dependent bias is removed with a dedicated *in situ* correction for momenta up to 450 GeV with a precision better than 0.03 TeV–1.

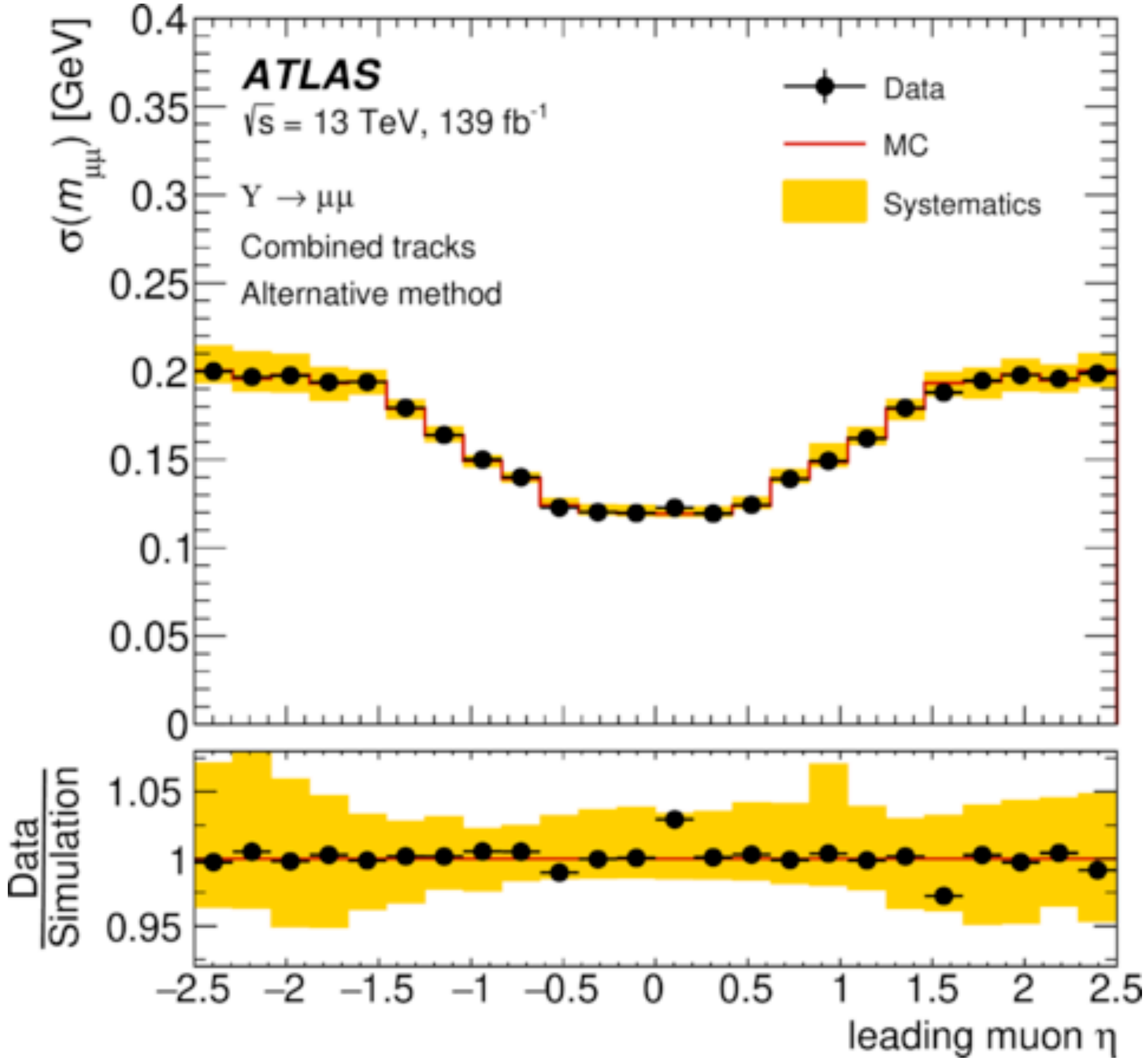

Tools for estimating fake/non-prompt lepton backgrounds with the ATLAS detector at the LHC

- https://atlas.web.cern.ch/Atlas/GROUPS/PHYSICS/PAPERS/EGAM-2019-01/
- Measurements and searches performed with the ATLAS detector at the CERN Large Hadron Collider often involve signatures with one or more prompt leptons. Such analyses are subject to `fake/non-prompt' lepton backgrounds, where either a hadron or a lepton from a hadron decay or an electron from a photon conversion satisfies the prompt-lepton selection criteria. These backgrounds often arise within a hadronic jet because of particle decays in the showering process, particle misidentification or particle interactions with the detector material. As it is challenging to model these processes with high accuracy in simulation, their estimation typically uses data-driven methods. Three methods for carrying out this estimation are described, along with their implementation in ATLAS and their performance.

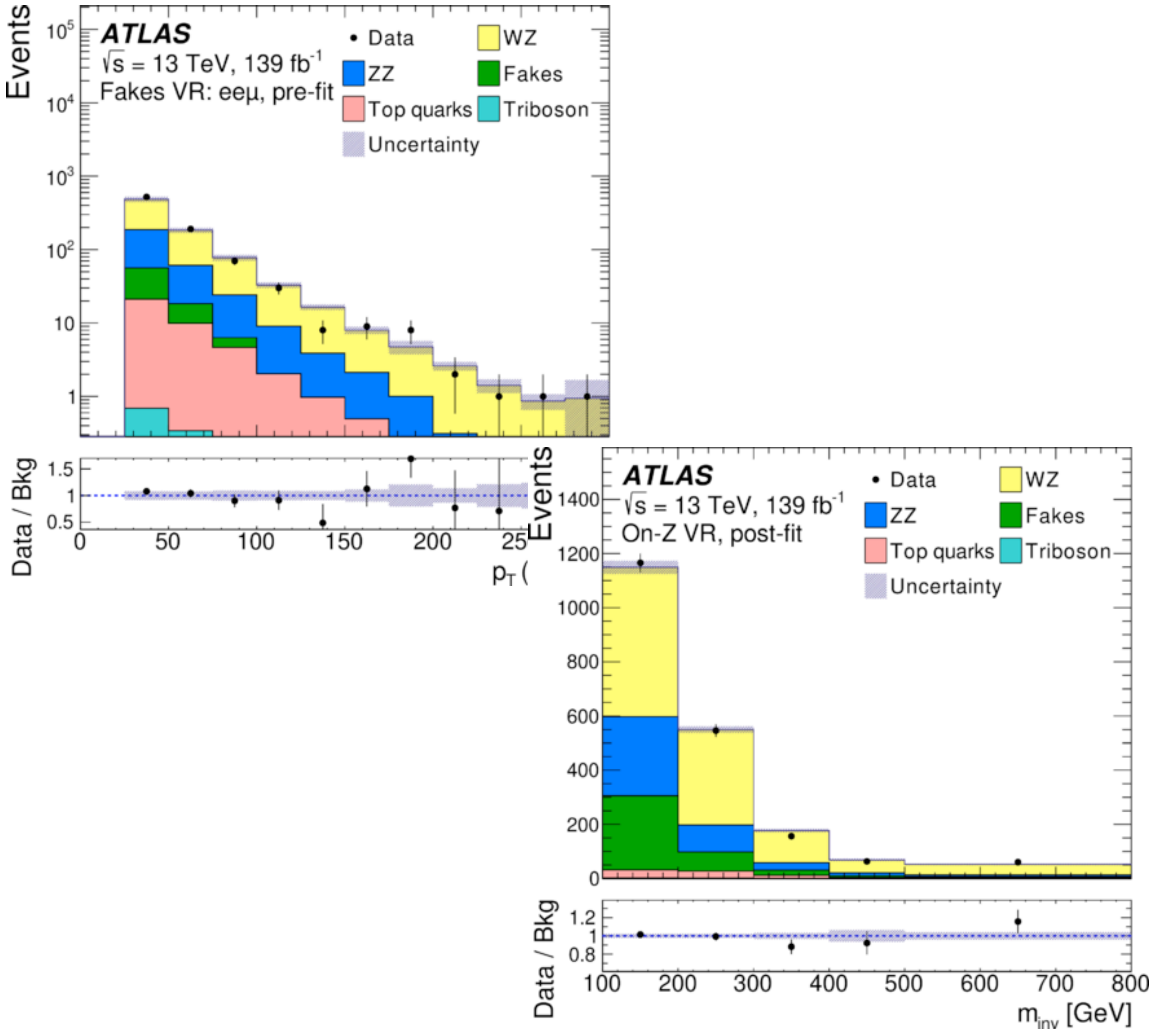

ATLAS flavour-tagging algorithms for the LHC Run 2 *pp* collision dataset

- https://atlas.web.cern.ch/Atlas/GROUPS/PHYSICS/PAPERS/FTAG-2019-07/
- The flavour-tagging algorithms developed by the ATLAS Collaboration and used to analyse its dataset of 13 TeV *pp* collisions from Run 2 of the Large Hadron Collider are presented. These new tagging algorithms are based on recurrent and deep neural networks, and their performance is evaluated in simulated collision events. These developments yield considerable improvements over previous jet-flavour identification strategies. At the 70% *b*-jet identification efficiency operating point, light-jet (charm-jet) rejection factors of 600 (11) are achieved in a sample of simulated Standard Model $t\bar{t}$ events; similarly, at a *c*-jet identification efficiency of 30%, a light-jet (*b*-jet) rejection factor of 70 (9) is obtained.

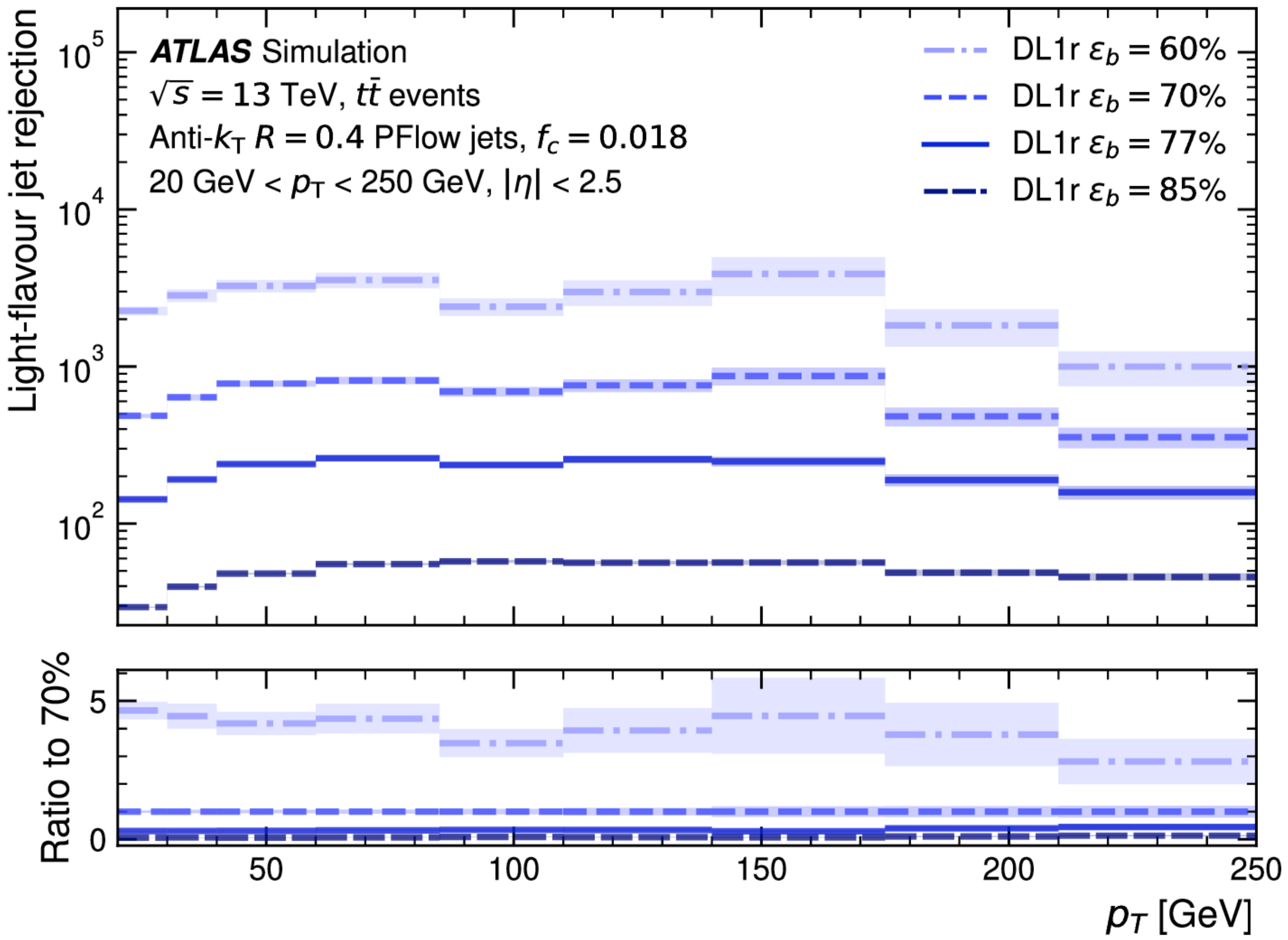

ATLAS Pixel detector readies to tackle Run 3

- https://atlas.cern/Updates/Briefing/ATLAS-Pixel-Detector-Run3
- https://atlas.web.cern.ch/Atlas/GROUPS/PHYSICS/PUBNOTES/ATL-PHYS-PUB-2022-033/

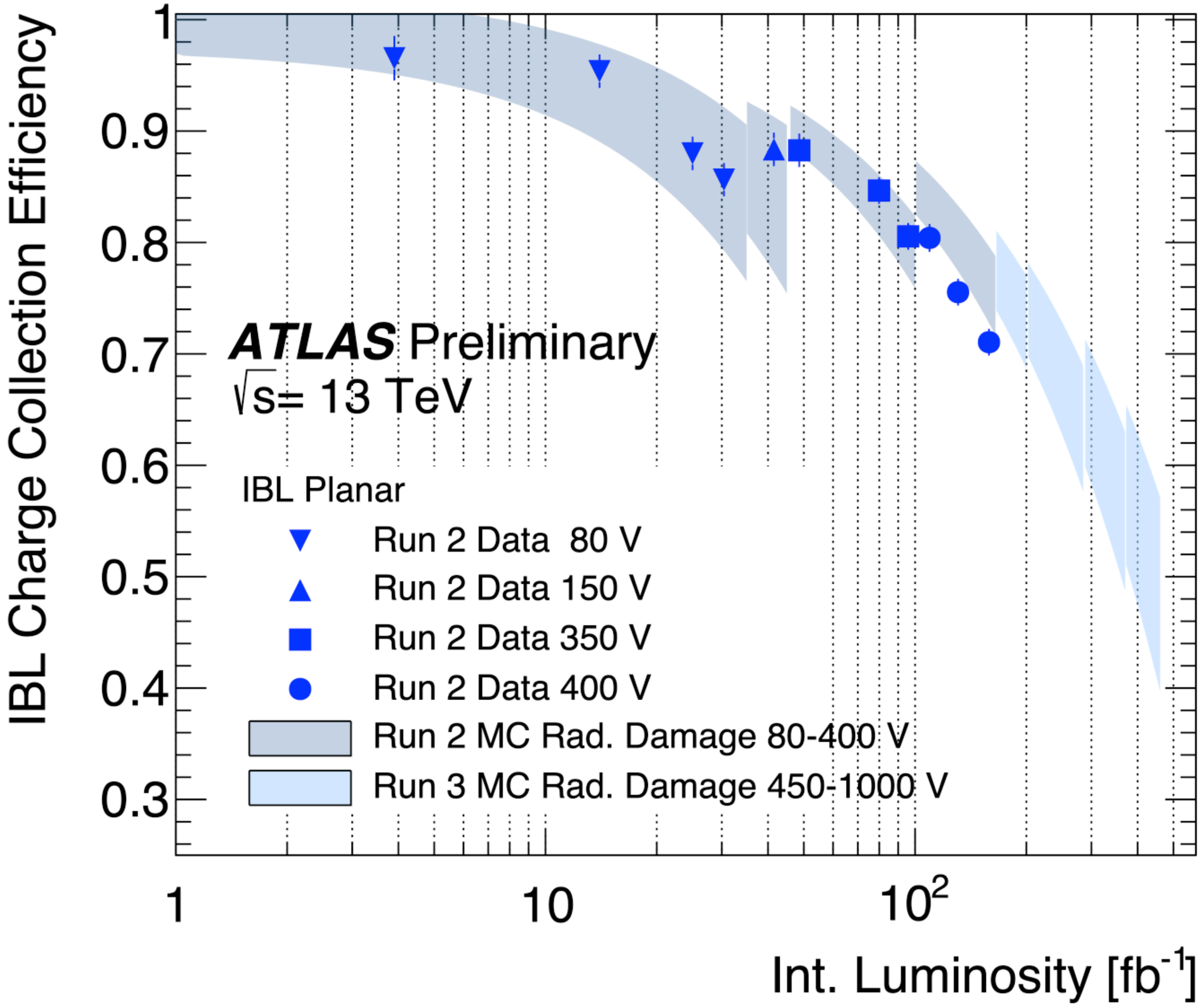

Status: October 2022

- Argentina
- Armenia
- Australia
- Austria
- Azerbaijan
- Belarus
- Brazil
- Canada
- Chile
- China
- Colombia
- Czech Republic
- Denmark
- France
- Georgia
- Germany
- Greece
- Israel
- Italy
- Japan
- Mongolia
- Morocco
- Netherlands
- Norway
- Palestine
- Philippines
- Poland
- Portugal
- Romania
- Russia
- Serbia
- Slovakia
- Slovenia
- South Africa
- Spain
- Sweden
- Switzerland
- Taiwan
- Türkiye
- UAE
- UK
- USA
- CERN
- JINR

ATLAS Collaboration

181 institutions (247 institutes) from 42 countries

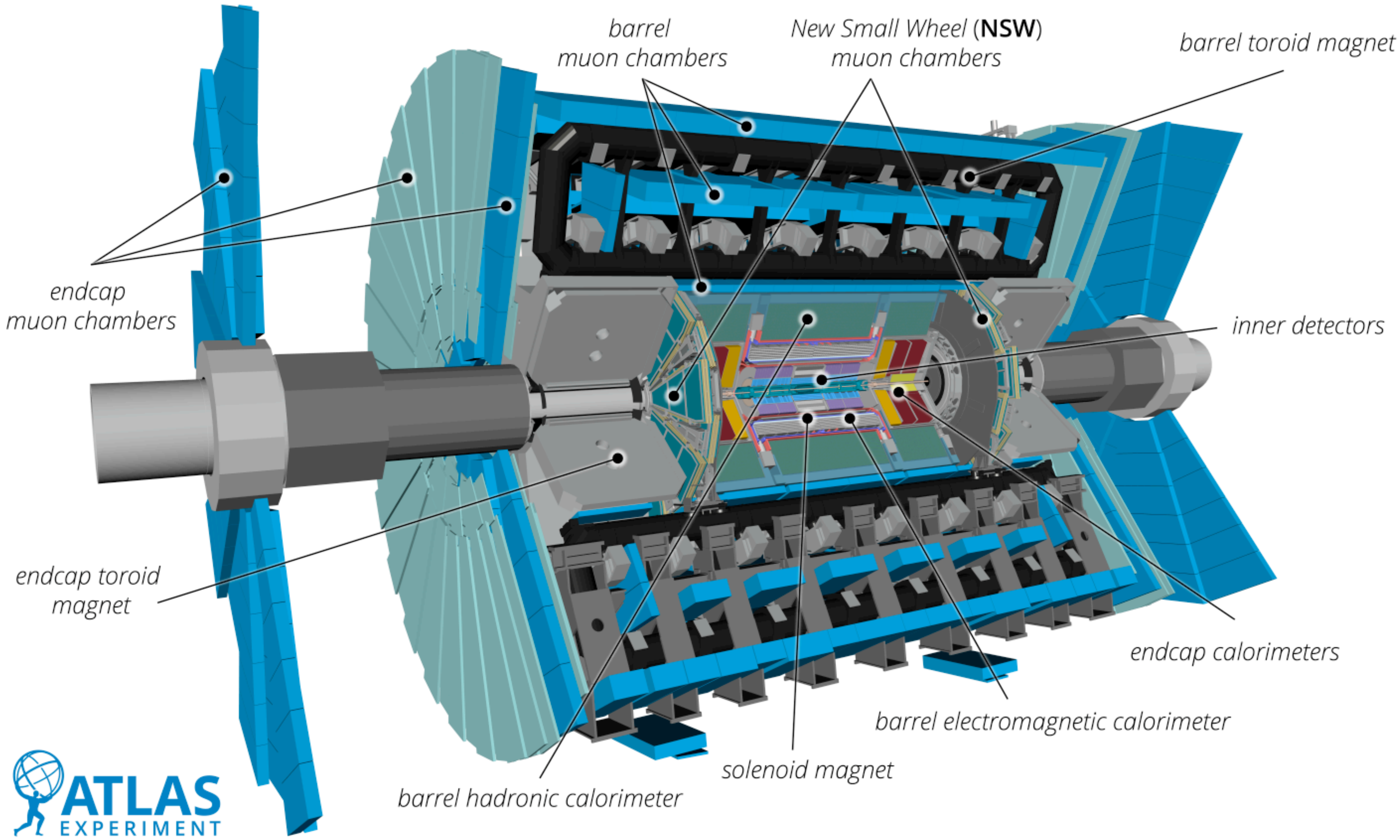
barrel muon chambers
New Small Wheel (**NSW**) muon chambers
barrel toroid magnet
endcap muon chambers
inner detectors
endcap toroid magnet
endcap calorimeters
barrel electromagnetic calorimeter
solenoid magnet
barrel hadronic calorimeter
ATLAS EXPERIMENT

ATLAS Long-lived Particle Searches* - 95% CL Exclusion

Status: July 2022

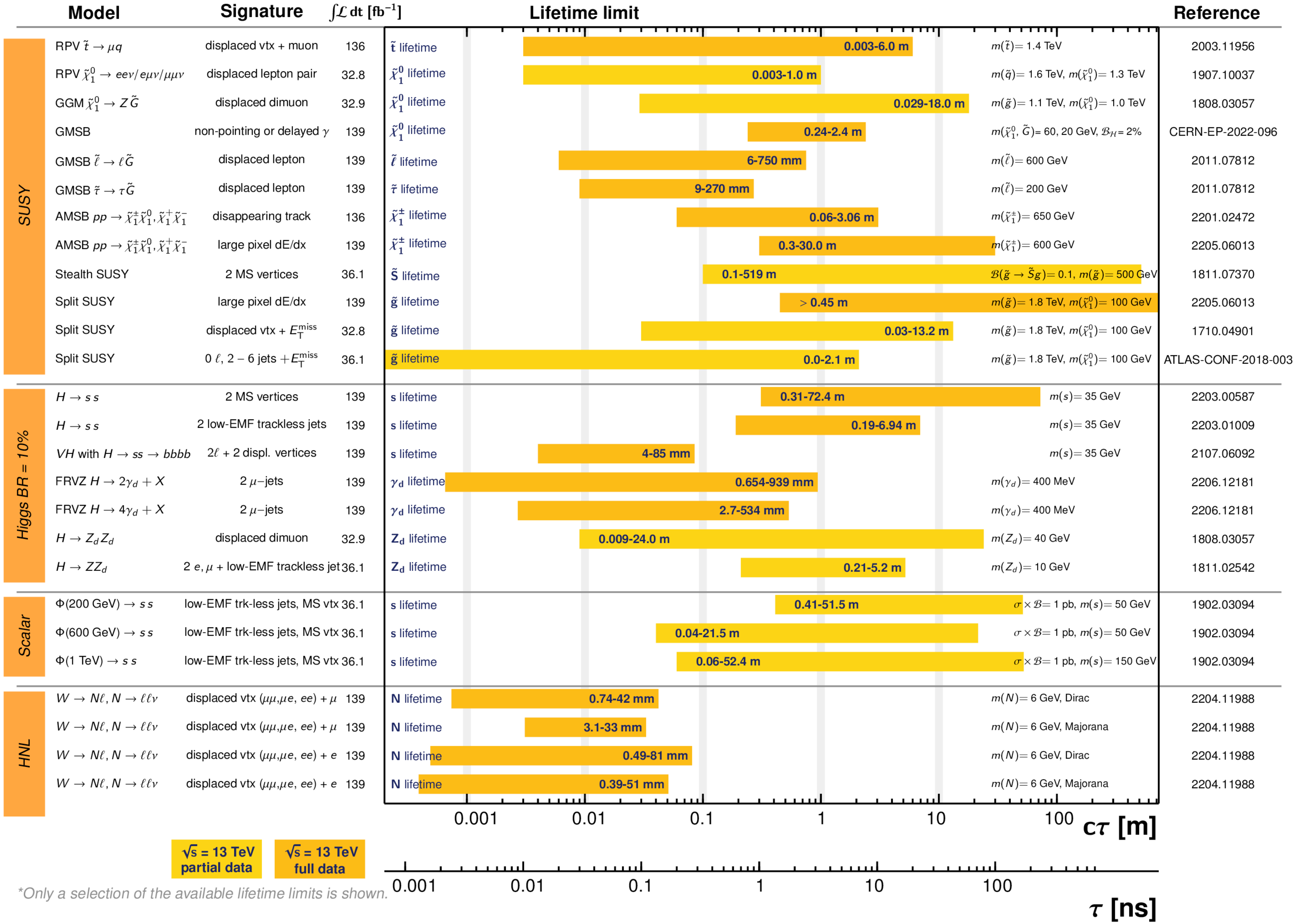

	Model	Signature	$\int\mathcal{L}\,dt$ [fb^{-1}]	Lifetime limit			Reference
SUSY	RPV $\tilde{t} \to \mu q$	displaced vtx + muon	136	$\tilde{t}$ lifetime	0.003-6.0 m	$m(\tilde{t})$= 1.4 TeV	2003.11956
	RPV $\tilde{\chi}_1^0 \to ee\nu/e\mu\nu/\mu\mu\nu$	displaced lepton pair	32.8	$\tilde{\chi}_1^0$ lifetime	0.003-1.0 m	$m(\tilde{q})$= 1.6 TeV, $m(\tilde{\chi}_1^0)$= 1.3 TeV	1907.10037
	GGM $\tilde{\chi}_1^0 \to Z\tilde{G}$	displaced dimuon	32.9	$\tilde{\chi}_1^0$ lifetime	0.029-18.0 m	$m(\tilde{g})$= 1.1 TeV, $m(\tilde{\chi}_1^0)$= 1.0 TeV	1808.03057
	GMSB	non-pointing or delayed γ	139	$\tilde{\chi}_1^0$ lifetime	0.24-2.4 m	$m(\tilde{\chi}_1^0, \tilde{G})$= 60, 20 GeV, $\mathcal{B}_{\mathcal{H}}$= 2%	CERN-EP-2022-096
	GMSB $\tilde{\ell} \to \ell\tilde{G}$	displaced lepton	139	$\tilde{\ell}$ lifetime	6-750 mm	$m(\tilde{\ell})$= 600 GeV	2011.07812
	GMSB $\tilde{\tau} \to \tau\tilde{G}$	displaced lepton	139	$\tilde{\tau}$ lifetime	9-270 mm	$m(\tilde{\ell})$= 200 GeV	2011.07812
	AMSB $pp \to \tilde{\chi}_1^{\pm}\tilde{\chi}_1^0, \tilde{\chi}_1^+\tilde{\chi}_1^-$	disappearing track	136	$\tilde{\chi}_1^{\pm}$ lifetime	0.06-3.06 m	$m(\tilde{\chi}_1^{\pm})$= 650 GeV	2201.02472
	AMSB $pp \to \tilde{\chi}_1^{\pm}\tilde{\chi}_1^0, \tilde{\chi}_1^+\tilde{\chi}_1^-$	large pixel dE/dx	139	$\tilde{\chi}_1^{\pm}$ lifetime	0.3-30.0 m	$m(\tilde{\chi}_1^{\pm})$= 600 GeV	2205.06013
	Stealth SUSY	2 MS vertices	36.1	$\tilde{S}$ lifetime	0.1-519 m	$\mathcal{B}(\tilde{g} \to \tilde{S}g)$= 0.1, $m(\tilde{g})$= 500 GeV	1811.07370
	Split SUSY	large pixel dE/dx	139	$\tilde{g}$ lifetime	> 0.45 m	$m(\tilde{g})$= 1.8 TeV, $m(\tilde{\chi}_1^0)$= 100 GeV	2205.06013
	Split SUSY	displaced vtx + E_T^{miss}	32.8	$\tilde{g}$ lifetime	0.03-13.2 m	$m(\tilde{g})$= 1.8 TeV, $m(\tilde{\chi}_1^0)$= 100 GeV	1710.04901
	Split SUSY	$0\ \ell$, $2-6$ jets $+E_T^{\mathrm{miss}}$	36.1	$\tilde{g}$ lifetime	0.0-2.1 m	$m(\tilde{g})$= 1.8 TeV, $m(\tilde{\chi}_1^0)$= 100 GeV	ATLAS-CONF-2018-003
Higgs BR = 10%	$H \to s\,s$	2 MS vertices	139	s lifetime	0.31-72.4 m	$m(s)$= 35 GeV	2203.00587
	$H \to s\,s$	2 low-EMF trackless jets	139	s lifetime	0.19-6.94 m	$m(s)$= 35 GeV	2203.01009
	VH with $H \to ss \to bbbb$	2ℓ + 2 displ. vertices	139	s lifetime	4-85 mm	$m(s)$= 35 GeV	2107.06092
	FRVZ $H \to 2\gamma_d + X$	2 μ–jets	139	γ_d lifetime	0.654-939 mm	$m(\gamma_d)$= 400 MeV	2206.12181
	FRVZ $H \to 4\gamma_d + X$	2 μ–jets	139	γ_d lifetime	2.7-534 mm	$m(\gamma_d)$= 400 MeV	2206.12181
	$H \to Z_d Z_d$	displaced dimuon	32.9	Z_d lifetime	0.009-24.0 m	$m(Z_d)$= 40 GeV	1808.03057
	$H \to ZZ_d$	2 e,μ + low-EMF trackless jet	36.1	Z_d lifetime	0.21-5.2 m	$m(Z_d)$= 10 GeV	1811.02542
Scalar	Φ(200 GeV) $\to s\,s$	low-EMF trk-less jets, MS vtx	36.1	s lifetime	0.41-51.5 m	$\sigma \times \mathcal{B}$= 1 pb, $m(s)$= 50 GeV	1902.03094
	Φ(600 GeV) $\to s\,s$	low-EMF trk-less jets, MS vtx	36.1	s lifetime	0.04-21.5 m	$\sigma \times \mathcal{B}$= 1 pb, $m(s)$= 50 GeV	1902.03094
	Φ(1 TeV) $\to s\,s$	low-EMF trk-less jets, MS vtx	36.1	s lifetime	0.06-52.4 m	$\sigma \times \mathcal{B}$= 1 pb, $m(s)$= 150 GeV	1902.03094
HNL	$W \to N\ell, N \to \ell\ell\nu$	displaced vtx ($\mu\mu$,μe, ee) + μ	139	N lifetime	0.74-42 mm	$m(N)$= 6 GeV, Dirac	2204.11988
	$W \to N\ell, N \to \ell\ell\nu$	displaced vtx ($\mu\mu$,μe, ee) + μ	139	N lifetime	3.1-33 mm	$m(N)$= 6 GeV, Majorana	2204.11988
	$W \to N\ell, N \to \ell\ell\nu$	displaced vtx ($\mu\mu$,μe, ee) + e	139	N lifetime	0.49-81 mm	$m(N)$= 6 GeV, Dirac	2204.11988
	$W \to N\ell, N \to \ell\ell\nu$	displaced vtx ($\mu\mu$,μe, ee) + e	139	N lifetime	0.39-51 mm	$m(N)$= 6 GeV, Majorana	2204.11988

*Only a selection of the available lifetime limits is shown.

ATLAS Heavy Particle Searches* - 95% CL Upper Exclusion Limits

Status: July 2022

ATLAS Preliminary

$\int\mathcal{L}\,dt = (3.6 - 139)\ \mathrm{fb}^{-1}$ $\sqrt{s} = 8, 13$ TeV

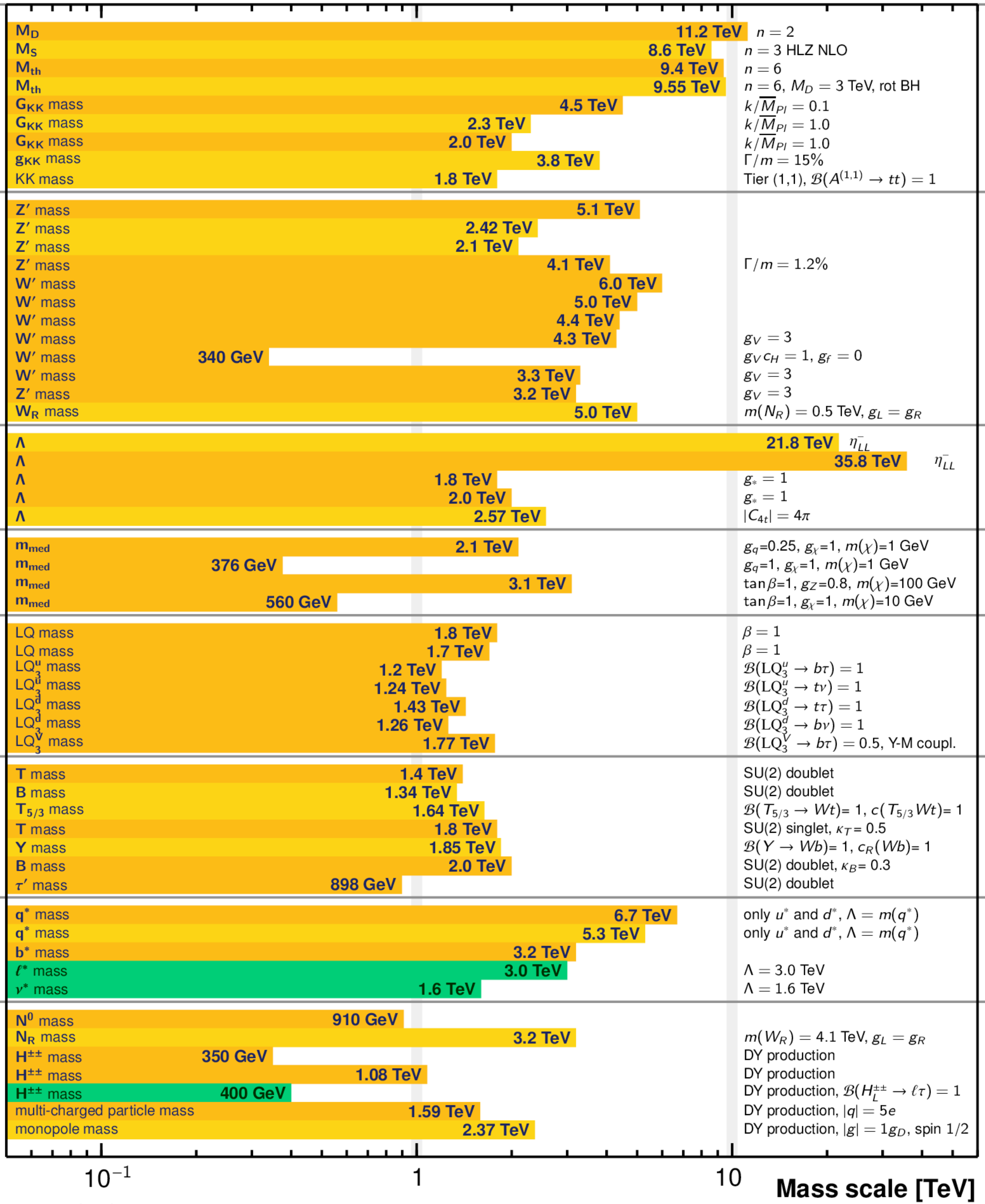

	Model	ℓ,γ	Jets†	E_T^{miss}	$\int\mathcal{L}\,dt[\mathrm{fb}^{-1}]$	Limit			Reference
Extra dimensions	ADD $G_{KK}+g/q$	$0\ e,\mu,\tau,\gamma$	1 – 4 j	Yes	139	M_D	11.2 TeV	$n=2$	2102.10874
	ADD non-resonant $\gamma\gamma$	$2\ \gamma$	–	–	36.7	M_S	8.6 TeV	$n=3$ HLZ NLO	1707.04147
	ADD QBH	–	2 j	–	139	M_{th}	9.4 TeV	$n=6$	1910.08447
	ADD BH multijet	–	≥3 j	–	3.6	M_{th}	9.55 TeV	$n=6$, $M_D=3$ TeV, rot BH	1512.02586
	RS1 $G_{KK}\to\gamma\gamma$	$2\ \gamma$	–	–	139	G_{KK} mass	4.5 TeV	$k/\overline{M}_{Pl}=0.1$	2102.13405
	Bulk RS $G_{KK}\to WW/ZZ$	multi-channel			36.1	G_{KK} mass	2.3 TeV	$k/\overline{M}_{Pl}=1.0$	1808.02380
	Bulk RS $G_{KK}\to WV\to\ell\nu qq$	$1\ e,\mu$	2 j / 1 J	Yes	139	G_{KK} mass	2.0 TeV	$k/\overline{M}_{Pl}=1.0$	2004.14636
	Bulk RS $g_{KK}\to tt$	$1\ e,\mu$	≥1 b, ≥1J/2j	Yes	36.1	g_{KK} mass	3.8 TeV	$\Gamma/m=15\%$	1804.10823
	2UED / RPP	$1\ e,\mu$	≥2 b, ≥3 j	Yes	36.1	KK mass	1.8 TeV	Tier (1,1), $\mathcal{B}(A^{(1,1)}\to tt)=1$	1803.09678
Gauge bosons	SSM $Z'\to\ell\ell$	$2\ e,\mu$	–	–	139	Z' mass	5.1 TeV		1903.06248
	SSM $Z'\to\tau\tau$	$2\ \tau$	–	–	36.1	Z' mass	2.42 TeV		1709.07242
	Leptophobic $Z'\to bb$	–	2 b	–	36.1	Z' mass	2.1 TeV		1805.09299
	Leptophobic $Z'\to tt$	$0\ e,\mu$	≥1 b, ≥2 J	Yes	139	Z' mass	4.1 TeV	$\Gamma/m=1.2\%$	2005.05138
	SSM $W'\to\ell\nu$	$1\ e,\mu$	–	Yes	139	W' mass	6.0 TeV		1906.05609
	SSM $W'\to\tau\nu$	$1\ \tau$	–	Yes	139	W' mass	5.0 TeV		ATLAS-CONF-2021-025
	SSM $W'\to tb$	–	≥1 b, ≥1 J	–	139	W' mass	4.4 TeV		ATLAS-CONF-2021-043
	HVT $W'\to WZ\to\ell\nu qq$ model B	$1\ e,\mu$	2 j / 1 J	Yes	139	W' mass	4.3 TeV	$g_V=3$	2004.14636
	HVT $W'\to WZ\to\ell\nu\,\ell'\ell'$ model C	$3\ e,\mu$	2 j (VBF)	Yes	139	W' mass	340 GeV	$g_V c_H=1$, $g_f=0$	ATLAS-CONF-2022-005
	HVT $W'\to WH\to\ell\nu bb$ model B	$1\ e,\mu$	1-2 b, 1-0 j	Yes	139	W' mass	3.3 TeV	$g_V=3$	2207.00230
	HVT $Z'\to ZH\to\ell\ell/\nu\nu bb$ model B	$0,2\ e,\mu$	1-2 b, 1-0 j	Yes	139	Z' mass	3.2 TeV	$g_V=3$	2207.00230
	LRSM $W_R\to\mu N_R$	$2\ \mu$	1 J	–	80	W_R mass	5.0 TeV	$m(N_R)=0.5$ TeV, $g_L=g_R$	1904.12679
CI	CI $qqqq$	–	2 j	–	37.0	Λ	21.8 TeV	η_{LL}^{-}	1703.09127
	CI $\ell\ell qq$	$2\ e,\mu$	–	–	139	Λ	35.8 TeV	η_{LL}^{-}	2006.12946
	CI $eebs$	$2\ e$	1 b	–	139	Λ	1.8 TeV	$g_*=1$	2105.13847
	CI $\mu\mu bs$	$2\ \mu$	1 b	–	139	Λ	2.0 TeV	$g_*=1$	2105.13847
	CI $tttt$	$\geq1\ e,\mu$	≥1 b, ≥1 j	Yes	36.1	Λ	2.57 TeV	$\lvert C_{4t}\rvert=4\pi$	1811.02305
DM	Axial-vector med. (Dirac DM)	$0\ e,\mu,\tau,\gamma$	1 – 4 j	Yes	139	m_{med}	2.1 TeV	g_q=0.25, g_χ=1, $m(\chi)$=1 GeV	2102.10874
	Pseudo-scalar med. (Dirac DM)	$0\ e,\mu,\tau,\gamma$	1 – 4 j	Yes	139	m_{med}	376 GeV	g_q=1, g_χ=1, $m(\chi)$=1 GeV	2102.10874
	Vector med. Z'-2HDM (Dirac DM)	$0\ e,\mu$	2 b	Yes	139	m_{med}	3.1 TeV	tanβ=1, g_Z=0.8, $m(\chi)$=100 GeV	2108.13391
	Pseudo-scalar med. 2HDM+a	multi-channel			139	m_{med}	560 GeV	tanβ=1, g_χ=1, $m(\chi)$=10 GeV	ATLAS-CONF-2021-036
LQ	Scalar LQ 1st gen	$2\ e$	≥2 j	Yes	139	LQ mass	1.8 TeV	$\beta=1$	2006.05872
	Scalar LQ 2nd gen	$2\ \mu$	≥2 j	Yes	139	LQ mass	1.7 TeV	$\beta=1$	2006.05872
	Scalar LQ 3rd gen	$1\ \tau$	2 b	Yes	139	LQ_3^u mass	1.2 TeV	$\mathcal{B}(\mathrm{LQ}_3^u\to b\tau)=1$	2108.07665
	Scalar LQ 3rd gen	$0\ e,\mu$	≥2 j, ≥2 b	Yes	139	LQ_3^u mass	1.24 TeV	$\mathcal{B}(\mathrm{LQ}_3^u\to t\nu)=1$	2004.14060
	Scalar LQ 3rd gen	$\geq2\ e,\mu,\geq1\ \tau$	≥1 j, ≥1 b	–	139	LQ_3^d mass	1.43 TeV	$\mathcal{B}(\mathrm{LQ}_3^d\to t\tau)=1$	2101.11582
	Scalar LQ 3rd gen	$0\ e,\mu,\geq1\ \tau$	0 – 2 j, 2 b	Yes	139	LQ_3^d mass	1.26 TeV	$\mathcal{B}(\mathrm{LQ}_3^d\to b\nu)=1$	2101.12527
	Vector LQ 3rd gen	$1\ \tau$	2 b	Yes	139	LQ_3^V mass	1.77 TeV	$\mathcal{B}(\mathrm{LQ}_3^V\to b\tau)=0.5$, Y-M coupl.	2108.07665
Vector-like fermions	VLQ $TT\to Zt+X$	2e/2μ/≥3e,μ	≥1 b, ≥1 j	–	139	T mass	1.4 TeV	SU(2) doublet	ATLAS-CONF-2021-024
	VLQ $BB\to Wt/Zb+X$	multi-channel			36.1	B mass	1.34 TeV	SU(2) doublet	1808.02343
	VLQ $T_{5/3}T_{5/3}\lvert T_{5/3}\to Wt+X$	2(SS)/≥3 e,μ	≥1 b, ≥1 j	Yes	36.1	$T_{5/3}$ mass	1.64 TeV	$\mathcal{B}(T_{5/3}\to Wt)$= 1, $c(T_{5/3}Wt)$= 1	1807.11883
	VLQ $T\to Ht/Zt$	$1\ e,\mu$	≥1 b, ≥3 j	Yes	139	T mass	1.8 TeV	SU(2) singlet, κ_T= 0.5	ATLAS-CONF-2021-040
	VLQ $Y\to Wb$	$1\ e,\mu$	≥1 b, ≥1 j	Yes	36.1	Y mass	1.85 TeV	$\mathcal{B}(Y\to Wb)$= 1, $c_R(Wb)$= 1	1812.07343
	VLQ $B\to Hb$	$0\ e,\mu$	≥2b, ≥1j, ≥1J	–	139	B mass	2.0 TeV	SU(2) doublet, κ_B= 0.3	ATLAS-CONF-2021-018
	VLL $\tau'\to Z\tau/H\tau$	multi-channel	≥1 j	Yes	139	τ' mass	898 GeV	SU(2) doublet	ATLAS-CONF-2022-044
Excited fermions	Excited quark $q^*\to qg$	–	2 j	–	139	q^* mass	6.7 TeV	only u^* and d^*, $\Lambda=m(q^*)$	1910.08447
	Excited quark $q^*\to q\gamma$	$1\ \gamma$	1 j	–	36.7	q^* mass	5.3 TeV	only u^* and d^*, $\Lambda=m(q^*)$	1709.10440
	Excited quark $b^*\to bg$	–	1 b, 1 j	–	139	b^* mass	3.2 TeV		1910.0447
	Excited lepton ℓ^*	$3\ e,\mu$	–	–	20.3	ℓ^* mass	3.0 TeV	$\Lambda=3.0$ TeV	1411.2921
	Excited lepton ν^*	$3\ e,\mu,\tau$	–	–	20.3	ν^* mass	1.6 TeV	$\Lambda=1.6$ TeV	1411.2921
Other	Type III Seesaw	$2,3,4\ e,\mu$	≥2 j	Yes	139	N^0 mass	910 GeV		2202.02039
	LRSM Majorana ν	$2\ \mu$	2 j	–	36.1	N_R mass	3.2 TeV	$m(W_R)=4.1$ TeV, $g_L=g_R$	1809.11105
	Higgs triplet $H^{\pm\pm}\to W^\pm W^\pm$	$2,3,4\ e,\mu$ (SS)	various	Yes	139	$H^{\pm\pm}$ mass	350 GeV	DY production	2101.11961
	Higgs triplet $H^{\pm\pm}\to\ell\ell$	$2,3,4\ e,\mu$ (SS)	–	–	139	$H^{\pm\pm}$ mass	1.08 TeV	DY production	ATLAS-CONF-2022-010
	Higgs triplet $H^{\pm\pm}\to\ell\tau$	$3\ e,\mu,\tau$	–	–	20.3	$H^{\pm\pm}$ mass	400 GeV	DY production, $\mathcal{B}(H_L^{\pm\pm}\to\ell\tau)=1$	1411.2921
	Multi-charged particles	–	–	–	139	multi-charged particle mass	1.59 TeV	DY production, $\lvert q\rvert=5e$	ATLAS-CONF-2022-034
	Magnetic monopoles	–	–	–	34.4	monopole mass	2.37 TeV	DY production, $\lvert g\rvert=1g_D$, spin 1/2	1905.10130

🟩 $\sqrt{s}$ = 8 TeV

🟨 $\sqrt{s}$ = 13 TeV partial data

🟧 $\sqrt{s}$ = 13 TeV full data

**Only a selection of the available mass limits on new states or phenomena is shown.*

†Small-radius (large-radius) jets are denoted by the letter j (J).

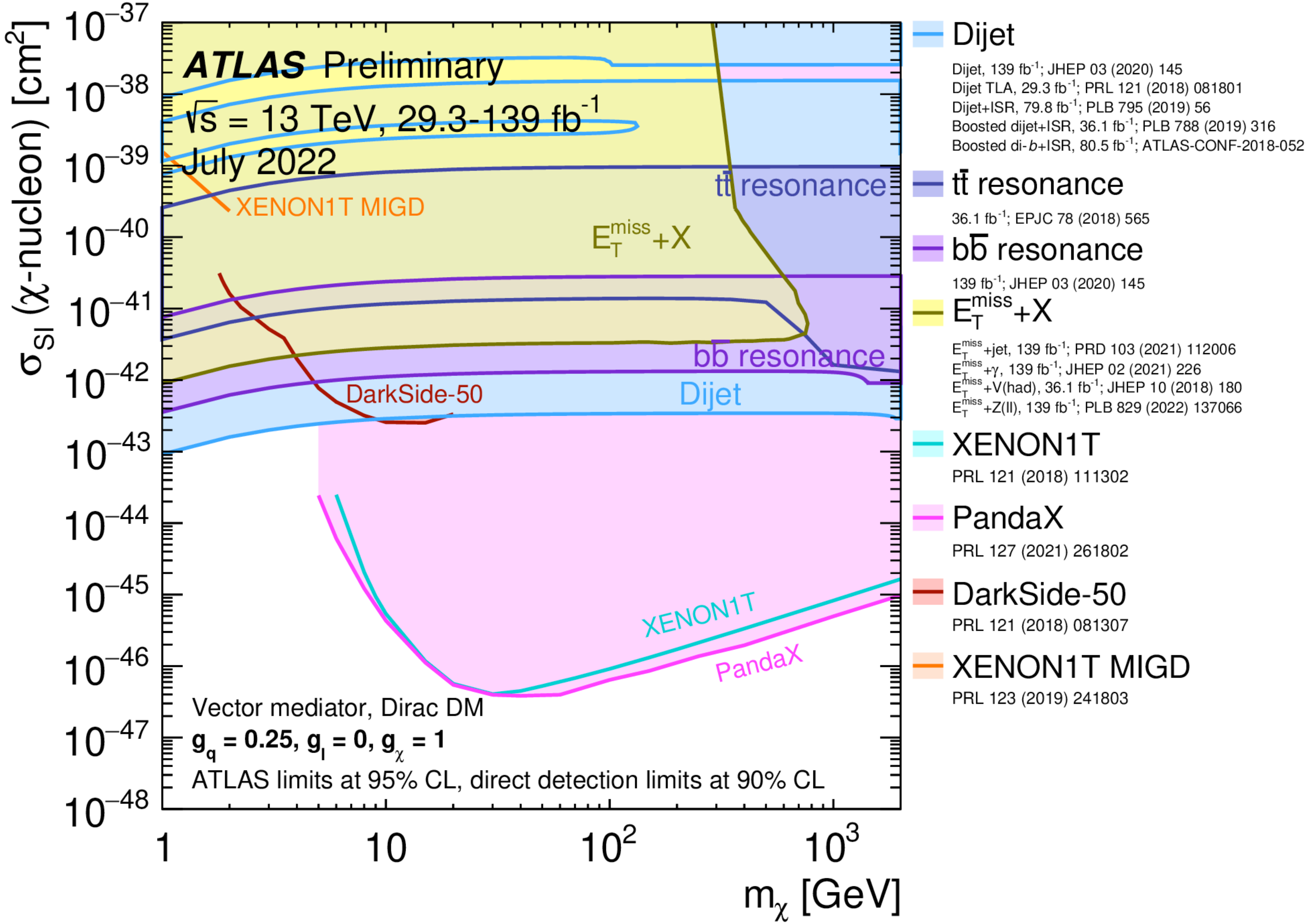
ATLAS Preliminary
$\sqrt{s}$ = 13 TeV, 29.3-139 fb^{-1}
July 2022
XENON1T MIGD
E_T^{miss}+X
$t\bar{t}$ resonance
$b\bar{b}$ resonance
DarkSide-50
Dijet
XENON1T
PandaX
Vector mediator, Dirac DM
$g_q = 0.25, g_l = 0, g_\chi = 1$
ATLAS limits at 95% CL, direct detection limits at 90% CL
σ_{SI} (χ-nucleon) [cm^2]
10^{-37}
10^{-38}
10^{-39}
10^{-40}
10^{-41}
10^{-42}
10^{-43}
10^{-44}
10^{-45}
10^{-46}
10^{-47}
10^{-48}
1
10
10^2
10^3
m_χ [GeV]
Dijet
Dijet, 139 fb^{-1}; JHEP 03 (2020) 145
Dijet TLA, 29.3 fb^{-1}; PRL 121 (2018) 081801
Dijet+ISR, 79.8 fb^{-1}; PLB 795 (2019) 56
Boosted dijet+ISR, 36.1 fb^{-1}; PLB 788 (2019) 316
Boosted di-b+ISR, 80.5 fb^{-1}; ATLAS-CONF-2018-052
$t\bar{t}$ resonance
36.1 fb^{-1}; EPJC 78 (2018) 565
$b\bar{b}$ resonance
139 fb^{-1}; JHEP 03 (2020) 145
E_T^{miss}+X
E_T^{miss}+jet, 139 fb^{-1}; PRD 103 (2021) 112006
E_T^{miss}+γ, 139 fb^{-1}; JHEP 02 (2021) 226
E_T^{miss}+V(had), 36.1 fb^{-1}; JHEP 10 (2018) 180
E_T^{miss}+Z(ll), 139 fb^{-1}; PLB 829 (2022) 137066
XENON1T
PRL 121 (2018) 111302
PandaX
PRL 127 (2021) 261802
DarkSide-50
PRL 121 (2018) 081307
XENON1T MIGD
PRL 123 (2019) 241803

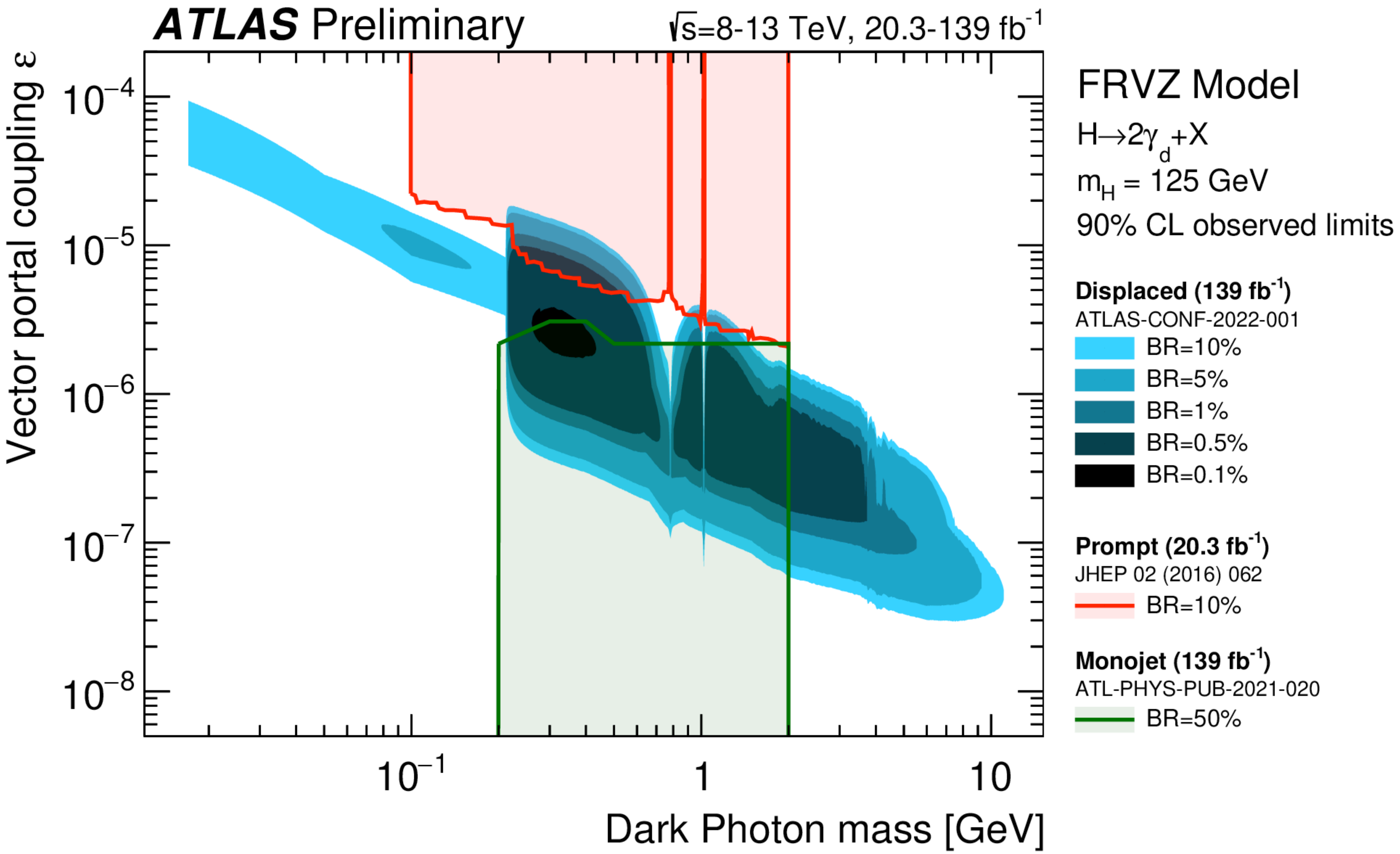
ATLAS Preliminary
√s=8-13 TeV, 20.3-139 fb⁻¹
Vector portal coupling ε
10⁻⁴
10⁻⁵
10⁻⁶
10⁻⁷
10⁻⁸
10⁻¹
1
10
Dark Photon mass [GeV]
FRVZ Model
H→2γd+X
mH = 125 GeV
90% CL observed limits
Displaced (139 fb⁻¹)
ATLAS-CONF-2022-001
BR=10%
BR=5%
BR=1%
BR=0.5%
BR=0.1%
Prompt (20.3 fb⁻¹)
JHEP 02 (2016) 062
BR=10%
Monojet (139 fb⁻¹)
ATL-PHYS-PUB-2021-020
BR=50%

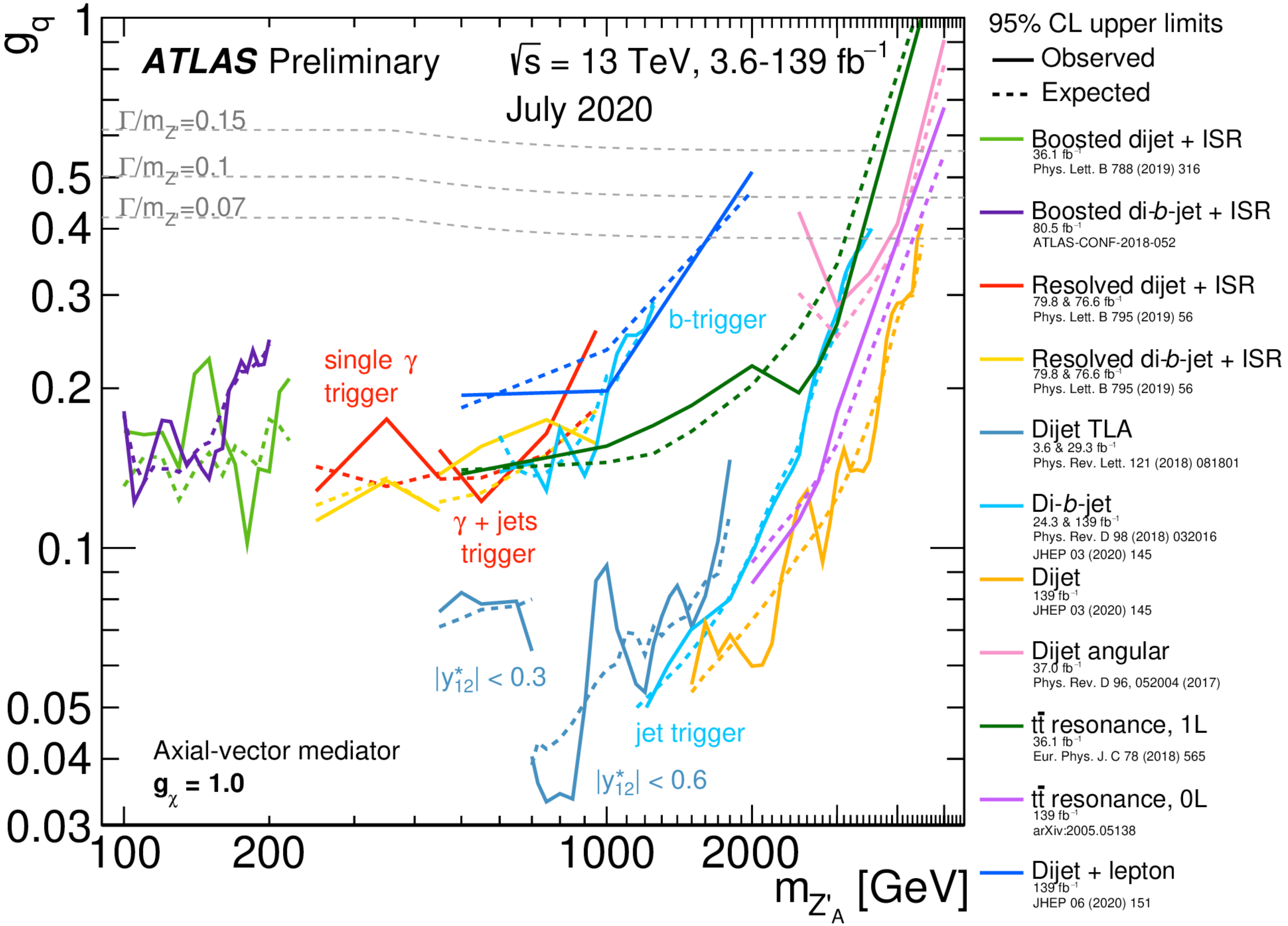
ATLAS Preliminary
$\sqrt{s}$ = 13 TeV, 3.6-139 fb^{-1}
July 2020
g_q
$m_{Z'_A}$ [GeV]
1
0.5
0.4
0.3
0.2
0.1
0.05
0.04
0.03
100
200
1000
2000
$\Gamma/m_{Z'}$=0.15
$\Gamma/m_{Z'}$=0.1
$\Gamma/m_{Z'}$=0.07
single γ trigger
γ + jets trigger
b-trigger
jet trigger
$|y^*_{12}|$ < 0.3
$|y^*_{12}|$ < 0.6
Axial-vector mediator
g_χ = 1.0
95% CL upper limits
Observed
Expected
Boosted dijet + ISR
36.1 fb^{-1}
Phys. Lett. B 788 (2019) 316
Boosted di-b-jet + ISR
80.5 fb^{-1}
ATLAS-CONF-2018-052
Resolved dijet + ISR
79.8 & 76.6 fb^{-1}
Phys. Lett. B 795 (2019) 56
Resolved di-b-jet + ISR
79.8 & 76.6 fb^{-1}
Phys. Lett. B 795 (2019) 56
Dijet TLA
3.6 & 29.3 fb^{-1}
Phys. Rev. Lett. 121 (2018) 081801
Di-b-jet
24.3 & 139 fb^{-1}
Phys. Rev. D 98 (2018) 032016
JHEP 03 (2020) 145
Dijet
139 fb^{-1}
JHEP 03 (2020) 145
Dijet angular
37.0 fb^{-1}
Phys. Rev. D 96, 052004 (2017)
$t\bar{t}$ resonance, 1L
36.1 fb^{-1}
Eur. Phys. J. C 78 (2018) 565
$t\bar{t}$ resonance, 0L
139 fb^{-1}
arXiv:2005.05138
Dijet + lepton
139 fb^{-1}
JHEP 06 (2020) 151

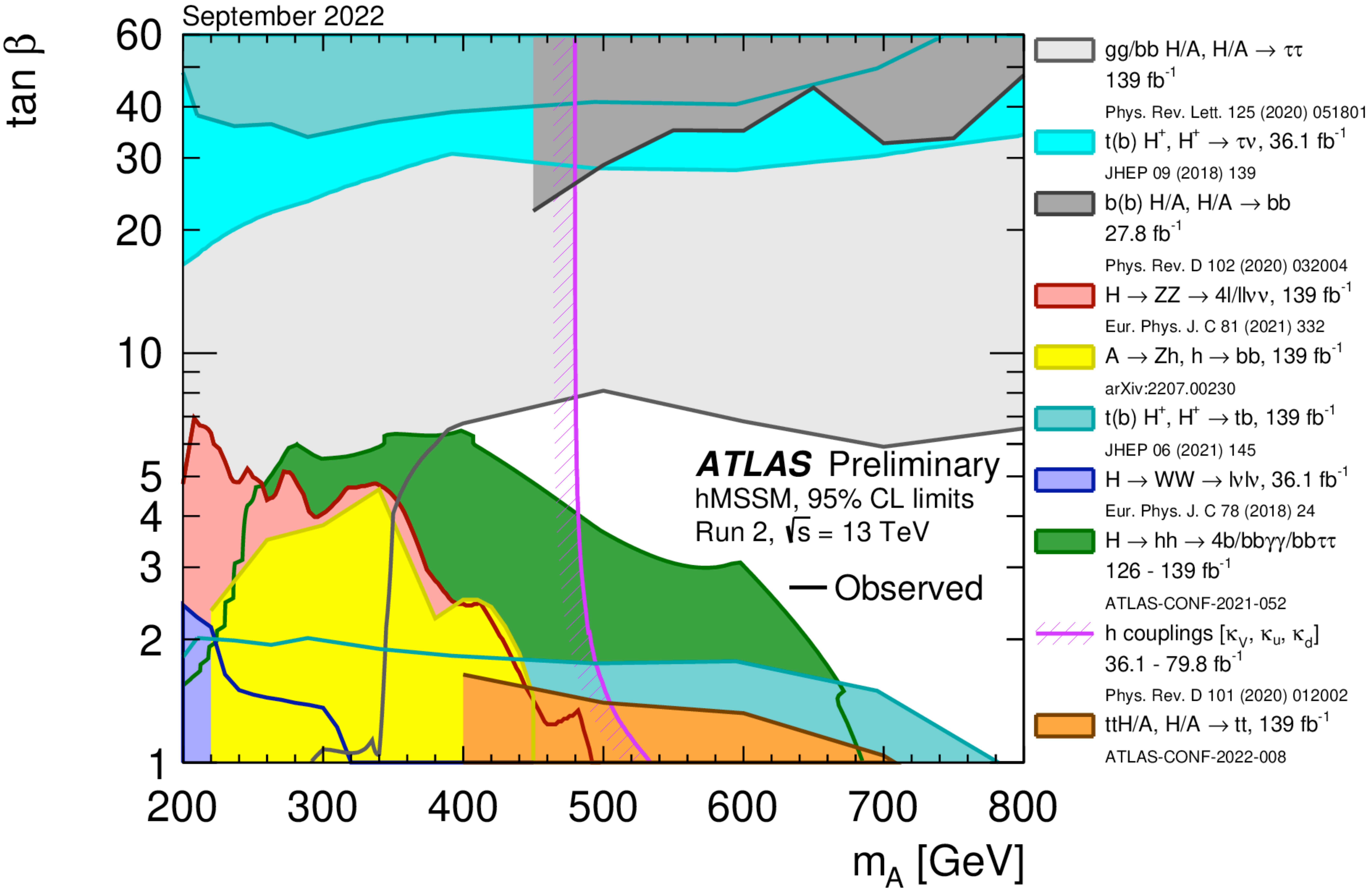September 2022
tan β
60
40
30
20
10
5
4
3
2
1
200
300
400
500
600
700
800
m_A [GeV]
ATLAS Preliminary
hMSSM, 95% CL limits
Run 2, √s = 13 TeV
— Observed
gg/bb H/A, H/A → ττ
139 fb^-1
Phys. Rev. Lett. 125 (2020) 051801
t(b) H+, H+ → τν, 36.1 fb^-1
JHEP 09 (2018) 139
b(b) H/A, H/A → bb
27.8 fb^-1
Phys. Rev. D 102 (2020) 032004
H → ZZ → 4l/llνν, 139 fb^-1
Eur. Phys. J. C 81 (2021) 332
A → Zh, h → bb, 139 fb^-1
arXiv:2207.00230
t(b) H+, H+ → tb, 139 fb^-1
JHEP 06 (2021) 145
H → WW → lνlν, 36.1 fb^-1
Eur. Phys. J. C 78 (2018) 24
H → hh → 4b/bbγγ/bbττ
126 - 139 fb^-1
ATLAS-CONF-2021-052
h couplings [κ_V, κ_u, κ_d]
36.1 - 79.8 fb^-1
Phys. Rev. D 101 (2020) 012002
ttH/A, H/A → tt, 139 fb^-1
ATLAS-CONF-2022-008

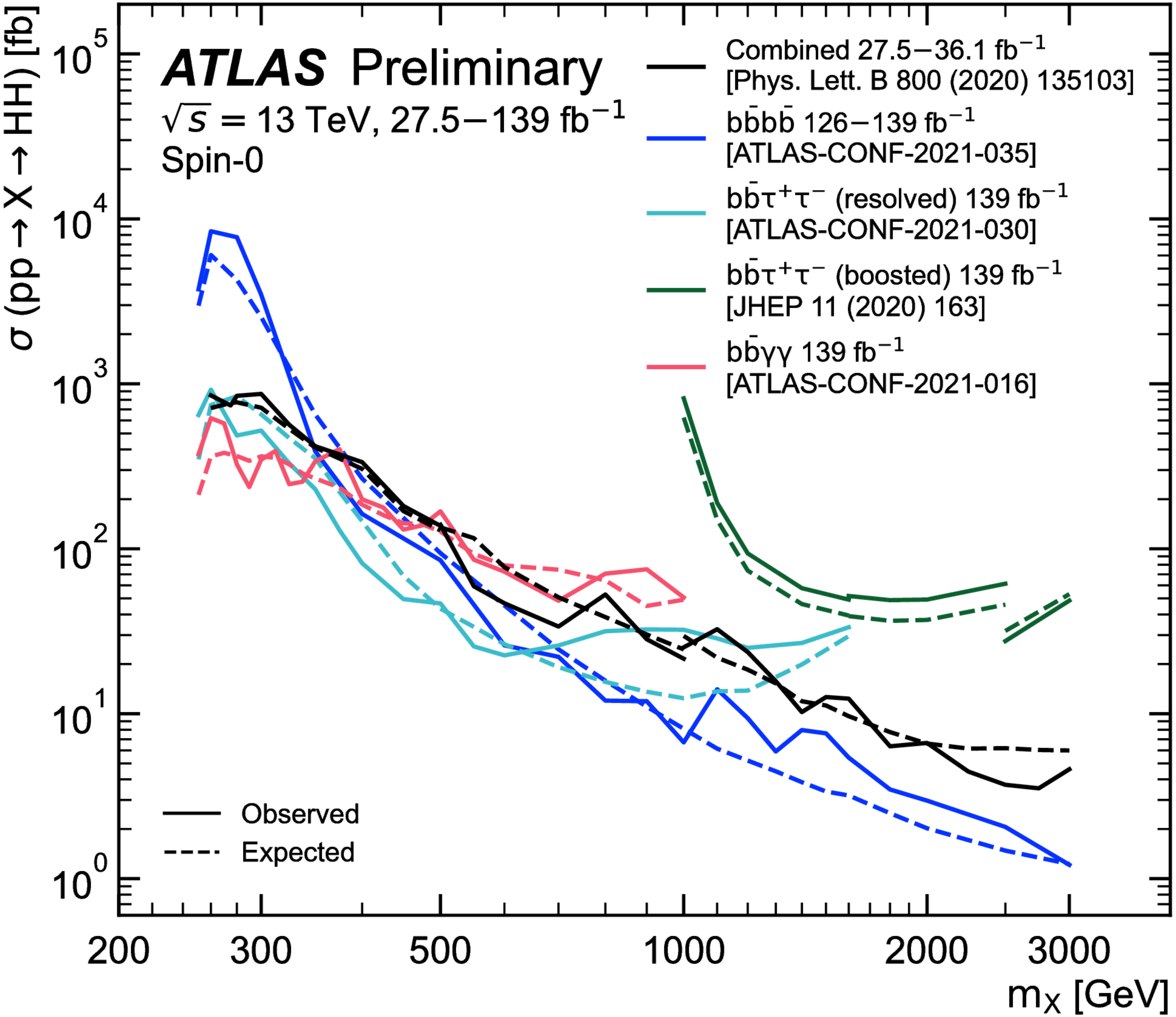

UPPSALA UNIVERSITET

ATLAS Diboson Searches - 95% CL Exclusion Limits

Status: June 2021

ATLAS Preliminary

$\mathcal{L}$ = (36.1 – 139) fb^{-1} $\sqrt{s}$ = 13 TeV

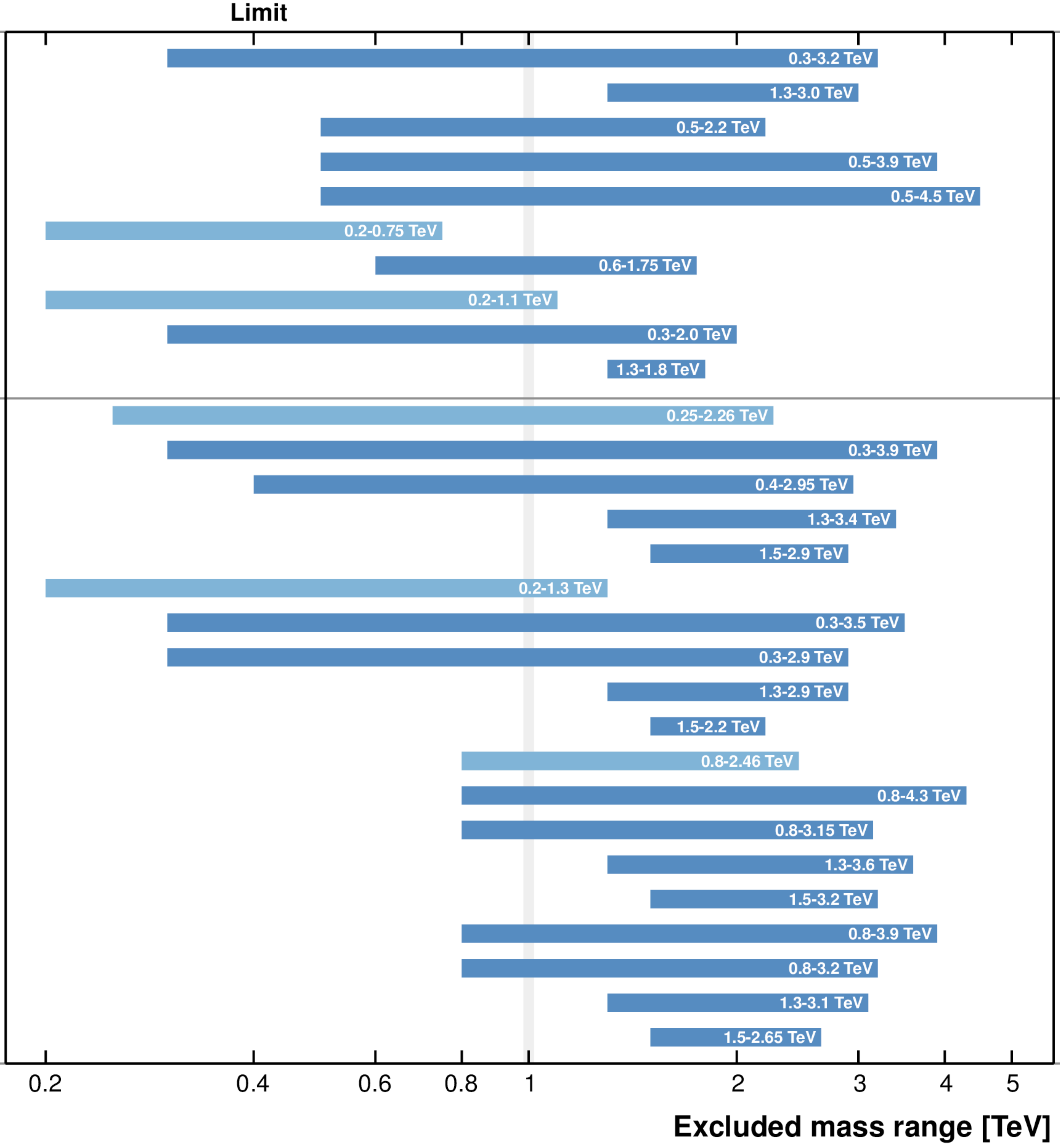

	Model	Channel†	Strategy*	Limit	Reference
Extra dimensions	Bulk RS ($k\pi r_c = 35$, $\Lambda_R = 3$ TeV)	$R \to WW, ZZ \to \nu\nu qq, \ell\nu qq, \ell\ell qq$	resolved, boosted	0.3-3.2 TeV	Eur. Phys. J. C 80 (2020) 1165
	Bulk RS ($k\pi r_c = 35$, $\Lambda_R = 3$ TeV)	$R \to WW, ZZ \to qqqq$	boosted	1.3-3.0 TeV	JHEP 06 (2020) 042
	RS1 ($k/\overline{M}_{Pl} = 0.01$)	$G_{KK} \to \gamma\gamma$	resolved	0.5-2.2 TeV	arXiv:2102.13405
	RS1 ($k/\overline{M}_{Pl} = 0.05$)	$G_{KK} \to \gamma\gamma$	resolved	0.5-3.9 TeV	arXiv:2102.13405
	RS1 ($k/\overline{M}_{Pl} = 0.1$)	$G_{KK} \to \gamma\gamma$	resolved	0.5-4.5 TeV	arXiv:2102.13405
	Bulk RS ($k/\overline{M}_{Pl} = 0.5$)	$G_{KK} \to WW \to e\nu\mu\nu$	resolved	0.2-0.75 TeV	Eur. Phys. J. C 78 (2018) 24
	Bulk RS ($k/\overline{M}_{Pl} = 1.0$)	$G_{KK} \to ZZ \to \ell\ell\ell'\ell', \nu\nu\ell\ell$	resolved	0.6-1.75 TeV	Eur. Phys. J. C 81 (2021) 332
	Bulk RS ($k/\overline{M}_{Pl} = 1.0$)	$G_{KK} \to WW \to e\nu\mu\nu$	resolved	0.2-1.1 TeV	Eur. Phys. J. C 78 (2018) 24
	Bulk RS ($k/\overline{M}_{Pl} = 1.0$)	$G_{KK} \to WW, ZZ \to \nu\nu qq, \ell\nu qq, \ell\ell qq$	resolved, boosted	0.3-2.0 TeV	Eur. Phys. J. C 80 (2020) 1165
	Bulk RS ($k/\overline{M}_{Pl} = 1.0$)	$G_{KK} \to WW, ZZ \to qqqq$	boosted	1.3-1.8 TeV	JHEP 06 (2020) 042
Gauge bosons	HVT ($g_F = -0.55$, $g_H = -0.56$)	$W' \to WZ \to \ell\nu\ell'\ell'$	resolved	0.25-2.26 TeV	Phys. Lett. B 787 (2018) 68
	HVT ($g_F = -0.55$, $g_H = -0.56$)	$W' \to WZ \to \nu\nu qq, \ell\nu qq, \ell\ell qq$	resolved, boosted	0.3-3.9 TeV	Eur. Phys. J. C 80 (2020) 1165
	HVT ($g_F = -0.55$, $g_H = -0.56$)	$W' \to WH \to \ell\nu bb$	resolved, boosted	0.4-2.95 TeV	ATLAS-CONF-2021-026
	HVT ($g_F = -0.55$, $g_H = -0.56$)	$W' \to WZ \to qqqq$	boosted	1.3-3.4 TeV	JHEP 06 (2020) 042
	HVT ($g_F = -0.55$, $g_H = -0.56$)	$W' \to WH \to qqbb$	boosted	1.5-2.9 TeV	Phys. Rev. D 102 (2020) 112008
	HVT ($g_F = -0.55$, $g_H = -0.56$)	$Z' \to WW \to e\nu\mu\nu$	resolved	0.2-1.3 TeV	Eur. Phys. J. C 78 (2018) 24
	HVT ($g_F = -0.55$, $g_H = -0.56$)	$Z' \to WW \to \ell\nu qq$	resolved, boosted	0.3-3.5 TeV	Eur. Phys. J. C 80 (2020) 1165
	HVT ($g_F = -0.55$, $g_H = -0.56$)	$Z' \to ZH \to \nu\nu bb, \ell\ell bb$	resolved, boosted	0.3-2.9 TeV	ATLAS-CONF-2020-043
	HVT ($g_F = -0.55$, $g_H = -0.56$)	$Z' \to WW \to qqqq$	boosted	1.3-2.9 TeV	JHEP 06 (2020) 042
	HVT ($g_F = -0.55$, $g_H = -0.56$)	$Z' \to ZH \to qqbb$	boosted	1.5-2.2 TeV	Phys. Rev. D 102 (2020) 112008
	HVT ($g_F = 0.14$, $g_H = -2.9$)	$W' \to WZ \to \ell\nu\ell'\ell'$	resolved	0.8-2.46 TeV	Phys. Lett. B 787 (2018) 68
	HVT ($g_F = 0.14$, $g_H = -2.9$)	$W' \to WZ \to \nu\nu qq, \ell\nu qq, \ell\ell qq$	resolved, boosted	0.8-4.3 TeV	Eur. Phys. J. C 80 (2020) 1165
	HVT ($g_F = 0.14$, $g_H = -2.9$)	$W' \to WH \to \ell\nu bb$	resolved, boosted	0.8-3.15 TeV	ATLAS-CONF-2021-026
	HVT ($g_F = 0.14$, $g_H = -2.9$)	$W' \to WZ \to qqqq$	boosted	1.3-3.6 TeV	JHEP 06 (2020) 042
	HVT ($g_F = 0.14$, $g_H = -2.9$)	$W' \to WH \to qqbb$	boosted	1.5-3.2 TeV	Phys. Rev. D 102 (2020) 112008
	HVT ($g_F = 0.14$, $g_H = -2.9$)	$Z' \to WW \to \ell\nu qq$	resolved, boosted	0.8-3.9 TeV	Eur. Phys. J. C 80 (2020) 1165
	HVT ($g_F = 0.14$, $g_H = -2.9$)	$Z' \to ZH \to \nu\nu bb, \ell\ell bb$	resolved, boosted	0.8-3.2 TeV	ATLAS-CONF-2020-043
	HVT ($g_F = 0.14$, $g_H = -2.9$)	$Z' \to WW \to qqqq$	boosted	1.3-3.1 TeV	JHEP 06 (2020) 042
	HVT ($g_F = 0.14$, $g_H = -2.9$)	$Z' \to ZH \to qqbb$	boosted	1.5-2.65 TeV	Phys. Rev. D 102 (2020) 112008

$\sqrt{s}$ = 13 TeV, $\mathcal{L}$ = 36.1 fb^{-1}

$\sqrt{s}$ = 13 TeV, $\mathcal{L}$ = 139 fb^{-1}

*small-radius (large-radius) jets are used in resolved (boosted) events

†with $\ell = \mu, e$

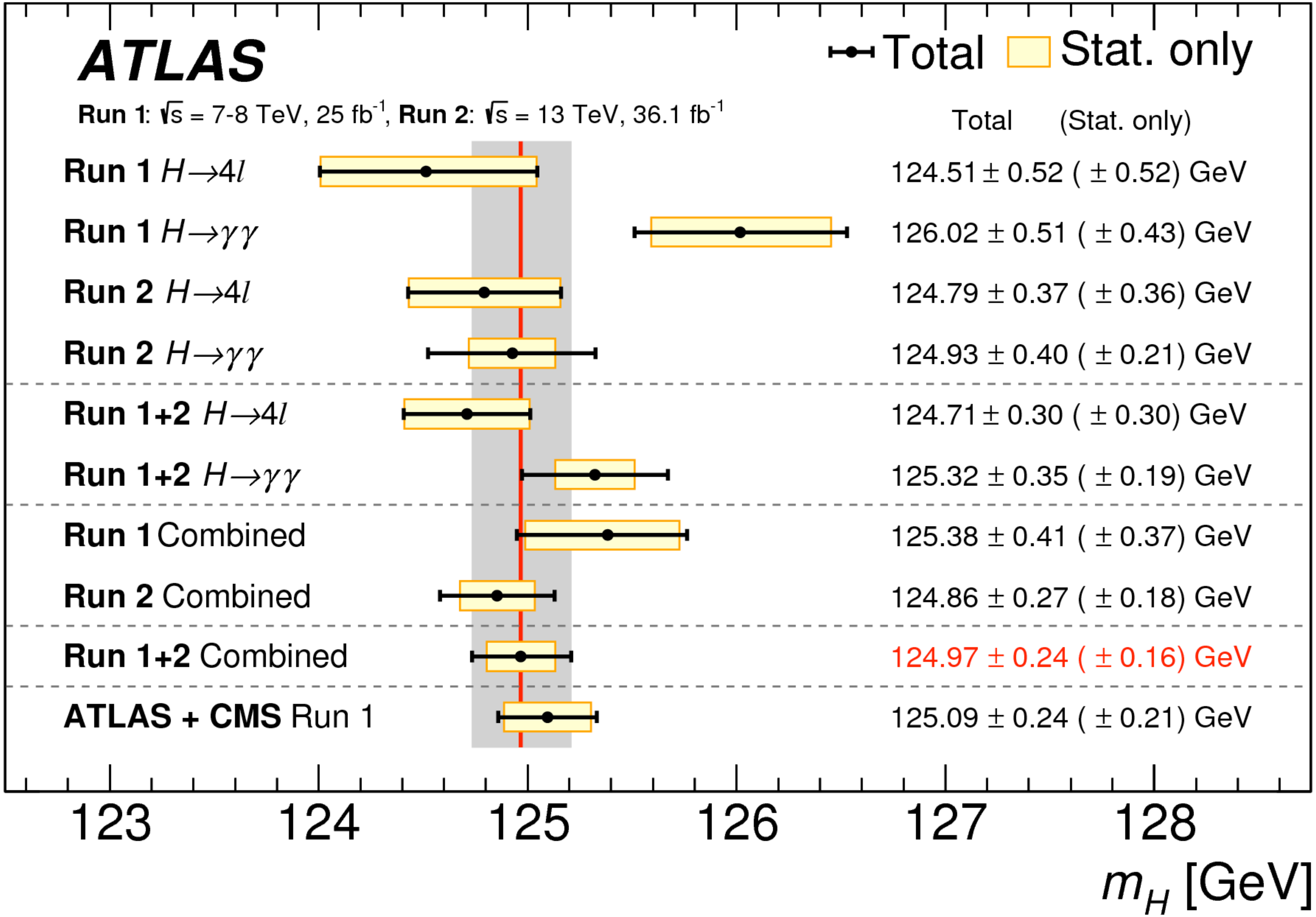
ATLAS
Total
Stat. only
Run 1: √s = 7-8 TeV, 25 fb^{-1}, Run 2: √s = 13 TeV, 36.1 fb^{-1}
Total (Stat. only)
Run 1 $H\rightarrow 4l$ 124.51 ± 0.52 (± 0.52) GeV
Run 1 $H\rightarrow\gamma\gamma$ 126.02 ± 0.51 (± 0.43) GeV
Run 2 $H\rightarrow 4l$ 124.79 ± 0.37 (± 0.36) GeV
Run 2 $H\rightarrow\gamma\gamma$ 124.93 ± 0.40 (± 0.21) GeV
Run 1+2 $H\rightarrow 4l$ 124.71 ± 0.30 (± 0.30) GeV
Run 1+2 $H\rightarrow\gamma\gamma$ 125.32 ± 0.35 (± 0.19) GeV
Run 1 Combined 125.38 ± 0.41 (± 0.37) GeV
Run 2 Combined 124.86 ± 0.27 (± 0.18) GeV
Run 1+2 Combined 124.97 ± 0.24 (± 0.16) GeV
ATLAS + CMS Run 1 125.09 ± 0.24 (± 0.21) GeV
123
124
125
126
127
128
m_H [GeV]

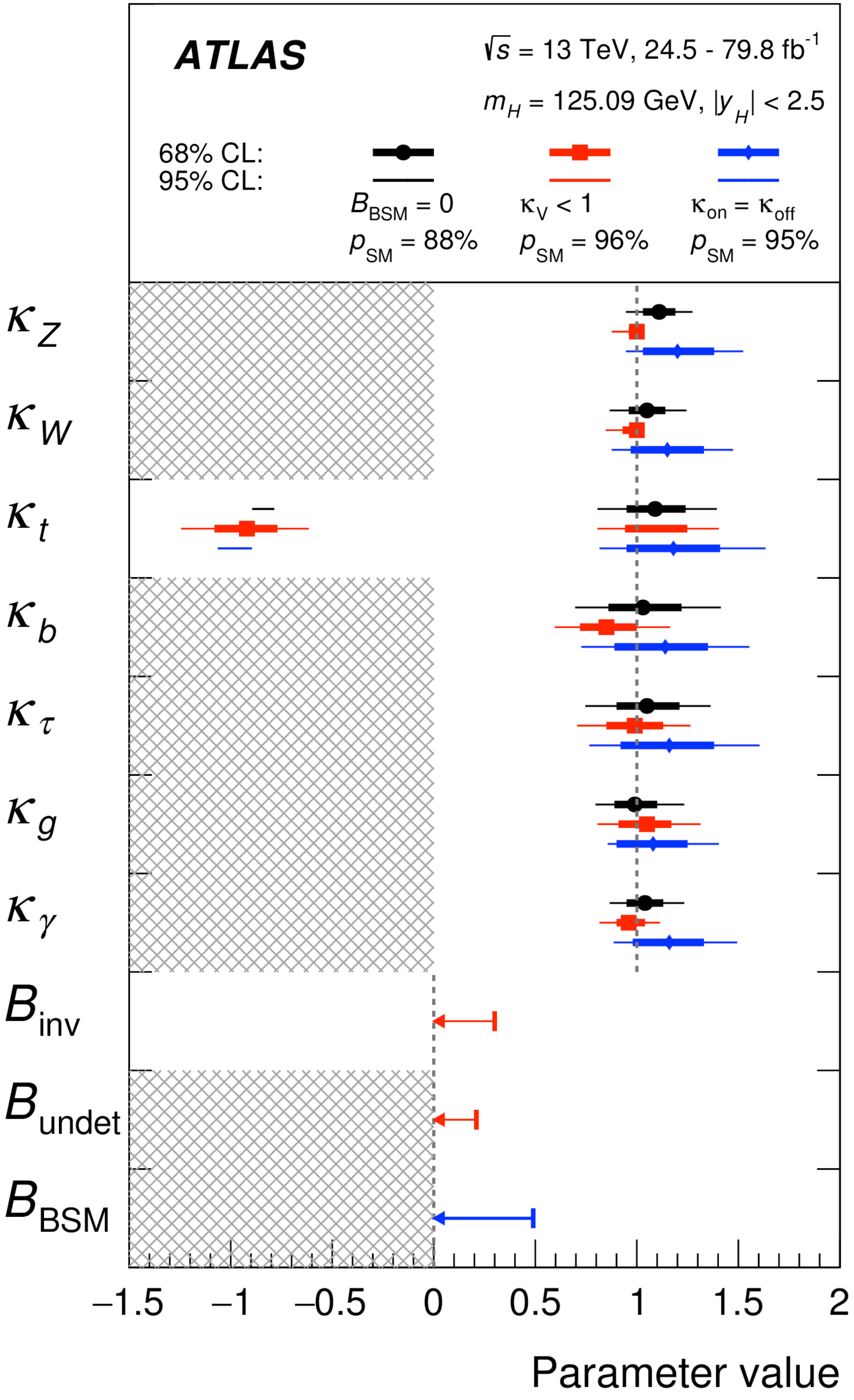
ATLAS
$\sqrt{s}$ = 13 TeV, 24.5 - 79.8 fb^{-1}
m_H = 125.09 GeV, $|y_H|$ < 2.5
68% CL:
95% CL:
$B_{BSM} = 0$
p_{SM} = 88%
$\kappa_V < 1$
p_{SM} = 96%
$\kappa_{on} = \kappa_{off}$
p_{SM} = 95%
κ_Z
κ_W
κ_t
κ_b
κ_τ
κ_g
κ_γ
B_{inv}
B_{undet}
B_{BSM}
–1.5
–1
–0.5
0
0.5
1
1.5
2
Parameter value

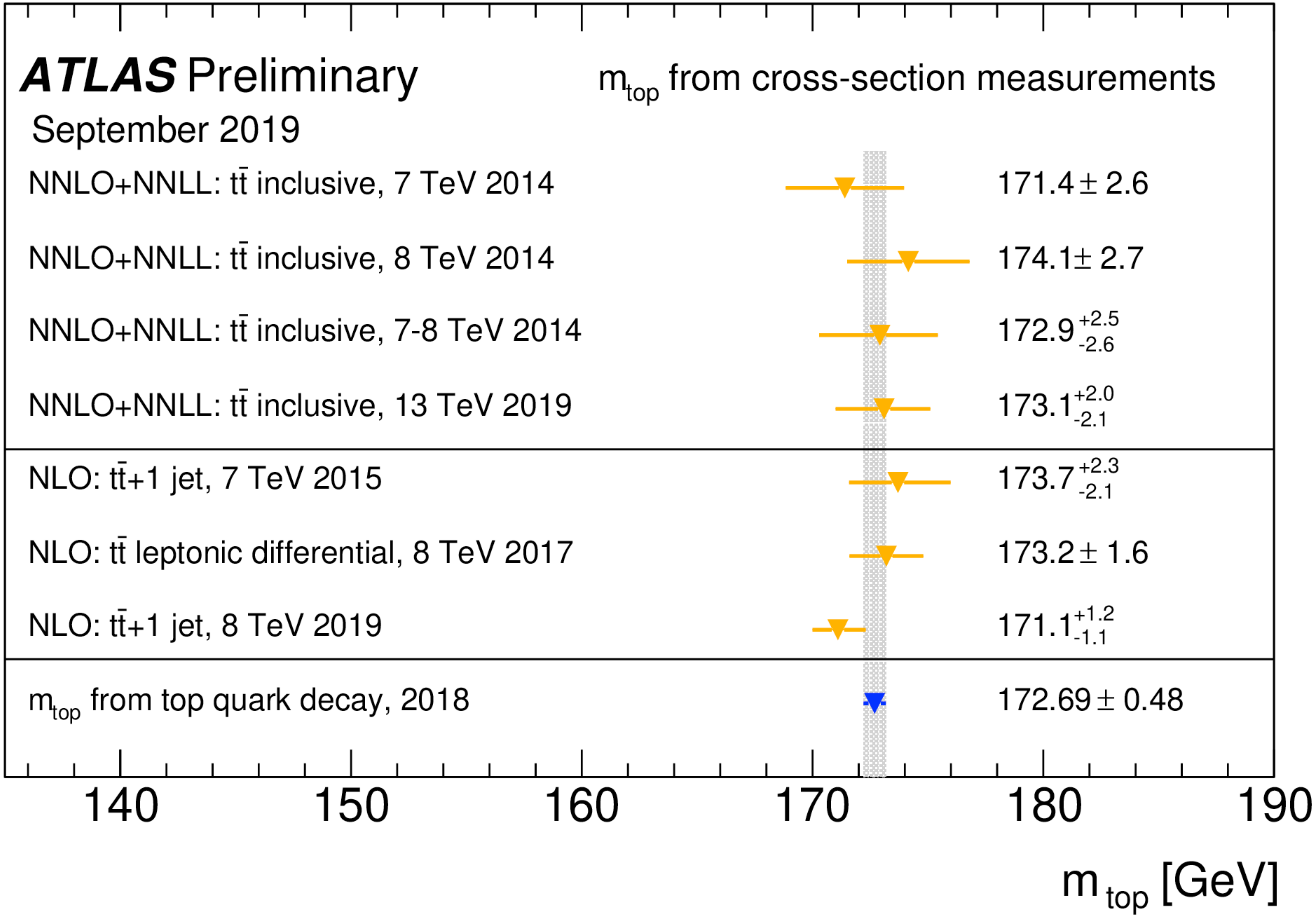
ATLAS Preliminary
September 2019
m_{top} from cross-section measurements
NNLO+NNLL: $t\bar{t}$ inclusive, 7 TeV 2014
171.4 ± 2.6
NNLO+NNLL: $t\bar{t}$ inclusive, 8 TeV 2014
174.1 ± 2.7
NNLO+NNLL: $t\bar{t}$ inclusive, 7-8 TeV 2014
$172.9^{+2.5}_{-2.6}$
NNLO+NNLL: $t\bar{t}$ inclusive, 13 TeV 2019
$173.1^{+2.0}_{-2.1}$
NLO: $t\bar{t}$+1 jet, 7 TeV 2015
$173.7^{+2.3}_{-2.1}$
NLO: $t\bar{t}$ leptonic differential, 8 TeV 2017
173.2 ± 1.6
NLO: $t\bar{t}$+1 jet, 8 TeV 2019
$171.1^{+1.2}_{-1.1}$
m_{top} from top quark decay, 2018
172.69 ± 0.48
140
150
160
170
180
190
m_{top} [GeV]

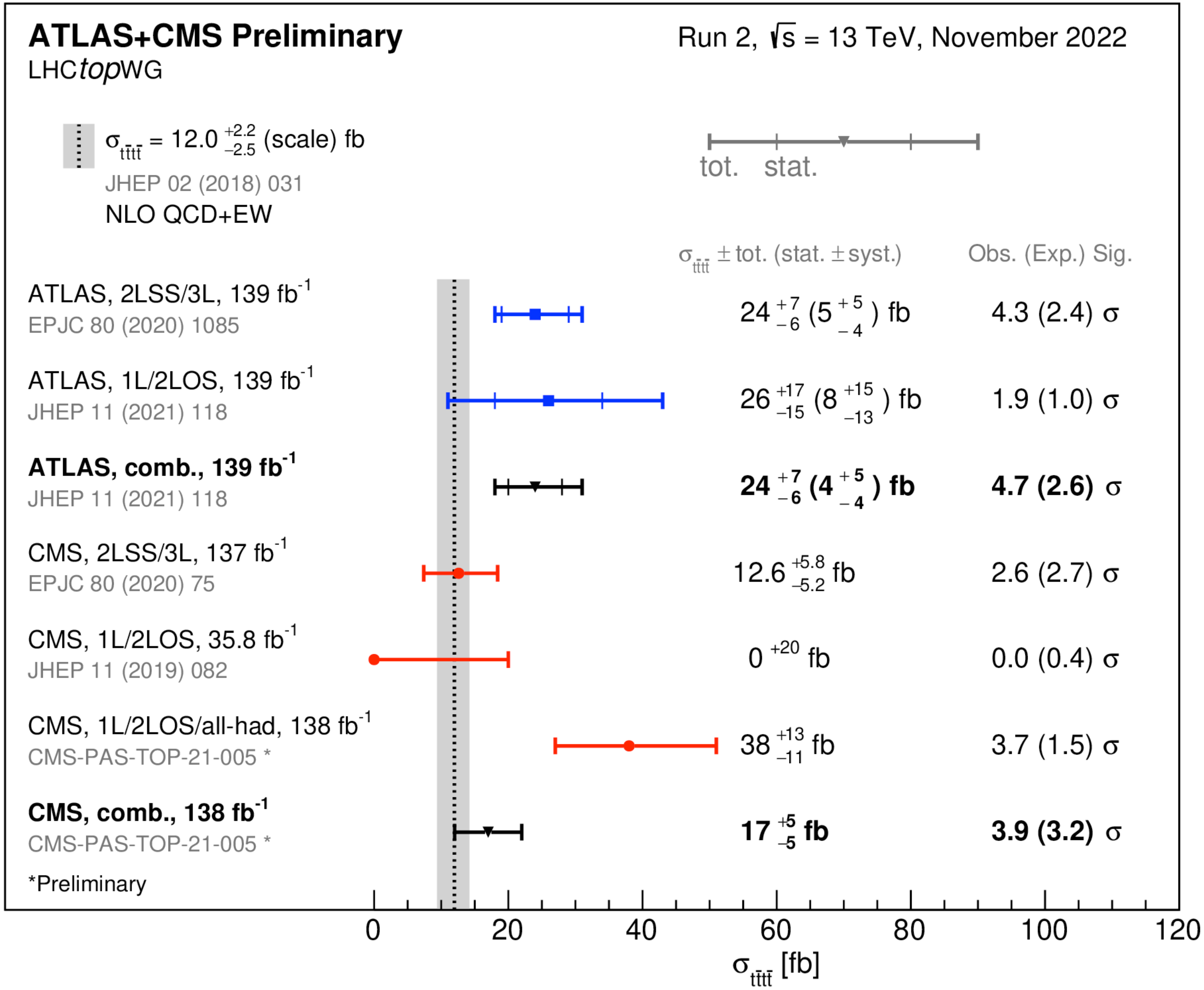
ATLAS+CMS Preliminary
LHC*top*WG
Run 2, $\sqrt{s}$ = 13 TeV, November 2022
$\sigma_{t\bar{t}t\bar{t}} = 12.0\,^{+2.2}_{-2.5}$ (scale) fb
JHEP 02 (2018) 031
NLO QCD+EW
tot.
stat.
$\sigma_{t\bar{t}t\bar{t}}$ ± tot. (stat. ± syst.)
Obs. (Exp.) Sig.
ATLAS, 2LSS/3L, 139 fb^{-1}
EPJC 80 (2020) 1085
$24\,^{+7}_{-6}\,(5\,^{+5}_{-4})$ fb
4.3 (2.4) σ
ATLAS, 1L/2LOS, 139 fb^{-1}
JHEP 11 (2021) 118
$26\,^{+17}_{-15}\,(8\,^{+15}_{-13})$ fb
1.9 (1.0) σ
ATLAS, comb., 139 fb^{-1}
JHEP 11 (2021) 118
$24\,^{+7}_{-6}\,(4\,^{+5}_{-4})$ fb
4.7 (2.6) σ
CMS, 2LSS/3L, 137 fb^{-1}
EPJC 80 (2020) 75
$12.6\,^{+5.8}_{-5.2}$ fb
2.6 (2.7) σ
CMS, 1L/2LOS, 35.8 fb^{-1}
JHEP 11 (2019) 082
$0\,^{+20}$ fb
0.0 (0.4) σ
CMS, 1L/2LOS/all-had, 138 fb^{-1}
CMS-PAS-TOP-21-005 *
$38\,^{+13}_{-11}$ fb
3.7 (1.5) σ
CMS, comb., 138 fb^{-1}
CMS-PAS-TOP-21-005 *
$17\,^{+5}_{-5}$ fb
3.9 (3.2) σ
*Preliminary
0
20
40
60
80
100
120
$\sigma_{t\bar{t}t\bar{t}}$ [fb]

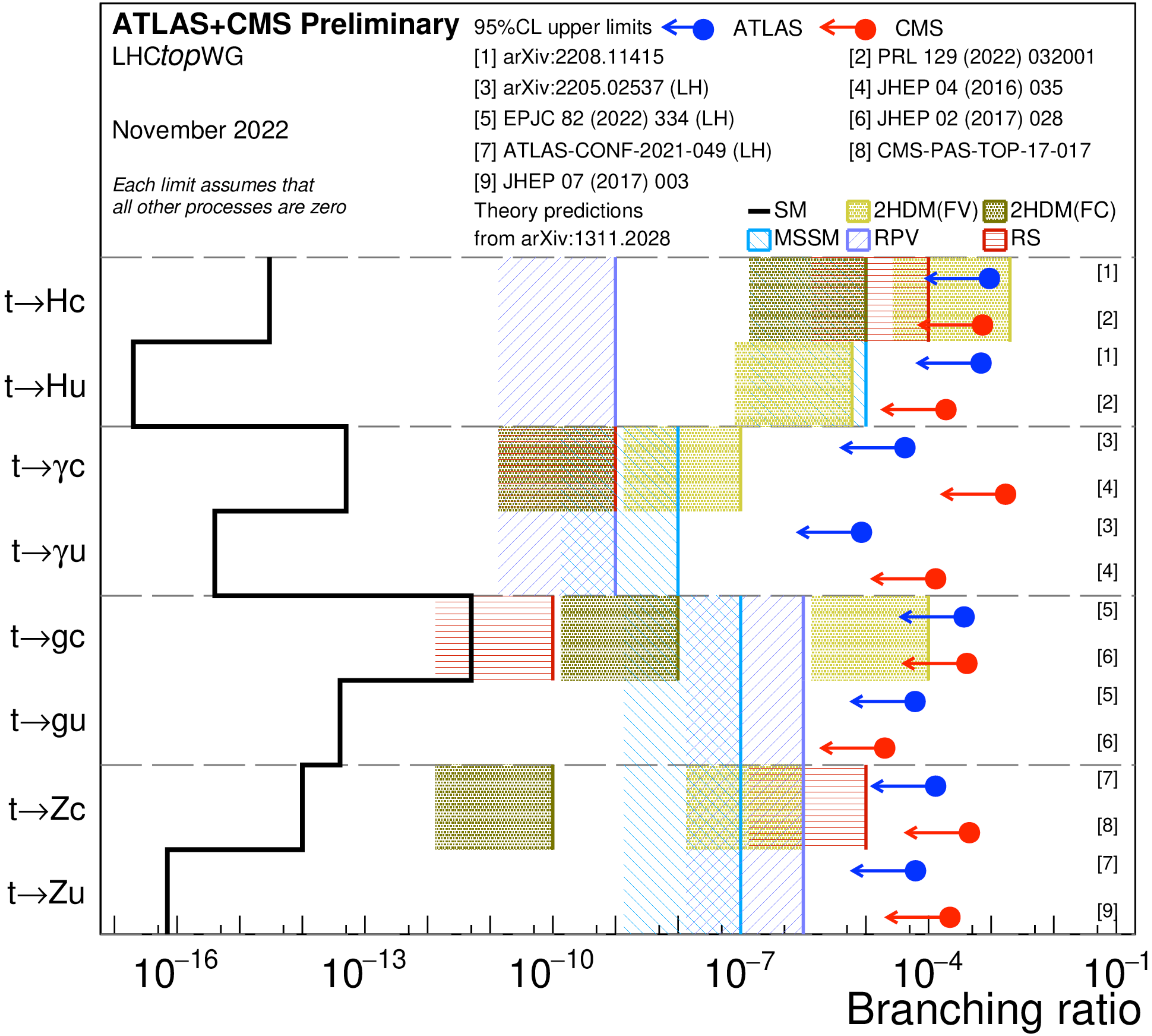
ATLAS+CMS Preliminary
LHC*top*WG
November 2022
Each limit assumes that all other processes are zero
95%CL upper limits
ATLAS
CMS
[1] arXiv:2208.11415
[2] PRL 129 (2022) 032001
[3] arXiv:2205.02537 (LH)
[4] JHEP 04 (2016) 035
[5] EPJC 82 (2022) 334 (LH)
[6] JHEP 02 (2017) 028
[7] ATLAS-CONF-2021-049 (LH)
[8] CMS-PAS-TOP-17-017
[9] JHEP 07 (2017) 003
Theory predictions from arXiv:1311.2028
SM
2HDM(FV)
2HDM(FC)
MSSM
RPV
RS
t→Hc
t→Hu
t→γc
t→γu
t→gc
t→gu
t→Zc
t→Zu
[1]
[2]
[1]
[2]
[3]
[4]
[3]
[4]
[5]
[6]
[5]
[6]
[7]
[8]
[7]
[9]
10^{-16}
10^{-13}
10^{-10}
10^{-7}
10^{-4}
10^{-1}
Branching ratio